Identification and Characterization of interacting partners of cytoplasmic domain of *Xenopus* Paraxial Protocadherin

DISSERTATION

submitted to the

Combined Faculties of the Natural Sciences and Mathematics

of the Ruprechtr-Karls University of Heidelberg, Germany

for the degree of

Doctor of Natural Sciences

presented by

Master of Sciences Yingqun Wang

born in Wuhan, P. R. China

Oral examination: ……

Identification and Characterization of interacting partners of cytoplasmic domain of *Xenopus* Paraxial Protocadherin

Referees: Prof. Dr. Herbert Steinbeisser

Prof. Dr. Thomas Holstein

DEDICATED TO THE MEMORY OF MY MOTHER

李竹生 ZHUSHENG LI

Table of Contents

1. SUMMARY

Gastrulation is one of the most crucial steps in early embryogenesis. A growing number of proteins contributing to the regulation of vertebrate gastrulation have been identified. Among them is *Xenopus* Paraxial Protocadherin (xPAPC). xPAPC modulates C-cadherin mediated cell adhesion and is involved in cell sorting. In addition it has signaling functions which are essential for convergent extension (CE) movements and tissue separation during gastrulation. xPAPC modulates the activities of Rho GTPase and c-jun-terminal kinase (JNK), which are effectors of the planar cell polarity (PCP) pathway. The cytoplasmic domain of xPAPC (xPAPCc) is indispensable for the signaling activities of xPAPC but until now no proteins have been reported to interact with xPAPCc and mediate intracellular signaling.

In this thesis three experimental strategies were employed to identify interaction partners of xPAPCc, with the aim to elucidate the mechanisms underlying xPAPC signaling. While candidate and GST pull-down approaches did not show satisfactory results, several putative interacting partners were revealed by yeast two-hybrid screen. Two proteins, Sprouty1 and CK2β, were characterized functionally. By coimmunoprecipitation assay the physical interaction of these two proteins with xPAPCc was verified. The interaction between xPAPCc and xSprouty is not dependent on the conserved 16 amino-acid region present in all four vertebrate PAPC homologs but on the phosphorylation of S741 and S955 residues of xPAPC. xPAPC functionally antagonizes xSpry in both CE movements and tissue separation. Mechanistically, xSpry1 inhibits membrane recruitment of the PCP components PKCδ and Dsh. Coexpression of xPAPC can rescue the recruitment of PKCδ and Dsh inhibited by xSpry1. Importantly, the interaction of xPAPC and xSpry1 is indispensable for the ability of xPAPC to antagonize xSpry1. xPAPC mutant in S741 and S955 residues is unable to bind and functionally antagonize xSpry1. This study therefore demonstrates clearly that the interaction between xPAPC and xSpry1 is crucial for the modulation of PCP pathway. xPAPC-mediated signaling promotes CE movements and tissue separation. This finding establishes for the first time a link between protocadherins and non-canonical Wnt signaling in vertebrates.

This study also demonstrates that xPAPC modulates Wnt/β-catenin signaling. CK2 stimulates the Wnt/β-catenin pathway by stabilization of β-catenin. xPAPC functionally antagonizes xCK2 in the *Xenopus* axis induction assay and inhibits the induction of Wnt target Xnr3 in animal cap explants. In conclusion, I propose that xPAPC acts as a switch between canonical Wnt and non-canonical Wnt signaling. By sequestration of Sprouty and CK2β, xPAPC promotes non-canonical Wnt signaling to modulate gastrulation movements while it inbibits canonical Wnt signaling to modify mesoderm specification.

Zusammenfassung

Die Gastrulation ist einer der entscheidenden Schritte der Embryogenese. Eine wachsende Anzahl von Proteinen, die zur Regulation der Gastrulation beitragen ist in den letzen Jahren identifiziert worden. Eines dieser Proteine ist das *Xenopus* Paraxiale Protocadherin (xPAPC). xPAPC kann die C-Cadherin-vermittelte Zelladhäsion modulieren und ist an der Trennung von Zellpopulationen beteiligt. xPAPC besitzt zusätzlich Signalfunktionen, welche für die Regulation von convergenten Extensionbewegungen (CE) und der Gewebstrennung während der Gastrulation notwendig sind. xPAPC beeinflusst die GTPase Rho und die C-jun terminale Kinase (JNK), welche Effektoren des planaren Polaritäts (PCP) Signalwegs sind. Die zytoplasmatische Domäne von xPAPC (xPAPCc) ist für diese Signalfunktion unabdingbar. Dennoch sind bisher keine Proteine identifiziert worden, die mit xPAPCc interagieren und die Signale intrazellulär vermitteln.
Im Rahmen dieser Arbeit wurden 3 Strategien zur Identifizierung und Charakterisierung von Proteinen, die mit xPAPCc interagieren angewandt mit dem Ziel, den Mechanismus der xPAPC-vermittelten Signalkette aufzuklären. Während ein „Kandidatansatz“ und eine GST-pull-down Strategie keine befriedigenden Ergebnisse lieferten, wurden einige potentielle Interaktionpartner durch einen Yeast-Two- Hybrid Ansatz identifiziert. Zwei dieser Proteine, Sprouty1(Spry1) und Casein Kinase 2β(CK2) wurden funktionell charakterisiert. Die physikalische Interaktion von xPAPCc mit diesen Proteinen wurde durch Co- Immunopäzipitations Experiment bestätigt. Die Interaktion von xPAPCc und Spry1 ist nicht von einer konservierten Region von 16 Aminosäuren abhängig, welche in allen 4 PAPC Homologen der Wirbeltiere vorhanden ist, sondern von der Phosphorylierung der Serine 741 und 955. xPAPC antagonisiert funktionell Spry1 im Kontext von CE Bewegungen und bei der Gewebstrennung. Spry1 inhibiert die Membranrekrutierung der PCP Komponenten Protein Kinase delta (PKCdelta) und Dishevelled (dsh). Koexpression von xPAPC kann die durch Spry 1 inhibierte Membranlokalisierung von PKCdelta und dsh retten. Die Interaktion von xPAPC und Spry1 ist für die Fähigkeit von xPAPC Spry1 zu antagonisieren essentiell. XPAPC Protein in dem S741 und S955 Reste mutiert sind kann nicht mehr an Spry1 binden und es nicht mehr antagonisieren. Diese Arbeit zeigt klar, dass die Interaktion von xPAPC und Spry1 für die Modulation des PCP Signalwegs ist. xPAPC vermittelte Signale stimulieren CE Bewegungen und Gewebstrennung. Durch diese Ergebnisse ist es erstmals möglich eine Verbindung zwischen Protocadherinen und nicht-canonischen Wnt-Signalwegen in Wirbeltieren herzustellen. Diese Arbeit zeigt auch, dass xPAPC den Wnt/β-Catenin Signalweg modulieren kann. CK2 stimuliert den Wnt/β-Catenin Signalweg durch die Stabilisierung von β-Catenin. xPAPC antagonisiert CK2βim *Xenopus* Achseninduktionstest und hemmt die Expression von des Wnt Ziegens xnr-3 in animalen Kappen Explantaten. Zusammenfassend kann xPAPC als „Schalter“zwischen canonischem und nicht-canonischem Wnt Signalweg angesehen werden. Durch die Bindung von Spry und CK2β kann xPAPC nicht-canonische Wnt Signale verstärken und so die Gastrulationsbewegungen modulieren. Gleichzeitig wird der canonische Wnt-Signalweg gehemmt, was einen Einfluss auf die Spezifizierung des Mesoderms hat.

2. INTRODUCTION

"It is not birth, marriage, or death, but **gastrulation**, which is truly the most important time in your life." Lewis Wolpert (1986)

Vertebrate embryogenesis is a fundamental process in which various aspects of cellular activities including proliferation, division, cell fate determination, apoptosis, movement and cell communication are delicately orchestrated. After induction of the germ layers, the blastula is transformed by gastrulation movements into a multilayered embryo with head, trunk and tail rudiments. Gastrulation is heralded by the formation of a blastopore, an opening in the blastula. The axial side of the blastopore is marked by the organizer, a signaling center that patterns the germ layers and regulates gastrulation movements. During internalization, endoderm and mesoderm cells move via the blastopore beneath the ectoderm. Epiboly movements expand and thin the nascent germ layers. Convergence movements narrow the germ layers from lateral to medial while extension movements elongate them from head to tail. Despite different morphology, parallels emerge with respect to the cellular and molecular mechanisms of gastrulation in different vertebrate species. Patterns of gastrulation cell movements relative to the blastopore and the organizer are similar from fish to mammals, and gastrulation movements are mediated by conserved molecular pathways (Solnica-Krezel 2005).

Gastrulation is the most crucial step in early vertebrate development. Haeckel coined the term gastrulation, derived from the Greek word "*gaste*" (meaning stomach or gut), to describe a set of morphogenetic processes that transform the rather unstructured early embryo into a gastrula with several significant characteristics:

1. The three primary germ layers including ectoderm, endoderm and mesoderm are established.
2. The basic body plan is established, including the physical construction of the rudimentary primary body axes.
3. The cells are brought into new positions, allowing them to interact with cells that were initially not close to them. This paves the way for inductive interactions, which are the hallmark of neurulation and organogenesis.

Therefore, to elucidate the mechanisms that control the complex cell movement and inductive processes during gastrulation remains a great challenge for development biologists over a century.

Fortunately the African frog *Xenopus laevis* has been a powerful model system for development biology since its embryos are large, can be obtained in large numbers and can be maintained easily and inexpensively in the laboratory. They are relatively easy to manipulate with microsurgical instruments, and they heal readily after surgery. Furthermore, the external surface of embryos is freely observable upon removal of the protective jelly coating, leading to the possibility to map early cell cleavage patterns, tissue fates, and gene expression patterns. This has allowed the generation of many highly informative embryo manipulation techniques as well as the ability to target treatments to specific tissues and examine gene expression patterns in specific tissues. As a result, great understanding of early development processes especially gastrulation movements has been achieved thanks to research based on *Xenopus* embryos.

2.1 Morphogenetic movements in gastrulation

During gastrulation, cell movements result in a massive reorganization of the embryo from a simple spherical ball of cells, the blastula, into a multi-layered organism and many of the cells at or near the surface of the embryo move to a new, more interior location.

The **primary germ layers** (endoderm, mesoderm, and ectoderm) are formed and organized in their proper locations during gastrulation. **Endoderm**, the most internal germ layer, forms the lining of the gut and other internal organs. **Ectoderm**, the most exterior germ layer, forms skin, brain, the nervous system, and other external tissues. **Mesoderm**, the middle germ layer, forms muscle, the skeletal system, and the circulatory system.

Although the details of gastrulation differ in various species of animals, the cellular mechanisms involved in gastrulation are common to all animals. Embryos use a limited stock of cell behaviors, but they use them in different combinations, in different geometric and mechanical contexts, and with different timings (Keller *et al.* 2003). It is important to note that a series of changes in cell motility, cell shape and cell adhesion occur during gastrulation. The major types of cell movements that take place during gastrulation are listed below (Fig. 1):

Invagination: a sheet of cells (called an epithelial sheet) bends inward.
Ingression: individual cells leave an epithelial sheet and become freely migrating mesenchyme cells.
Involution: an epithelial sheet rolls inward to form an underlying layer.
Epiboly: a sheet of cells spreads by thinning.
Intercalation: rows of cells move between one another, creating an array of cells that is longer (in one or more dimensions) but thinner.
Convergent extension (CE): rows of cells intercalate, but the intercalation is highly directional.

Tissue separation: mesendodermal and ectodermal cells are prevented from mixing. Brachet's cleft is formed between the neuroectoderm and the mesendoderm.

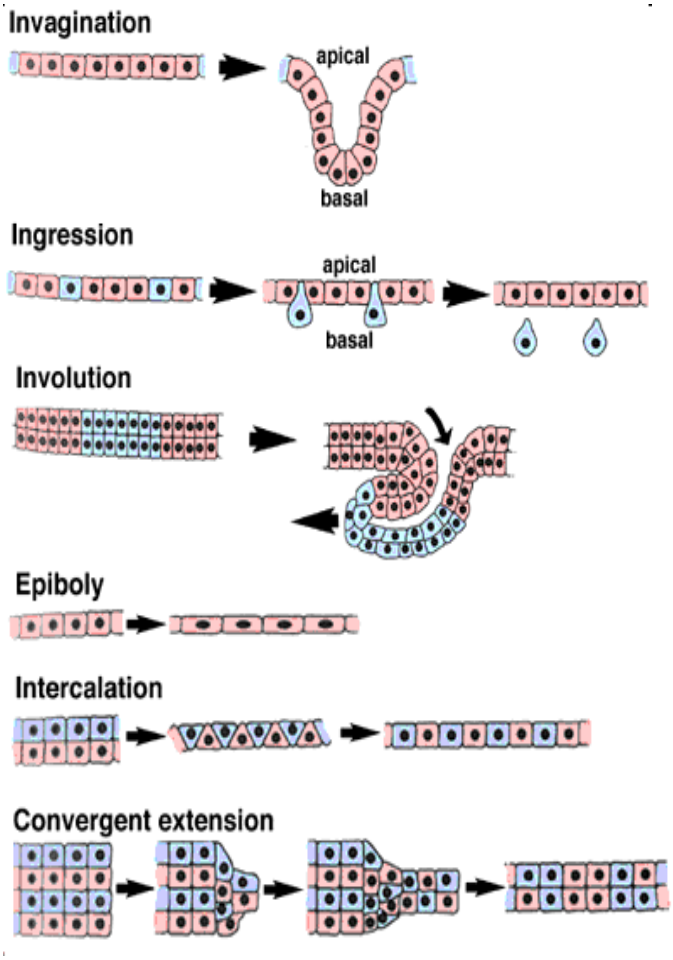

Figure 1. Major types of cell movements occur during gastrulation (modified from http://worms.zoology.wisc.edu/frogs/**).**

Since mechanisms of CE movements and tissue separation will be addressed in my research, a detailed description of these two gastrulation morphogenesis is given below.

2.1.1 CE movements

CE movements are considered as the main driving force of *Xenopus* gastrulation (Kuhl *et al.* 2001). These movements narrow (converge) the mediolateral aspect and elongate (extend) the anterior-posterior aspect of the embryo, thus contributing to the establishment of morphological and functional polarity, with the head on one end and the tail on the other (Keller 2002). In fact, CE movements elongate the body axis from its initial "egg shape" in all chordate species examined so far, as shown in Fig. 2a. Furthermore, CE movements are driven by internal forces, independent of other tissues, and independent of external substrates according to the fact that presumptive notochordal, somitic, and neural tissues that converge and extend in the embryo also do so when explanted in a culture dish as shown in Fig. 2b (Keller 2002).

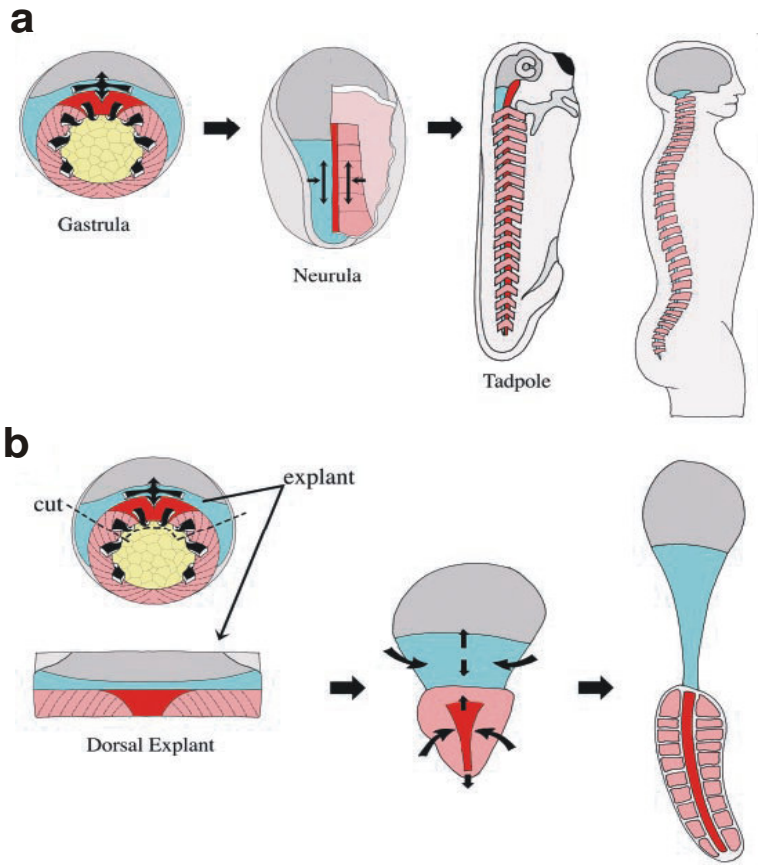

Figure 2. CE movements elongate the anterior-posterior axis of the vertebrate body plan. a. The notochordal (red) and somitic (pink) tissues turn inside and converge (narrow) and extend (lengthens) in the gastrula and neurula stages of the frog embryo. The overlying presumptive hindbrain and spinal cord (blue) tissues converge and extend coordinately but on the outside of the embryo. These movements push the head away from the tail and elongate the body axis of the tadpole. **b.** Cultured explants of the same tissues also converge and extend, showing that CE movements are driven by internal forces (Keller 2002).

Cell tracing and time-lapse recording of live cells show that CE movements involve two types of cell intercalation. First, several layers of deep cells intercalate along the radius of the embryo (**radial intercalation**) to produce fewer layers (thinning) of greater length (extension) (Fig. 3a). Then the deep cells intercalate mediolaterally (**mediolateral intercalation**) to produce a narrower (convergence), longer (extension) array (Fig. 3b). Radial intercalation predominates in the first half of gastrulation (Fig. 3a) and mediolateral intercalation predominates in the second half of gastrulation and through neurulation (Fig. 3b) in both the dorsal mesodermal tissue and the prospective posterior neural tissue (spinal cord and hindbrain).

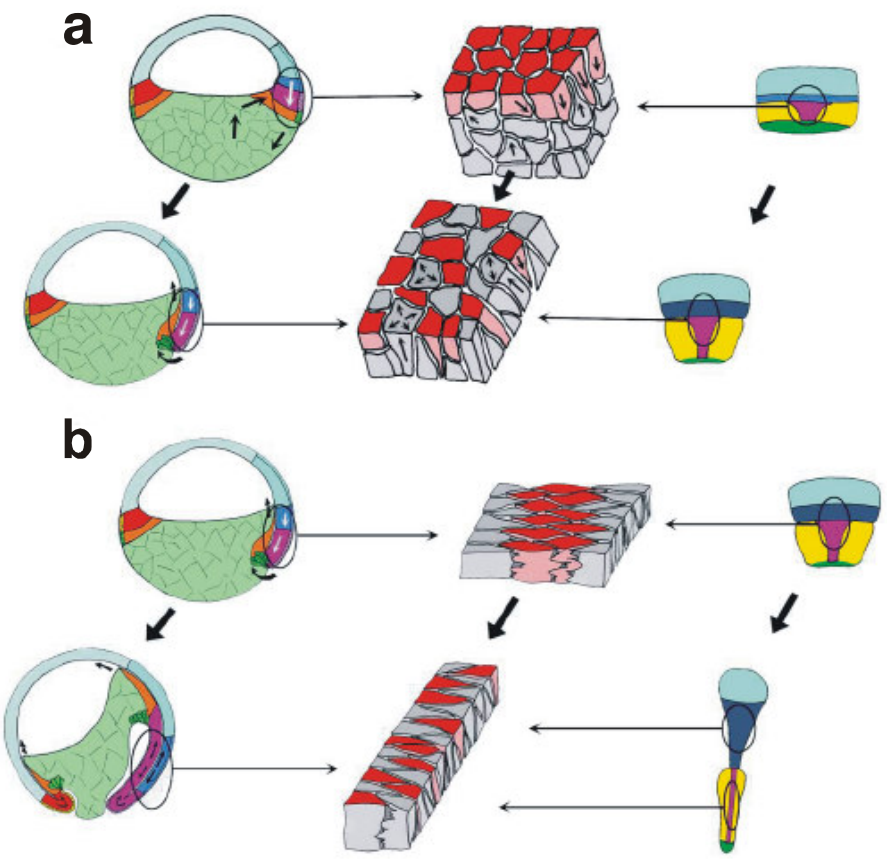

Figure 3. Cell intercalation in CE movements. Early in gastrulation, the dorsal deep mesoderm and posterior neural tissue undergoes a thinning and extension (white arrows, **a.** left panel) that is driven by radial intercalation of multiple layers of deep cells to form fewer layers of greater area (**a.** center panel). From the midgastrula stage onward, these same tissues undergo convergence and extension (black arrows, **b.** bottom left panel), which is driven by mediolateral cell intercalation (**b.** middle panel **a.** left panel). These movements of thinning and extension and convergence and extension also occur independent of other tissues in explants (**a, b** right panel) (Keller *et al.* 2003).

2.1.2 Tissue seperation

The formation of tissue boundaries in the embryo is essential for the establishment of the body plan and the formation of the organs. Tissues have to develop separation behaviors to prevent cell from mixing and define borders between different groups of cells. Therefore the term "**tissue separation**" was introduced to define "a strong form of cell sorting, where not only mixing of two cell populations is prevented, but a visible cleft between tissues is established, perhaps to allow or shear movement between tissues" (Ibrahim and Winklbauer 2001).

In the amphibian blastula, a thin blastocoel roof (BCR) is formed as a wall enclosing the blastocoel cavity and most of the BCR will form ectoderm in later stages. During the gastrulation, mesendodermal cells move as a coherent mass toward the animal pole and BCR serves as the substrate for their translocation. Although BCR and internalized mesendoderm are in direct contact during the process, they do not fuse into a single cell mass but maintain a stable interface as a prerequisite for the movement of the two tissues past each other (Wacker *et al.* 2000). In other words, they display tissue separation behaviors. As a result of the separation, a visible cleft called Brachet´s cleft is formed between the mesendoderm and the ectoderm (Fig. 1). The anterior part of Brachet´s cleft is generated by vegetal rotation in which the anterior endoderm moves actively toward BCR (Wacker *et al.* 2000). The posterior part of Brachet´s cleft develops when the mesoderm invaginates through the blastopore lip and the anteroposterior axis of the embryo forms. Therefore it is postulated that separation behavior is implemented in three steps, each controlled by different mechanisms as shown in Fig. 4 (Wacker *et al.* 2000).

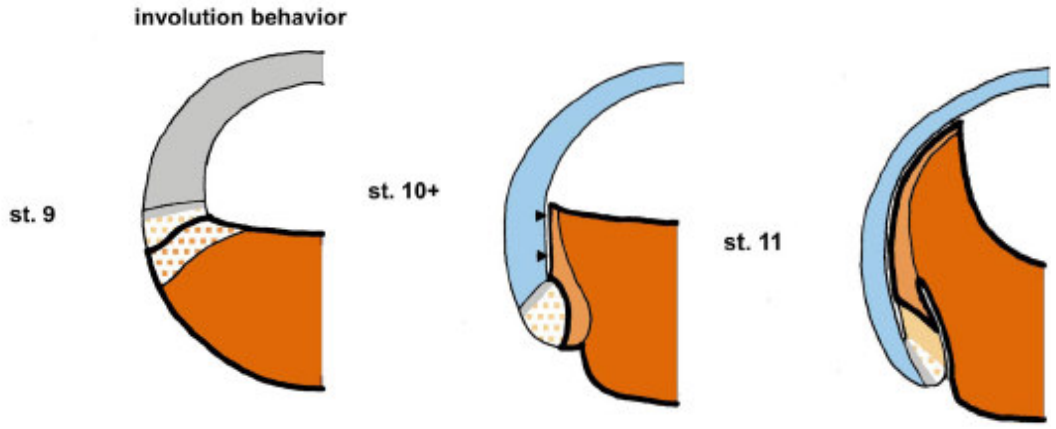

Figure 4. Tissue spearation behaviors in early amphibian embryo. Dorsal part of embryo at late blastula (st.9), early gastrula (st.10+), and midgastrula (st.11). Germ layers are outlined; the vegetal motility domain is indicated by a bold line. Regions of indiscriminate behavior are shown in gray, differential repulsion behavior in blue, separation behavior in orange, with lighter shading indicating later expression of behavior. Prospective regions of separation behavior are dotted in orange. Arrowheads indicate Brachet's cleft (Wacker *et al.* 2000).

Tissue separation behaviors in early embryo development show spatiotemporal variation, indicating that the Brachet´s cleft is not a uniform structure. The anterior portion of the cleft depends on the separation behaviors of the endoderm whereas the posterior portion is formed by the mesoderm via a different mechanism (Wacker *et al* 2000).

Tissue separation and the formation of tissue boundaries also occur in later stages of development. Multilayered structures with defined tissue boundaries will develop during the formation of various organs including heart. In contrast, one noteworthy demonstration of loss of boundaries and defects in separation behaviors is metastasis in which tumors cross boundaries and invade new tissues.

2.2 Molecular basis of gastrulation movements

A great knowledge of morphogenetic processes during gastrulation (as partially described in **2.1**) has been accumulated thanks to centuries of macroscopic analysis and the arrival of new imaging techniques. But to get an in-depth understanding we have to address the question: what are the molecular mechanisms underlying these morphogenetic movements? By use of powerful forward and reverse genetic approaches much progress has been made recently to identify and characterize pathways and molecules implicated in modulation of morphogenetic movements, especially in the context of CE movements. Two key concepts emerge when summarizing these new findings: (1) Molecules from a variety of categories contribute to the regulation of gastrulation movements in vertebrate. These include classic signaling pathways such as Wnt, BMP, Nodal and FGF; transcriptional factors like Brachyury and Snail; adhesion molecules like catenin, cadherin and protocadherin; extracellular matrix like fibronectin, cyr61 and syndecan; regulators of cytoskeleton like Rho, Rac, cdc42, JNK; axon guidance molecules like ephrin and slit; and even molecules involved in endocytosis including dynamin, Rab5 and μ2-adaptin. This fact may emphases the complexity of gastrulation movements and indicates that different molecules have to be engaged to make sure that these movements go through perfectly.
(2) Despite the difference in morphology, different vertebrate species employ similar molecules and signaling pathways in gastrulation movements, thus showing the conserved aspect of vertebrate gastrulation movements. Below are described some pathways and molecules involved in gastrulation movements, with emphasis on CE movements and tissue separation.

2.2.1 Wnt signaling pathway

The name Wnt was derived from *Wg* (*wingless*) and *Int* (Rijsewijk *et al.* 1987). The *wingless*

gene had originally been identified as a segment polarity gene in *Drosophila melanogaster* that functions during embryogenesis while the Int genes were originally identified as vertebrate genes near several integration sites of mouse mammary tumor virus (MMTV). Surprisingly, the *Int-1* gene and the *wingless* gene were found to be homologous, and the ensuing effort to understand how similar genes produce different effects has revealed that Wnts are a major class of secreted glycoproteins with diverse functions in pattern establishment.

Wnt signaling pathway is highly conserved in complex eukaryotes ranging from worm to human. It is essential for development by regulating a variety of processes such as cell proliferation, cell differentiation, cell polarity and cell migration. Additionally, deregulation of the Wnt signaling has been implicated in a broad range of pathological processes including degenerative diseases and cancer (Logan and Nusse 2004). Despite the complexity of this pathway, a combination of developmental, genetic, and biochemical analyses have greatly enriched our understanding of Wnt pathway and the list of Wnt signaling components has exploded. It is evident that multiple extracellular, cytoplasmic, and nuclear regulators intricately modulate Wnt signaling and a preliminary sketch of Wnt signaling emergs as describe below (Fig. 5).

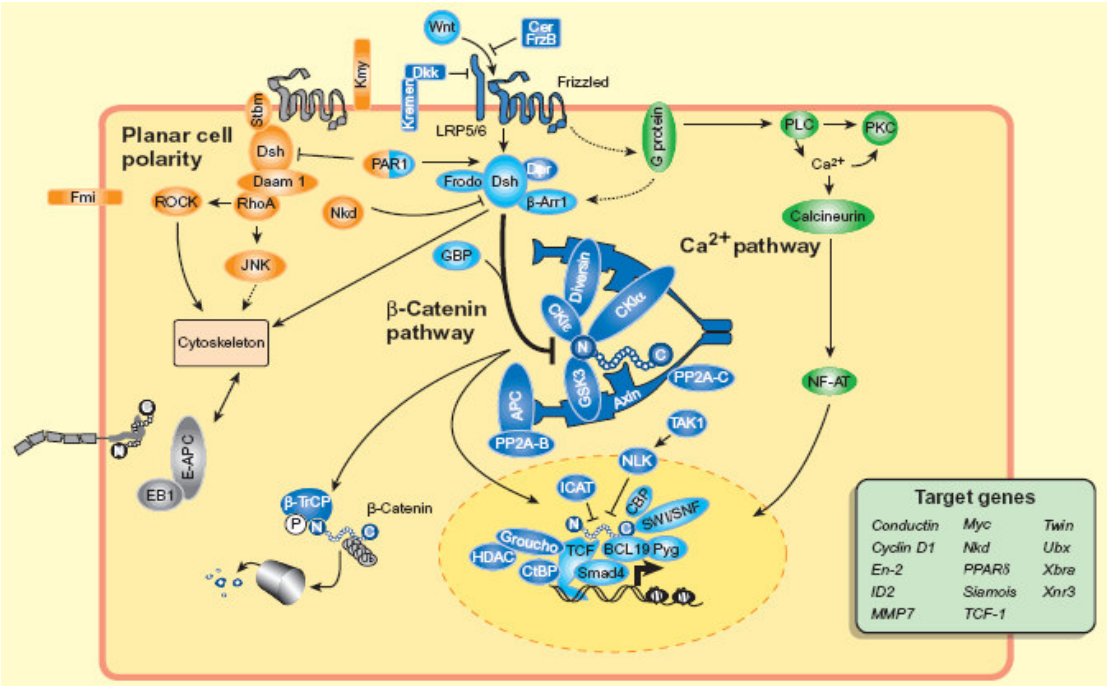

Figure 5. Distinct downstream signaling pathways mediated by Wnt. Depending on the available receptors and intracellular effectors, different cells respond to various Wnt ligands to execute different branches of Wnt signaling pathways. In the middle panel is shown canonical Wnt/β-Catenin pathway, while in the left and right panel are shown non-canonical Wnt pathway, i.e. Planar cell polarity pathway and Wnt/Ca^{2+} pathway, respectively (Huelsken and Behrens 2002).

2.2.1.1 Canonical Wnt/β-catenin pathway

In this pathway, Wnt binds to seven-transmembrane receptor Frizzled (Fz), which may be coupled to heterotrimeric G proteins. Members of the low-density lipoprotein receptor-related protein (LRP) family LRP5/6 act as co-receptors of Wnt ligands. Various secreted factors such as cerberus and FrzB bind toWnt and block the interaction with Fz. Dickkopf antagonises Wnt action by blocking access to the LRP co-receptor and induction of LRP endocytosis in cooperation with kremen. Intracellularly, Wnt signaling leads to stabilization of cytosolic β-catenin. In the absence of Wnt, β-catenin is phosphorylated by casein kinase I at Ser45; this in turn enables glycogen synthase kinase (GSK) 3β to phosphorylate serine/threonine residues 41, 37 and 33. Phosphorylation of these residues triggers ubiquitylation of β-catenin by bTrCP and degradation in proteasomes. Phosphorylation of β-catenin occurs in a multiprotein complex containing the scaffold protein axin, the tumor suppressor gene APC and diversin. In the presence of Wnt, dishevelled (Dsh) blocks β-Catenin degradation by recruiting GBP/Frat-1, which displaces GSK3β from axin. Dsh activity is modulated by the kinase PAR1, which potentiates Wnt activation of β-catenin pathway but blocks the JNK pathway. Other Dsh-interacting molecules include frodo and β-arrestin 1, which synergize with Dsh.

Stabilized β-catenin enters the cell nucleus and associates with LEF/TCF transcription factors, which leads to the transcription of Wnt-target genes (Fig. 5). Transcriptional activation is mediated by the interaction of β-catenin with the histone acetyl transferase CBP, the chromatinremodeling SWI/SNF complex and Bcl9 bound to pygopus (Pyg). Interaction of TCF with Smad4 might lead to crosstalk of Wnt and BMP signaling. When β-catenin is absent, certain TCFs repress transcription by interacting with the corepressors CtBP and groucho bound to histone deacetylase (HDAC). Phosphorylation of TCFs by Nemo-like kinase (NLK), a target of TAK1 (a MAP kinase kinase kinase), as well as interaction of β-catenin with ICAT negatively regulates Wnt signaling (Huelsken and Behrens 2002).

2.2.1.2 Planar cell polarity pathway

Planar cell polarity (PCP) signaling is extensively studied with *Drosophila* as a model system due to the fact that PCP occurs visibly in several external structures including the precisely aligned hairs on wing cells, the perfectly arranged ommatidia in the facet eye and the bristles on the thorax. In fact the term "**planar cell polarity**" is derived from study on these epithelial cells to define the tissue polarity shown by these epithelia to become polarized within the plane of the epithelium, along an axis perpendicular to the apical-basal axis of the cell (Nubler-Jung 1987).

PCP pathway is composed of several core proteins that induce intracellular cytoskeletal rearrangements in response to extracellular polarity cues. Fz mediates the polarity cue in both *Drosophila* and vertebrates. While PCP signaling in Drosophila is independent of *Wg* (Lawrence *et al.* 2002) and it is still under debate whether Fz ligand really exists or not, in vertebrates in some circumstance PCP is mediated by noncanonnical Wnts like Wnt5a and Wnt11, i.e. Wnts that do not signal by means of β-catenin (Moon *et al.* 1993; Heisenberg *et al.* 2000). Whatever the mechanism, upon activation, Fz signals to the core PCP effectors Dsh, the atypical cadherin Flamingo (Fmi), the transmembrane PDZ-containing protein Strabismus (Stbm). In vertebrates downstream effect of Wnt/Fz signaling is mediated by Daam1 (Disheveled-associated activator of morphogenesis) (Habas *et al.* 2001). Daam1 contains forming homology domains that mediate protein-protein interaction. Daam1 binds Dsh by its carboxyl terminus and Rho by its amino terminus, thus acting as a scaffold to assemble proteins complex of Dsh, Rho, Rho-associated kinase (ROCK) and JNK, which then regulate the cytoskeleton, cell polarity, etc.

2.2.1.3 Wnt/Ca^{2+} pathway

While PCP signaling is largely characterized in *Drosophila*, Wnt/Ca^{2+} signaling was first postulated based on research data on *Xenopus* and zebrafish (Kuhl *et al.* 2000). In this pathway, Fz is persumed to behave like G-protein-coupled receptors (GPCRs) due to the existence of seven transmemrbane domains and a heptihelical structures conserved among all memebers of the superfamily of GPCRs (Wang and Malbon 2003). Upon binding to ligands such as Wnt5a, Fz is activated, leading to activation of heterotrimetric G proteins. Then the Gβγ subunits activate phospholipase C (PLC), which hydrolyzes phosphatidylinositol 4,5-bisphosphate to inositol 1,4,5-trisphosphate (IP3) and diacylglycerol (DAG). IP3 catalyzes intracellular Ca^{2+} release, resulting in activation of Ca^{2+}-calmodulin–sensitive CamKII and Ca^{2+}-sensitive protein phosphatase calcineurin (Calcn). Calcn can dephosphorylate transcriptional facotr NF-AT and contribute to its nuclear accumulation to regulate gene expression. On the other hand, DAG can activate PKC directly (Fig 5). A range of biochemical evidence supports this model: (1) Wnts show chemical similarity to other secreted glycoprotein ligands like gonadotropins that act through GPCRs; (2) Ca^{2+} release mediated by Wnts is inhibited by pertussis toxin or by depletion of specific G protein subunits; (3) Functional chimeras of Frizzleds can be made with ectodomains and transmembrane domains of other GPCRs; (4) Wnt signaling is sensitive to inhibitors of enzymes integral to GPCR signaling (Wang and Malbon, 2003).

2.2.1.4 Regulation of gastrulation by Wnt signaling

All three branches of Wnt signaling can regulate different aspects of gastrulation. Here I just focus on the regulation of CE movements and tissue separation by non-canonical Wnt signaling.

The first hint that Wnt signaling is involved in CE movements came from the observation that overexpression of Xwnt5 blocks CE movements (Moon *et al.*, 1993). Subsequently it was showed that Xdd1, a dominant-negative (DN) form of Dsh, blocked CE movements (Sokol 1996), but it was not yet clear whether canonical Wnt or non-canonical Wnt pathway is responsible. Detailed analysis of Dsh deletion constructs showed the differential requirements for Dsh domains in canonical Wnt and PCP pathway (Axelrod *et al.* 1998). Furthermore, DN Wnt11 blocks CE movements in *Xenopus* and this can be rescued by either full-length Dsh or delected form of Dsh that functions in PCP but not canonical Wnt pathway, but not rescued by components of canonical Wnt signaling like β-catenin (Tada and Smith 2000). Similarly, *slb/Wnt11* mutant zebrafish displayed CE defect selectively rescued by Dsh constructs that activate PCP signaling, but not by activation of canonical Wnt signaling (Heisenberg *et al.* 2000). Later it was shown that vertebrate homologs of Drosophila PCP gene Stbm/Vang play important role in CE movements. Both gain-of-function and loss-of-function studies reveal a role for Stbm in mediating CE movements during gastrulation in *Xenopus* and zebrafish (Park and Moon 2002). Based on all these data, it is generally accepted that PCP pathway regulates CE movements in vertebrates.

Although no genetic evidence exists yet to demonstrate the engagement of Wnt/Ca^{2+} pathway in regulation of CE movements in zebrafish, it was shown that XCdc42 (*Xenopus* Cdc42) acts downstream of the Wnt/Ca^{2+} signaling pathway involving PKC activation to regulate CE movements in *Xenopus* and importantly XCdc42 does not seem to act downstream or upstream of Dsh (Choi and Han 2002), strongly indicating that this pathway is different from PCP pathway which involves Dsh. Furthermore, Gβγ was shown to signal downstream of Wnt-11/xFz7 and upstream of PKC to regulate Cdc42 activity and play a role in CE movements in *Xenopus* (Penzo-Mendez *et al.* 2003). All together these two studies provide strong evidence that Wnt/Ca^{2+} pathway regulates CE movements in *Xenopus*.

Wnt/Ca^{2+} signaling is also implicated in the regulation of tissue separation (Winklbauer *et al.* 2001). Loss of Fz7 function by morpholino (MO) led to a defective separation of mesodermal and ectodermal germ layers and this defect could be rescued by PKC but not by Dsh, Cdc42, β-catenin or Tcf3. Furthermore, tissue separation behavior was blocked by heterotrimeric G protein

inhibitor pertussin toxin and could be rescued by PKC but not by Fz7 (Winklbauer *et al.* 2001). These results clearly showed that Fz7 mediates tissue separation via Wnt/Ca^{2+} branch distinct from Wnt/PCP or Wnt/β-catenin branch.

2.2.2 FGF signaling

FGF signaling plays important roles in embryogenesis. FGF receptors (FGFRs) are a subfamily of cell surface receptor tyrosine kinases (RTKs). Upon binding to FGF ligands, FGFRs undergo dimerization, which activates tyrosine kinase activity. These kinases autophosphorylate intracellular domains and initiate downstream signaling. At least three signaling pathways are transducted downstream of FGFRs, the main signal involves the activation of the Ras G protein and the MAP kinase cascade. In addition, the activated receptor stimulates PLC to split PIP_2 into IP_3 and DAG. A third signal involves the activation of phosphatidylinositol-3 kinase (PI3 kinase) and Akt kinase (Fig. 6). By these signaling branches, FGFs regulate mesoderm formation and gastrulation, neural induction and anteroposterior patterning and endoderm formation in early vertebrate development (Bottcher and Niehrs 2005). Here I just focus on gastrulation movements regulated by FGF signaling in *Xenopus*.

In *Xenopus* embryos, FGF signaling impacts CE movements both directly and indirectly. In a direct manner, FGF signaling may crosstalk with PCP pathway to regulate CE movements. FGF signaling activates PLCγ, with the production of IP3 and DAG. DAG leads to recruitment of PKCδ to membrane, where it activates Dsh and regulates CE movements by PCP pathway (Kinoshita *et al.* 2003). Sproutys are induced by FGF signaling early in gastrulation and inhibit both calcium release and PKCδ translocation, therefore blocking FGF-mediated CE movements but permitting FGF-mediated cell specification (Fig.7 left). However, in late gastrulation and neurulation stages the expression of Sproutys declines and that of Spred (Sprouty-related proteins) increases dramatically, blocking cell specification while permitting mesodermal CE movements induced by FGF (Fig.7 right). In this way, FGF signaling fine-tunes both cell fate and cell motility in the same cell (Sivak *et al.* 2005).

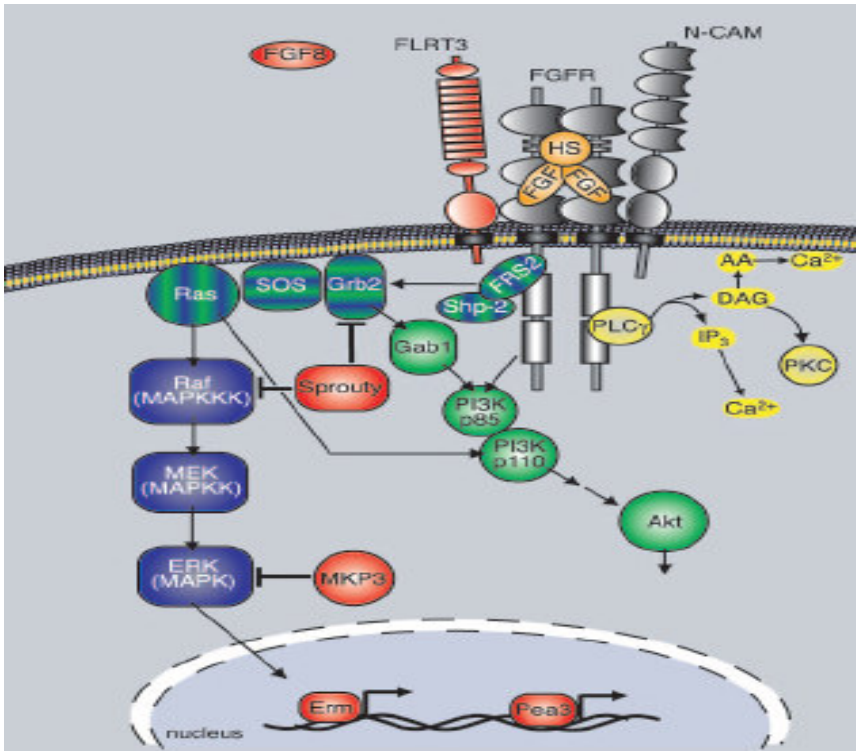

Figure 6. FGF signaling. Upon binding to FGF ligands, FGFRs trigger intrinsic tyrosine kinase activity and activate downstream signaling via Pas/MAP kinase branch (shown in blue), PI3 kinase/Akt branch (shown in green) and PLC/Ca^{2+} branch (shown in yellow). Components involved in both branches are striped and members of FGF synexpression group are shown in red. Sprouty is induced by FGF and acts at different levels to block FGF signaling, forming a negative feedback loop (Bottcher and Niehrs 2005).

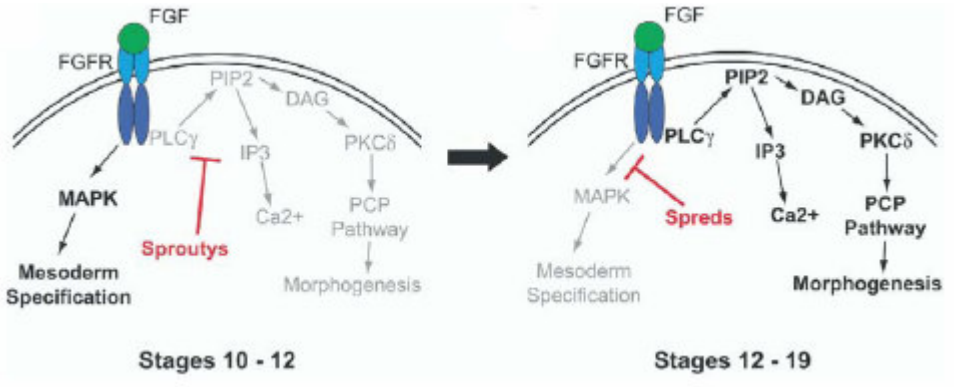

Figure 7. Interpretation of FGF signaling by Sprouty and Spred to fine-tune mesoderm morphogenesis and specification in *Xenopus*. Left: Sproutys are expressed early to block PLCγ/Ca^{2+} pathway that regulates morphogenesis downstream of FGFR, while MAPK pathway that controls mesoderm specification is not affected. Right: With the completion of mesoderm specification, expression of Spreds increases to inhibit mesoderm specification induced by MAPK pathway, while expression of Sproutys diminishes to permit PCP pathway to drive morphogenesis (modified from Sivak *et al*., 2005).

In an indirect manner, FGF signaling regulates the induction and maintenance of Xbra, which functions as a switch to promote CE movements and inhibit cell migration (Kwan and Kirschner 2003). Furthermore, Xbra as a transcription factor directly induces Xwnt11 (Tada and Smith, 2000) and prickle (Takeuchi *et al.* 2003), both of which regulate CE movements by PCP pathway as described in **2.2.1.4**. Xmc (*Xenopus* marginal coil), another gene induced by FGF signaling, regulates CE movements while has no impact on mesoderm induction or maintenance per se (Frazzetto *et al.* 2002). FGF target gene neurotrophin receptor homolog (NRH) regulates the protrusive activity necessary for CE movements (Chung *et al.* 2005). NRH activates GTPases including Rho, Rac and Cdc42 as well as the cascade of MKK7-JNK independently of Dsh, suggesting that NRH signaling interacts with PCP pathway downstream of Dsh (Sasai *et al.* 2004).

2.2.3 BMP and Nodal signaling

A ventral to dorsal gradient of BMP activity is established under control of Spemann organizer and this gradient coordinates cell fate determination with morphogenetic movements during early embryogenesis (Myers *et al.* 2002b). In *Xenopus*, high BMP activity blocks extension of dorsal mesodermal explants, whereas DN BMP receptor instigates ectopic CE movements of ventral mesoderm explants (Graff *et al.* 1994). In zebrafish, the BMP activity gradient has been shown to play an instructive role in determining domains of distinct CE movements, possibly in parallel with, rather than downstream of cell-fate specification (Myers *et al.* 2002a). High ventral BMP activity levels inhibit CE movements and specify the NCEZ (No convergence no extension zone); decreasing BMP activity levels in the lateral gastrula increase CE movements; dorsally, low BMP activity promotes substantial extension with limited convergence. The three morphogenetic domains are reduced or expanded in mutants with excess or deficit of BMP activity, supporting the roles of BMP in regulation of CE movements (Myers *et al.* 2002b). Mechanistically, different BMP activity thresholds might regulate genes that mediate cell movement behavior and fate specification. For example, high BMP activity negatively regulates the expression of Wnt11 and Wnt5a, therefore limiting CE movements (Myers *et al.* 2002b).

The nodal class of TGFβ proteins plays critical roles in early vertebrate development, essential for the establishment of mesodermal and endodermal lineages and cell movements involved in gastrulation. Xnr3 is a special nodal-related protein in *Xenopus* in that it is structurally different from other Xnrs, and, uniquely among them, induces cellular finger-like protrusions when ectopically expressed. This led to the investigation of its role in CE movements during embryogenesis. Loss of Xnr3 function by MO led to CE defects in embryos and explants.

Moreover, Xnr3 requires the FGF receptor FGFR1 to activate Xbra xpression and induce CE movements (Yokota *et al.* 2003). So this finding demonstrates the crosstalk of Nodal signaling and FGF signaling in morphogenesis.

2.2.4 Endocytosis

Signaling and endocytosis are inseparable companion. On one hand, endocytosis downregulates signaling initiated on the membrane. On the other hand, recently endocytosis has been shown to play more important and active roles in signal transduction, especially in aspect of regulating the activity and distribution of developmental signals. For example, endocytosis of Delta, the Notch ligand, is required for signal activation. In Hedgehog signaling, endocytic trafficking segregates an inhibitory receptor (Patched) from the positive effector (Smoothened). Endocytosis also powers the transport of morphogens along epithelia (Piddini and Vincent 2003). Unfortunately, how endocytosis is engaged in morphogenetic movements is seldom addressed although a variety of signals have impact on gastrulation morphogenesis as described in **2.2.1-2.2.3**. Nevertheless, it is encouraging that a recent report demonstrated that Fz endocytosis plays active roles in PCP signaling to regulate CE movements (Yu *et al.* 2007). In this case, Dsh was found to interact with μ2-adaptin, a subunit of the clathrin adaptor AP-2; this interaction is required to engage activated Fz4 with the endocytic machinery and for its internalization. Functionally, Dsh mutants unable to bind AP-2 had no effect on canonical Wnt/β-catenin pathway since they could induce dorsal axis duplication and activate TOPFlash reporter to a similar extent to wild-type (wt) Dsh. However, these mutants failed to inhibit CE movements or activate JNK while wt Dsh could (Yu *et al.* 2007). Thus gastrulation movements are regulated by Fz endocytosis via the engagement of Dsh with AP-2. In this line it was observed earlier that DN dynamin, a GTPase essential for clathrin-mediated endocytosis, significantly blocked the elongation of animal cap explants induced by activin, accompanied by inhibition of C-cadherin endocytosis. The authors proposed that dynamin-dependent endocytosis of C-cadherin is crucial in remodelling adhesive contacts during CE movements (Jarrett *et al.* 2002). But taking into account of the new results, we can assume that the effect of dynamin on CE movements is mediated not only by C-cadherin endocytosis, but also by endocytosis of other molecules like Fz. In another interesting study, Wnt11 was shown to regulate the cohesion and migration of mesendodermal progenitor cells during zebrafish gastrulation by modulating endocytosis of E-cadherin through Rab5c, another GTPase engaged in early endocytosis (Ulrich *et al.* 2005). It is expected that more detailed mechanisms by which endocytosis controls gastrulation morphogenesis will be revealed in the near future.

2.2.5 Cytosketon remodeling

Cytoskeleton contains three kinds of cytoplasmic filaments: microtubules, actin filaments and intermediate filaments, forming a complex and dynamic network that play critical roles in the establishment and maintenance of cell and embryonic polarity, cell shape, cell adhesion and cell motility. Rho family of GTPases including Rho, Rac and Cdc42 are good candidates to be mediators of morphogenetic events in gastrulation due to their ability to regulate cytoskeleton remodeling underling cell motility and shape changes. Rho mediates formation of stress fibers, contractile microfilaments bundles spanning the cell, and focal adhesions, the attachments of stress fibers to the substrate. Rac mediates formation of lamellipodia, flattened protrusions important in cell motility. Cdc42 mediates cell polarity and formation of filipodia, thin protrusions that mediate cell motility and contact interactions (Nobes and Hall 1999). In *Xenopus* embryos, Rho GTPases are expressed in tissues undergoing extensive morphogenesis and are activated downstream of non-canonical Wnt signaling during gastrulation as described in **2.2.1**. The picture of how Wnts mediate cytoskelecton remodeling to control gastrulation movements emerges with the identification of an increasing number of effectors that link Rho GTPases with cytoskelecton (Fig. 8).

WGEF, a guanine nucleotide exchange factor (GEF), was identified to form complex with Dsh and Daam1 and activate RhoA specially. WGEF can rescue CE movements impaired by DN Wnt11, providing the missing link between Dsh/Daam1 and Rho activation in PCP signaling (Tanegashima K *et al.* 2006). xNET1, another RhoA specific GEF, was found to impair CE movements when overexpressed. Although xNET1 co-immunoprecipitated with Dsh, its localization in animal caps was not changed upon the activation of PCP signaling (Miyakoshi *et al.* 2004). Thus upstream events other than Wnts may regulate the activity of xNET1 to activate RhoA. Eps8 acts as a scaffold to promote the formation of complexes including Abi1 that are essential for Rac activation and Rac-dependent actin remodeling and membrane ruffling (Scita *et al.* 1999). Interestingly, Eps8 was shown to recruit Dsh to actin filaments and cell membrane in *Xenopus* and impair CE movements (Roffers-Agarwal *et al.* 2005). Dsh can activate both RhoA and Rac and Daam1 is required for Dsh-mediated RhoA but not Rac activation (Habas *et al.* 2001). Therefore Eps8 may provide a crucial link between Dsh, Rac and the actin cytoskeleton during gastrulation. That Rho and Rac are activated via different branch downstream of Dsh is in accordance with the distinct and overlapping roles that Rho and Rac play in cytoskeleton remodeling necessary for CE movements. Rac is important for filopodia formation along the elongate sides of intercalating mesoderm cells while Rho regulates their bipolar morphology.

Both Rac and Rho contribute to the mediolateral extension of tractive lammelipodia (Tahinci and Symes 2003). Cdc42 is not activated by PCP pathway (Habas *et al.* 2003), but by Wnt/Ca^{2+} pathway and functions in gastrulation by regulating Ca^{2+}-mediated cell adhesion (Winklbauer *et al.* 2001; Choi and Han 2002). XCEP2 (*Xenopus* Cdc42 effector protein 2) and X-PAK5 (*Xenopus* p21-activated kinase 5) were identified to act downstream of Cdc42 to modulate Ca^{2+}-mediated cell-cell adhesion, therefore balancing the need for tissue integrity and plasticity during the dynamic cellular rearrangements of gastrulation (Nelson and Nelson 2004; Faure *et al.* 2005). Recently, Profilin1 was found as an interacting partner of Daam1 and localized with Daam1 to actin stress fibers in response to Wnt signaling. Inhibition or depletion of Profilin1 inhibited stress fiber formation and specifically inhibited blastopore closure but not CE movements, tissue separation or neural fold closure in *Xenopus* (Sato *et al.* 2006). Taken together, it seems that different effectors downstream of Wnts mediate different aspects of cytoskeleton reorganization both independently and cooperationally and contribute to the coordination of gastrulation movements (Fig. 8).

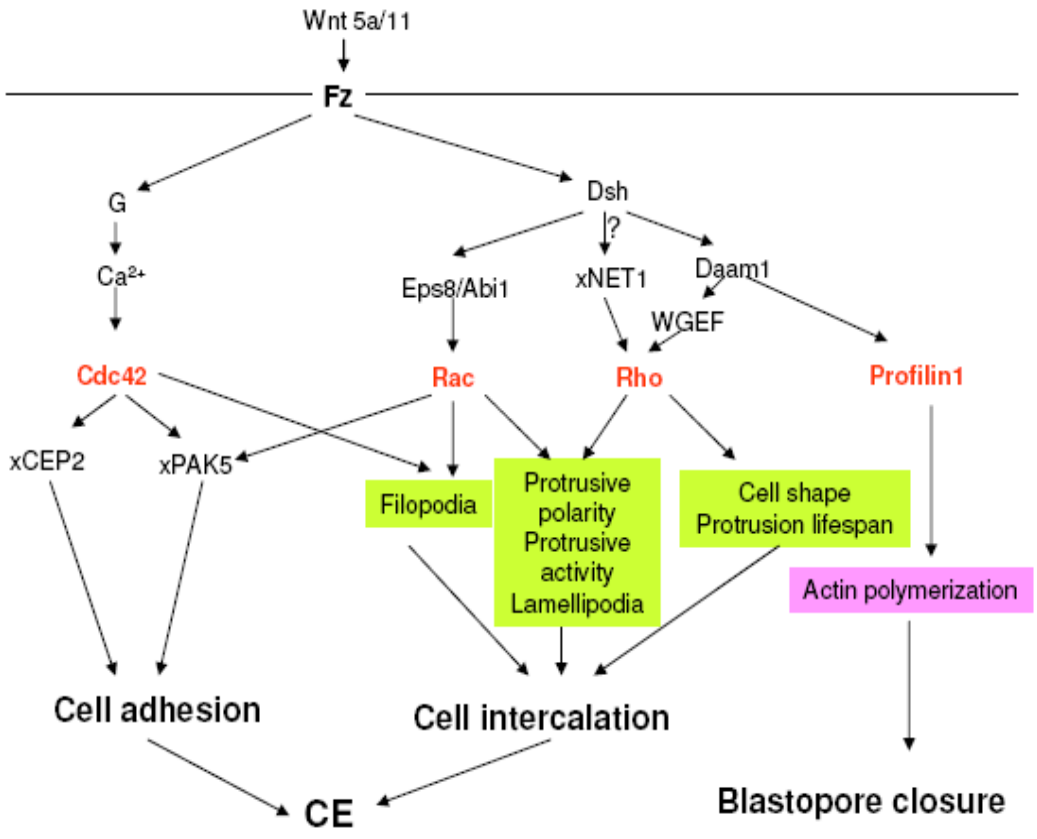

Figure 8. Cytoskelecton remodeling mediated by Wnts and their effectors during gastrulation movements in *Xenopus*. See text for details.

2.2.6 Extracelluar matrix

Extracelluar matrix (ECM) consists of collagen, proteoglycans, and a variety of glycoproteins secreted by cells. Cell adhesion, cell migration and the formation of epithelial sheets and tubes all depend on the ability of cells to form attachments to ECM. In some cases, as in the formation of epithelia, these attachments have to be extremely strong. In other instances, as in the migration of cells, attachments have to be made, broken and made again. In some cases, ECM serves as a permissive substrate to which cells can adhere, or upon which they can migrate. In other instances, ECM provides the direction for cell movements or the signals for a development event. Therefore it is not surprising that ECM plays important roles in morphogenesis. Here only the impact of ECM on CE movements and tissue separation is summarized.

In *Xenopus* embryos, Integrin-ECM interaction modulates cadherin-mediated cell adhesion and is required for mediolateral cell intercalation behaviors that drive CE movements (Marsden and DeSimone 2003). It was demonstrated recently that ECM component fibronectin may play instructive role in the coordination of protrusive activity underlying CE movements (Davidson *et al.* 2006). Cyr61, a CCN-family, secreted, heparin-binding ECM-associated protein, is an important regulator of CE movements in *Xenopus* by both assembling ECM to regulate cell-cell and cell-matrix adhesion and modulating Wnt signaling (Latinkic *et al.* 2003).

Heparan sulphate proteoglycans (HSPG) are abundant molecules in ECM, consisted of a protein core to which heparan sulphate glycosaminoglycan (GAG) chains are attached. Glypicans and syndecans represent the two main cell-surface HSPGs. Glypicans are HSPGs that are linked to the cell membrane by a glycosylphosphatidylinositol (GPI) anchor while syndecans are type I transmembrane proteins with up to five GAG attachment sites. In mammals six glypican and four syndecan genes have been identified and they are of interest in the context of morphogen gradient formation (Hacker 2005). Glypican Knypek potentiates Wnt11/PCP signaling to regulate CE movements in zebrafish (Topczewski *et al.* 2001). *Xenopus* glypican 4 (Xgly4, *Xenopus* ortholog of *kny*) physically binds Wnt ligands and Fz7 and functions as a positive regulator (likely as a co-receptor) of PCP pathway to modulate CE movements (Ohkawara *et al.* 2003). Recently *Xenopus* syndecan-4 (xSyn4) was also shown to regulate CE movements specially with no impact on cell-fate determination. Mechanistically, xSyn4 interacts biochemically and functionally with Fz7 and Dsh to recruit Dsh to plasma membrane, resulting in the activation of PCP pathway. Importantly the recruitment of Dsh by xSyn4 is regulated by fibronectin (Munoz *et al.* 2006; Munoz and Larrain 2006). Therefore a model was proposed in which xSyn4 and fibronectin cooperate with

xFz7 and Wnt in the specific activation of PCP pathway (Munoz *et al.* 2006). In this aspect, xSyn4 also functions as a co-receptor for PCP signaling, similar to Xgly4 as described above.

2.2.7 Cell adhesion molecules

The formation, maintenance and turnover of adhesion between cells is crucially involved in all morphogenetic events. A myriad of cell adhesion molecules control these adhesive contacts between cells. Among them, cadherins are major players for dynamic regulation of adhesive contacts associated with diverse morphogenetic processes. Perhaps the large size and the structural and functional diversity of the cadherin family members have evolved to allow different cell interactions necessary for tissue morphogenesis in complex organisms (Halbleib and Nelson 2006). Cadherins are a superfamily of membrane proteins characterized by the presence of extracellular cadherin (EC) repeats in the extracellular domain. Different cadherins are classified into several subfamilies by the gross organization of their extracellular cadherin motifs and sequence similarities in their extracellular and cytoplasmic domains (Fig. 9). These subfamilies of cadherins and their functions in development are briefly described below.

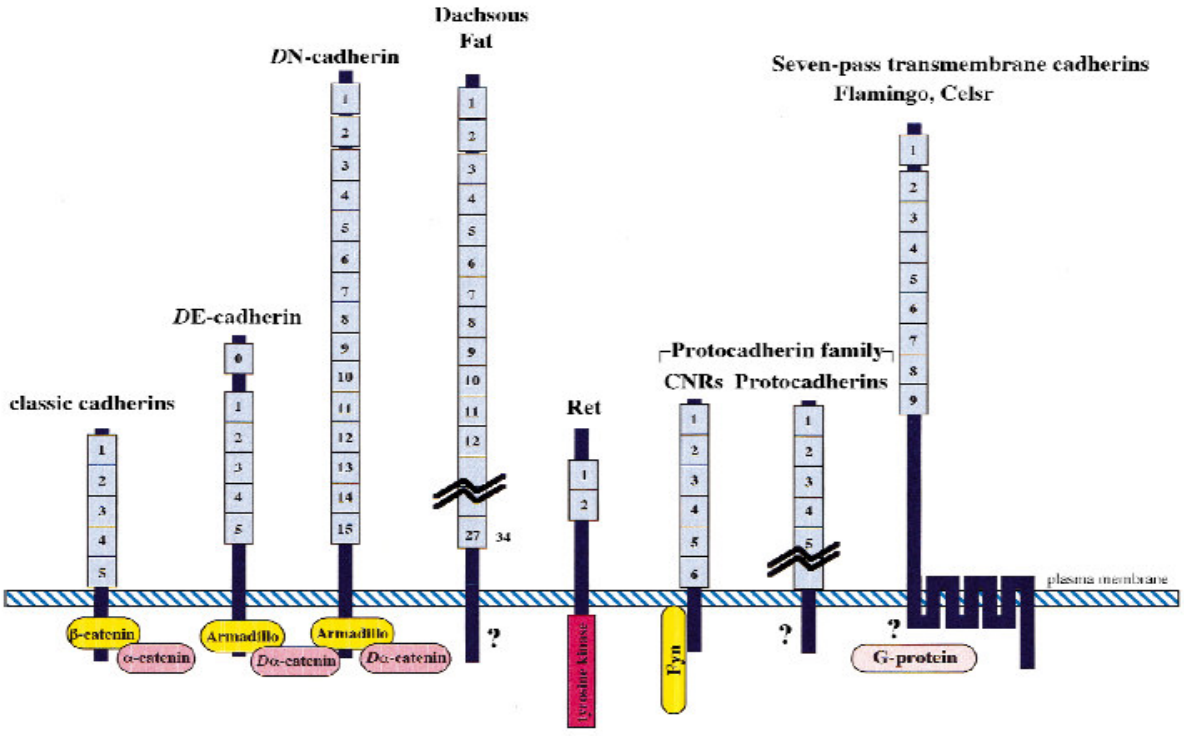

Figure 9. Molecular structure of the cadherin superfamily (blue) and their cytoplasmic interactors (yellow or pink). The number represents how many EC repeats are present in the extracellular domain. DE- and DN-cadherin are Drosophila orthologs of E-and N-cadherin, respectively (Yagi and Takeichi 2000).

2.2.7.1 Classic cadherins

Classic cadherins are identified first among cadherin superfamily (so named as “classic”) and defined by their characteristic cytoplasmic sequence for binding to catenins. More than 20 different classic cadherin subtypes found so far are further divided into 2 subfamilies based on the amino acid sequences of the cytoplasmic domain. Type I classical cadherins mediate strong cell–cell adhesion and have a conserved HAV motif in the most distal EC (EC1). They include epithelial (E), neuronal (N), placental (P) and retinal (R) cadherin, named according to the tissues where they were first identified. In contrast, type II classical cadherins, such as vascular epithelium (VE) cadherin, lack this motif.

2.2.7.1.1 Classical cadherins in morphogenesis

Classical cadherins play key roles in a variety of morphogenetic processes by mediating cell sorting, coordinated cell movements, planar cell division (Halbeleib and Nelson 2006). During gastrulation, modulation of adhesion plays major roles in cell rearrangements within cell sheets like CE movements and in epithelial mesenchymal transitions. CE movements in the sea urchin archenteron are accompanied by a loss of E-cadherin (Miller and McClay 1997). E-cadherin is also essential for the epiboly of the animal cap (Levine *et al.* 1994) and modulation of the adhesive function of C-cadherin is engaged in CE movements in *Xenopus* (Marsden and DeSimone 2003). Cadherins are also involved in the tissue separation of germ layers in *Xenopus* (Wacker *et al.* 2000).

2.2.7.1.2 Catenins in morphogenesis

Function of classical adherins is modulated by a group of cytoplasmic proteins called catenins that interact with the cadherin intracellular domain. A major role of catenins is to anchor the cadherin complex to the actin cytoskeleton. β-catenin and plakoglobin (γ-catenin) bind the C-terminal region of cadherin, acting as bridges connecting E-cadherin to α-catenin, which in turn associates with actin filaments directly or indirectly. β-catenin also has signaling roles in the Wnt/β-catenin pathway as described before. In contrast, p120 catenin subfamily members including p120 and armadillo repeat gene deleted in velo-cardio-facial syndrome (ARVCF) bind the juxtamembrane region of cadherin. Although p120 does not interact with α-catenin, it associates with kinesin and microtubules (Chen *et al.* 2003; Franz and Ridley 2004). p120 regulates cell adhesion and motility positively or negatively depending on its effects on cadherin stability and clustering or on small GTPases and the cell cytoskeleton. p120 and ARVCF act as a guanine nucleotide dissociation inhibitor (GDI) by binding to and preventing RhoA activity while

activate both Rac1 and Cdc42 through its interaction with VAV2, a Rho GEF (Fang *et al.* 2004). p120 and ARVCF are essential for CE movements in *Xenopus*, perhaps resulting from the modulation of cadherin and Rho GTPase activity (Fang *et al.* 2004). Moreover, p120 can bind transcriptional repressor Kaiso and relieve repression of Kaiso target genes like Wnt11, contributing to gastrulation movements indirectly by upregulation of PCP pathway (Kim *et al.* 2004). Thus p120 acts as two-edged sword to regulate morphogenesis by modulating not only adhesion but also gene expression, in a way similar to β-catenin.

2.2.7.2 Protocadherins

Protocadherins make up the largest subfamily of cadherins, expressed mostly in but not limited to nervous system. Compared with classical cadherins, protocadherins have six to seven EC repeats in the extracellular domains while have no catenin-binding sites in the intracellular domains. Much less is known about the function of protocadherins, but increasing evidence demonstrates their roles in tissue morphogenesis and neural development (Hirano *et al.* 2003). Here I just focus on the roles of *Xenopus* protocadherins in embryogenesis, how their orthologs function in other species will be described if available.

2.2.7.2.1 Axial protocadherin

Axial protocadherin (AXPC) is expressed exclusively in the axial mesoderm notochord. At the tailbud stage, it is also expressed in the pronephros, somites, heart, optic vesicle, otic vesicle, and distinct parts of the brain. AXPC is necessary and sufficient for prenotochord cell sorting in the gastrulating embryo. Importantly, cell sorting require extracellular domain, implying that EC mediated cell adhesion is involved in cell sorting (Kuroda *et al.* 2002).

Protocadherin-1 (Pcdh1) is the mammal ortholog of AXPC. In transfected cells Pcdh1 localizes to cell-cell junction and mediates weak homophilic cell-cell adhesion. In rats, Pcdh1 is expressed mainly in brain (Sano *et al.* 1993). Except for mediating cell-cell adhesion, no other function of AXPC or Pcdh1 has been reported yet.

2.2.7.2.2 NF-protocadherin

NF-protocadherin (NFPC) is predominantly expressed within the deep sensorial layer of ectoderm and in a restricted group of cells in the neural folds (Bradley *et al.* 1998). NFPC contributes to neurulation since its disruption inhibits neural tube closure due to a lack of proper cell organization in neural folds (Rashid *et al.* 2006). NFPC mediates cell adhesion within the

ectoderm and blistering caused by DN NFPC can be rescued by C-cadherin but not N- or E-cadherin (Bradley *et al.* 1998). This suggests that adhesion alone is not enough to rescue NFPC function but signaling induced by NFPC may be involved. Indeed TAF1 was identified to bind the NFPC cytoplasmic domain and rescue the ectodermal disruptions caused by DN NFPC. Moreover, disruptions in either NFPC or TAF1 result in essentially identical defects, indicating that NFPC and TAF1 acts in the same pathway to modulate neural tube formation (Heggem and Bradley 2003a; Heggem and Bradley 2003b).

Protocadherin-7 (Pcdh7, also named BH-protocadherin for its prominent expression in brain and heart of man) was regarded as ortholog of NFPC since they show high sequence similarity (Yoshida *et al.* 1998). Pcdh7 is predominantly expressed in cerebral cortex neurons in the adult mouse brain. Interestingly, cytoplasmic domain of Pcdh7 binds protein phosphatase type I isoform alpha (PP1alpha) and inhibits PP1alpha activity towards glycogen phosphorylase (Yoshida *et al.* 1999). This interaction may mediate a role of Pcdh7 in synaptic modulation.

2.2.7.2.3 Paraxial protocadherin

Paraxial protocadherin (PAPC) incites more research interest, perhaps due to its initial specific expression in Spemann organizer. It is expressed in the dorsal marginal zone at gastrula and in paraxial mesoderm at later stage. Interestingly, PAPC is expressed in a complementary pattern to AXPC, and this pattern is important for boundary formation and sorting of cells into the paraxial (PAPC) and axial (AXPC) mesoderm that form the somites and notochord, respectively (Kim *et al.* 1998; Yamamoto *et al.* 1998; Kuroda *et al.* 2002). Surprisingly, PAPC expression is regulated strongly by both the maternal β-catenin and Nodal-related signaling in gastrulation (Wessely *et al.* 2004), highlighting the important roles that PAPC may play in gastrulation movements.

Indeed PAPC has been revealed to have multiple functions in a variety of developmental systems. During *Xenopus* gastrulation, the extracellular domain of PAPC may mediate cell sorting but in an indirect manner by modulating C-cadherin adhesion through an unknown mechanism (Chen and Gumbiner 2006), while the intracellular domain is implicated in the regulation of CE movements and tissue separation (Kim *et al.* 1998; Medina *et al.* 2004; Unterseher *et al.* 2004). Importantly, the regulation of CE movements and tissue separation by PAPC depends on the signaling function of PAPC to modulate the activity of Rho GTPase and JNK and may involve the interaction of PAPC and Fz7 ectodomains (Medina *et al.* 2004; Unterseher *et al.* 2004). PAPC is also required for CE movements during gastrulation in zebrafish; in this context, PAPC is a

downstream target of spadetail, a transcription factor required for mesodermal morphogenetic movements (Yamamoto *et al.* 1998).

It is not currently well established whether the function of PAPC in gastrulation is conserved in mammals. On one hand, the putative mammalian PAPC ortholog, Pcdh8, while expressed in the primitive streak, paraxial mesoderm, somites, and CNS, does not have a significant loss-of function phenotype as the authors observed (Yamamoto *et al.* 2000). But another study suggested that PAPC regulates gastrulation movements in mice. Lim1 is a transcriptional factor that promotes PAPC expression in both mice and frog. *Xenopus* embryos depleted of Lim1 lack anterior head structures and fail to form a proper axis as a result of a failure of gastrulation movements. Similar disruption of cell movements in the mesoderm is also observed in Lim1 knockout mice. PAPC expression is lost in the nascent mesoderm of Lim1 knockout mouse embryos and in the organizer of Lim1-depleted *Xenopus* embryos. Importantly the defects caused by loss of Lim1 can be rescued to a considerable extent by supplying PAPC exogenously (Hukriede *et al.* 2003). Therefore it is likely that Lim1 and its downstream target PAPC function in gastrulation movements in both *Xenopus* and mammals. In conclusion, PAPC represents a link between regulatory genes in the Spemann´s organizer and the execution of cell movements during morphogenesis.

2.2.7.2.4 Protocadherin in Neural crest and Somites

Recently a novel protocadherin was identified in *Xenopus* that is initially expressed in the mesoderm during gastrulation, followed by expression in the cranial neural crest (CNC) and somites. Therefore it is named as Protocadherin in Neural crest and Somites (PCNS). PCNS has 65% amino acid identity to *Xenopus* PAPC and 42-49% amino acid identity to Pcdh 8 in human, mouse, and zebrafish genomes. Overexpression of PCNS resulted in gastrulation failure but conferred little if any specific adhesion on ectodermal cells while loss of function resulted in failure of CNC migration, leading to severe defects in the craniofacial skeleton. Somites and axial muscles also failed to undergo normal morphogenesis in these embryos. Thus, PCNS is essential for CNC migration and somite morphogenesis in *Xenopus* (Rangarajan *et al.* 2006).

2.2.7.3 Atypical cadherins

Atypical cadherins are large cadherins that have great number of EC repeats in the extracelluar domains. For example, Dachsous and Fat have 27 and 34 ECs, respectively, while Flamingo is the only member of cadherins family that has seven-pass rather than single transmembrane

domain (Fig. 9). These three atypical cadherins have been shown to interact with each other and regulate asymmetrical localization of Fz and hence PCP signaling, therefore coordinating the polarity required for a variety of morphogenesis in *Drosophila* (Strutt and Strutt 2005). Characterization of these atypical cadherins orthlogs in vertebrates is undergoing and limited study have already shown that these atypical cadherins function in vertebrate in a similar manner.

CE movements and neural tube closure are the major morphogenetic processes regulated by PCP signaling in vertebrates. Flamingo mediates CE movements during gastrulation in zebrafish (Formstone and Mason 2005a). Further study recently showed that in zebrafish embryos, Wnt11-induced Fz7 accumulation partially depends on Flamingo to increase cell contact persistence, but independent of Wnt11 downstream signaling via RhoA and Rok. Thus Flamingo can interact with Fz7 and Wnt11 to modulate local cell contact persistence to coordinate cell movements during gastrulation (Witzel *et al.* 2006). This study for the first time showed that Flamingo performs a conserved role in PCP signaling by recruiting other PCP components to local sites on plasma membrane to regulate cell adhesion both in fly and in vertebrates. Interestingly, mice with Flamingo mutations exhibited failure of neural tube closure (Curtin *et al.* 2003) and Flamingo is upregulated in the chick neural epithelium at the initiation of neural tube closure (Formstone and Mason 2005b). How these atypical cadherins are engaged in gastrulation movements in *Xenopus* awaits further study. But taken into account available data it seems that atypical cadherins participate in a complex and highly conserved signaling cascade to maintain polarity in a range of tissues and coordinate morphogenetic movements during development.

2.3 Aim of the study

As described above, *Xenopus* PAPC (xPAPC) is an important molecule that links regulatory genes in the Spemann´s organizer with the execution of morphogenesis including CE movements and tissue separation. Importantly, the signaling activity of xPAPC revealed recently is critical for xPAPC to modulate these morphogenetic processes. xPAPC promotes CE movements by activating Rho and JNK (Unterseher *et al.* 2004). On the other hand, xPAPC can interact with Fz7 and activate Rho and JNK to modulate tissue separation (Medina *et al.* 2004). Therefore, detailed analysis of the mechanisms by which xPAPC activates Rho and JNK will reveal the mode of action of xPAPC in morphogenesis. The cytoplasmic domain of xPAPC (**xPAPCc**) is essential for the signaling activity of xPAPC since M-PAPC, a mutant form of xPAPC anchored to membrane but without cytoplasmic domain, can not promote CE movements (Kim *et al.* 1998) or promote

tissue separation (Medina *et al.* 2004). Hence it is important to identify and characterize proteins that interact with xPAPCc to elucidate the mechanisms underlying PAPC signaling.

Up to date no proteins have been reported to interact with xPAPCc. So in this study, three experimental strategies will be employed to identify xPAPCc interacting partners and the roles of their interactions in CE movements and tissue separation will be characterized.

1. **Candidate approach**. Bioinformatics tools will be used to predict potential protein-protein interaction domains or motifs present in xPAPCc. On the other hand, candidate proteins will be selected based on literature regarding their expression patterns, protein structure and function with those of xPAPC.
2. **GST-pull down assay**. GST-xPAPCc fusion protein will be expressed and purified from *E. coli* and subjected to lysates from gastrulation stage *Xenopus* embryos. The proteins pulled down by GST-xPAPCc will be separated on SDS-PAGE gels and identified by matrix assist laser desorption/ionization-time of flight mass spectrometry (MALDI-TOF MS)
3. **Yeast two-hybrid screen**. Matchmaker *Xenopus laevis* oocyte cDNA library will be screened with xPAPCc as the bait.

It is expected that proteins interacting with xPAPCc will be identified by the above approaches and their interaction will be further functionally analyzed in *Xenopus* embryos to elucidate the mechanisms of PAPC mediated signaling activity.

3. Materials and Methods

3.1 Materials

3.1.1 Chemicals

General laboratory chemicals	Roth, Merck, Sigma
Acrylamid/Bisacrylamid (30 : 1)	Roth
Ampicillin (Sodium salt)	Biomol
Bacto-Trypton and yeast extract	BD
DNA-Marker	MBI Fermentas
dNTPs	MBI Fermentas
Hi-Di Formamide	Roche
Human Chorionic Gonadotropin	Sigma
L-Cysteine	Biomol
NP40	Calbiochem
Okadaic acid	Calbiochem
Phosphatase inhibitor cocktail I and II	Sigma
Protease inhibitor cocktail	Calbiochem
Ultralink Immobilized Protein G	Pierce

3.1.2 Enzyme and Kit systems

Big Dye Terminator Cycle Sequencing	Applied Biosystems
General Enzymes for molecular biology	NEB, Amersham, Gibco BRL, MBI Fermentas, Finnzymes
JETQuick Plasmid Mini Kit	Genomed GmbH
JETQuick PCR Purification Kit	Genomed GmbH
JETQuick Gel Extraction Kit	Genomed GmbH
JETStar Plasmid Midi Kit	Genomed GmbH
MEGAscript Kit for SP6 and T7	Ambion
Qiagen Miniprep Kit	Qiagen
Qiagen Maxiprep Kit	Qiagen

3.1.3 Laboratory instruments and accessories

Analytical balance	Mettler
Blot equipment	Invitrogen
Camera CC-12	Soft Imagining System
DNA Thermal Cycler	Biometra
Electrophoresis	Biometra
Electroporation cuvette	Peq Lab
Film developing machine	MS Laborgeräte
Filter paper (3-MM)	Whatman
Glass centrifuge tube	DuPont
Incubation shaker	Infors
Injection machine IM300 Microinjector	Narishige
Micromanipulator	Micro Instruments
Micropipette puller	Narishige
Microscope Axiovert 135	Zeiss
NanoDrop ND-1000 spectrophotometer	NanoDrop Technologies
Nitrocellulose membranes	Schleicher&Schuell
PCR-tube (0.2ml)	Peq Lab
Petri plates	Sarstedt
pH-Meter	Mettler
Plastic centrifuge tube (15 and 50ml)	Sarstedt
Protein Gel Novex	Invitrogen
Scanner Snapscan e50	AGFA
Table centrifuge	Eppendorf
UV fotocamera Darkroom	UVP
Vortexer	Janke& Kunkel
Water bath	BFL
Confocal microscopy facility	Nikon Imaging Center, University Heidelberg

3.1.4 General buffers and media

Blocking buffer	0.1% Tween 20 (w/v), 5% Milk (w/v) in PBS
buffer H (for GST pull-down)	50 mM Tris, pH 7.5, 250 mM KCl, 5 mM EDTA, 1 mM DTT, 0.1% Triton X-100, protease inhibitors
Cysteine	2% L-Cysteine in H_2O and adjust pH to 8.0
6x DNA loading buffer	40% (v/v) Glycerin, 0.25% Bromphenol blue
Ethidium bromide stock solution	10 mg/ml Ethidium bromide, stored at RT in the dark
Gurdons buffer	88 mM NaCl, 10mM Tris-Hcl (pH 7.4), filter sterile
LB-Medium pH7.4	10 g/l Bacto-Trypton, 5 g/l yeast extract, 10 g/l NaCl in H_2O, autoclaved (121°C, 20 min)
LB-Agar plates	LB-Medium with 1.5% agar
LB/Amp-medium	100 µg/ml Ampicillin in LB-medium
LB/Amp-Agar plates	LB-Medium with 1.5% agar, 100 µg/ml Ampicillin
MBSH	88 mM NaCl, 1 mM KCl, 2.4 mM NaHCO3, 0.8 mM MgSO4, 0.33 mM NaNO3, 0.4 mM CaCl2, 10 mM HEPES pH 7.4, 10 µg/ml Streptomycin, 10 µg/ml Penicilin
MEMFA	0.1 M MOPS pH 7.4, 2 mM EGTA, 1 mM MgSO4, 3.7% Formaldehyde
NP40 lysis buffer	10 mM Tris-HCl pH 7.5, 100 mM NaCl, 2 mM EDTA, 1 mM EGTA, 0.5% NP40, 10% glycerol with a cocktai of phosphatase and proteinase inhibitors
PBS	8 g/l NaCl, 0.2 g/l KCl, 1.44 g/l Na_2HPO_4, 0.24 g/l KH_2PO_4 in H_2O adjusted to pH 7.4 with 2 M NaOH
PBS-T	PBS with 0.1% Tween 20
3x SDS-PAGE loading buffer	150 mM Tris-HCl pH 6.8, 6% (w/v) SDS, 300 mM DTT, 30% (w/v) Glycerin, 0.3% (w/v) Bromphenol blue
SDS-PAGE running buffer	24.8 mM Tris, 192 mM Glycine, 0.1% SDS
Stripping buffer	62.5 mM Tris-HCl pH 6.8, 2% SDS, 100 mM β-mercaptoethanol
10x TBE	108 g/l Tris, 55 g/l Boric acid, 7.4 g/l EDTA, pH 8.0 autoclaved (121°C, 20 min)
TE	10 mM Tris-HCl pH 8.0, 1.0 mM EDTA
Transfer buffer	24.8 mM Tris, 192 mM Glycine, 20% Methanol
2x YTA	16 g/l tryptone, 10 g/l yeast extract, 5 g/l NaCl, 100 µg/ml Ampicillin, pH 7.0

3.1.5 Stock solutions, media and buffers for yeast work

Single-stranded carrier DNA: Weigh 200 mg of salmon sperm DNA Type III Sodium Salt (Sigma D1626) into 100 ml of TE buffer (pH 8.0) or ddH_2O. Disperse the DNA into solution by drawing it up and down repeatedly with a 25-ml plastic pipette. Mix vigorously on a magnetic stirrer for 2-3 hours or o/n in a cold room. Aliquot the DNA in 1 ml and store at -20°C.

1 M LiOAc: Adjust to pH 7.5 with dilute acetic acid and autoclave.

50% PEG (w/v): Weigh 50 g PEG (MW 3350, Sigma P3640) into a beaker and add 80 ml ddH_2O. Stir with a magnetic stirring bar until dissolved. Transfer all of the liquid to a 100 ml graduated cylinder. Wash beaker with a small amount of ddH_2O and add this to the graduated cylinder containing the PEG solution, and bring the volume to exactly 100 ml. Mix well by inversion. Autoclave at 121°C for 15 min.

1 M 3-AT: prepare in ddH_2O and filter sterilize. Store at 4°C. Store plates containing 3-AT at 4°C for up to 2 months.

X-Gal (20 mg/ml in DMF): dissolve X-Gal in DMF. Store in the dark at -20°C.

40% Galactose: dissolve 40 g Galactose in 100 ml H_2O, autoclave at 121°C for 15 min.

40% Raffinose: dissove 40 g Raffinose in 100 ml H_2O, autoclave at 121°C for 15 min.

10 x BU salts: 70 g/L $Na_2HPO_4 \bullet 7H_2O$, 30 g/L NaH_2PO_4, add H_2O to 1 L, dissolve and autoclave and store at RT.

5 x M9 Salts: 64 g/L $Na_2HPO_4 \bullet 7H_2O$, 15 g/L KH_2PO_4, 2.5 g/L NaCl, 5 g/L NH_4Cl, add H_2O to 1 L and autoclave at 121°C for 15 min.

YPAD media

50 g/L YPD powder, 0.03 g/L adenine hemisulfate, 20 g/L agar (for plates only).

Add H_2O to 1 L, autoclave at 121°C for 15 min.

2x YPAD media

100 g/L YPD powder, 0.03 g/L adenine hemisulfate.

Add H_2O to 1 L,autoclave at 121°C for 15 min.

SD media

27 g/L DOB (dropout base) powder, CSM-Amino acid (Complete Supplement Mixture minus the above amino acid), 0.03 g/L adenine hemisulfate, 20 g/L agar (for plates only).

Add H_2O to 1 L, dissolve and autoclave at 121°C for 15 min.

For SD plates containing 3-AT, cool SD media to 55°C and add appropriate amount of 1 M 3-AT stock solution and swirl to mix well before pouring to plates.

SD-Trp/-Leu/-His/+10mM 3-AT/+X-Gal plate

27 g/L DOB powder, 0.62 g/L CSM-Trp-Leu-His, 0.03 g/L adenine hemisulfate, 20 g/L agar.
Add H_2O to 820 ml, dissolve and autoclave at 121°C for 15 min. Cool to 55°C, add
50 ml 40% Galactose, 25 ml 40% Raffinose, 100 ml 10 x BU salts, 4 ml X-Gal stock,
10 ml 1 M 3-AT stock. Pour and store plates inverted in the dark at 4°C.

M9/Amp minimal medium plates (for selection of prey plasmid in KC8 cells)
0.69 g/L CSM-Leu, 20 g/L agar, 750 ml H_2O.
Autoclave at 121°C for 15 min. Cool to 55°C, add
200 ml 5x M9 salts, 20 ml 20 % glucose, 2 ml 1 M $MgSO_4$, 0.1 ml 1 M $CaCl_2$, 1 ml 1 M thiamine HCl (filter-sterilized), 1 ml 50 mg/ml ampicillin. Pour and store plates at 4°C.

Buffers for β-galactosidase filter assay

Z buffer	$Na_2HPO_4 \cdot 7H_2O$ 16.1 g/L $NaH_2PO_4 \cdot H_2O$ 5.50 g/L KCl 0.75 g/L $MgSO_4 \cdot 7H_2O$ 0.246 g/L Adjust to pH 7.0 and autoclave.
X-gal stock solution	Dissolve X-Gal in DMF at a concentration of 20 mg/ml. Store in the dark at –20°C
Z buffer/X-gal solution	100 ml Z buffer 0.27 ml β-ME 1.67 ml X-gal stock solution

Buffers for yeast protein extraction

NaOH/β-ME buffer	1.85 M NaOH 7.5% β-Mercaptoethanol
55% TCA (w/v)	To new bottle containing 500 g of TCA, add 227 ml H_2O to get 100% TCA (w/v). Then mix 55 ml to 45 ml H_2O.
SU buffer	5% SDS (w/v) 8 M Urea 125 mM Tris-HCl (pH 6.8) 0.1 mM EDTA 0.005% bromophenol blue (w/v) Store at -20°C Add 15 mg of DTT/ ml of SU buffer prior to use

3.1.6 Antibodies

Primary antibodies

Name	description	Dilution	Source
Ab1	anti-c-myc Mouse monoclonal Ab	1: 3000	Oncogene
M2	anti-flag Mouse monoclonal Ab	1:3000	Sigma
3F10	anti-HA high affinity Rat monoclonal Ab	1:3000	Roche

Secondary antibodies

Name	dilution	source
Anti-mouse Peroxidase coupled antibody produced in goat	1:5000	Dianva
Anti-rat Peroxidase coupled antibody produced in goat	1:5000	Dianva

3.1.7 Bacterial, yeast strains and yeast two-hybrid cDNA library

***E. coli* XL1-Blue:** *recA1 endA1 gyrA96 thi-1 hsdR17 supE44 relA1 lac* [F´ *proAB lacI*^{q}*ZΔM15* Tn*10* (Tet^{r})].

***E. coli* BL21**: F^{-} *ompT hsdS*$_B$(r_B^- m_B^-) *gal dcm*

Saccharomyces cerevisiae* L40**: *MATa** *ade2 his3 leu2 trp1 LYS2*::*lexA-HIS3 URA3*::*lexA-lacZ*

***Xenopus laevis* oocyte Matchmaker cDNA library (Clontech):** kindly provided by Staub O as frozen glycerol stock of *E. coli* transformed with the library.

3.1.8 Oligonucleotides

The sequences of all oligonucleotides are in 5' - 3' direction as specified.

For **sequencing**
pACT2-derived plasmids:
pACT2-U2: GTGAACTTGCGGGGTTTTTCAGTATCTACG

pACT2-D2: ATACGATGTTCCAGATTACGCTAGCTTGGG

pCS2-derived plasmids:

SP6: ATTTAGGTGACACTATAG

T7: TAATACGACTCACTATAG

For **cloning** (restriction site underlined)
Clone xPAPCc into pNLX3:
Forward: CGCGGATCCGTTGTACTTGTAAAAAGAAAG
Reverse: CGTCTGCAGAAAGGTTGTAGCAATTTCTG
Clone hPcdh8c into pNLX3:
Forward: ATTGAATTCTGCAACCGCCGCAAGAAGGAG
Reverse: GGCGTCGACTTACACATTTTCATTGGCTCC
Clone xSpry2 into pACT2:
Forward: GGATGCGGAATTCGAATGGAGACGAGAGTACA
Reverse: GCGCCTCGAGCTATGTTGGTTTTTCTAAGTTC
Clone xSpred1 into pACT2:
Forward: AATTGGATCCGAATGAGCGGCGAACAGGAG
Reverse: GCGAGATCTTCCAGCTGCTTTATGCTTCCC
Clone dSpry into pACT2:
Forward: GCGCGAATTCGAATGGATCGCAGAAATGG
Reverse: ATATCTCGAGGTAGTCGGGACTGGAGTCC
Clone hSpry1 into pACT2:
Forward: CGCGAATTCACATGGATCCCCAAAATCAAC
Reverse: ATTCTCGAGTCATGATGGTTTACCCTGACC
Clone hSpry2 into pACT2:
Forward: ATAGAATTCACATGGAGGCCAGAGCTCAG
Reverse: GCGCCTCGAGCTATGTTGGTTTTTCAAAGTTC
Clone xPAPCc into pGEX6p2:
Forward: GGCGTCGACGTGTACTTGTAAAAAGAAAGC
Reverse: ATGCGGCCGCAAAGGTTGTAGCAATTTCTG
Clone xAXPCc into pGEX6p2:
Forward: CAGGGTCGACGCGGTATTGCAGGCAAAAAG
Reverse: ATATAGCGGCCGCCCACACGTCAGTCCAAGCTAG
Clone xPAPCc into pCS2-flag:
Forward: GCCTCGAGATGTGTACTTGTAAAAAGAAAG
Reverse: AGGTCTAGAAAAGGTTGTAGCAATTTCTG
Clone xAXPCc into pCS2-flag:
Forward: ATCTCGAGATGCGGTATTGCAGGCAAAAAG
Reverse: ATATCTAGACCACACGTCAGTCCAAGCTAG
Clone xTubulinβ into pCS2MT:
Forward: GATCTCGAGATGAGGGAAATCGTGCACTTG
Reverse: GCGTCTAGATTAGGCATTTTCCTCCTCTTC
Clone xCK2β into pCS2MT:
Forward: AGTGAATTCAATGAGTAGCTCGGAGGAGG
Reverse: AGCCTCGAGTCAACGCATGGTCTTCAC
Clone xSpry1 into pCS2-EGFP-C1:
Forward: ATTAGATCTATGGAGCTACAAAGTCAACATGG
Reverse: ATATCTAGATCAGGAGGGCTTGCCCTGGCC

For **site-directed mutagenesis of xPAPC** (mutant sites underlined)
S741 to A741:
Forward: CGCCTGTTAGCCACCCCATCTCCCCAGTCG
S741 to E741:
Forward: CGCCTGTTAGAAACCCCATCTCCCCAGTCG
Reverse: TTCTTCATTGCATGTTCCATGTTGTTCAGG

T947 to A947:
Forward: AGAAGTGCAGCGTTATCTCCGCAGAGATCG
Reverse: GTTGACTAAATCTCTTTCATATTCCGCGTG

S955 to A955:
Forward: AGATCGTCTGCCAGATACCAAGAATTCAAT
S955 to E955:
Forward: AGATCGTCTGAGAGATACCAAGAATTCAAT
Reverse: CTGCGGAGATAACGTTGCACTTCTGTTGAC

For **deletion mutagenesis of xPAPC** (deletion of conserved residues 818-833)
Forward: GAATCACAAAAGAAGAGCATTGAGCAGCC
Reverse: AATGTGCCCCATGTGAGAATGTCCACTTA

xPAPC MO: provided by Steinbeisser H (Medina *et al.* 2004).

3.1.9 Plasmids

3.1.9.1 Plasmids for yeast two-hybrid assay

Empty bait plasmid pNLX3 was provided by Moreau J (Iouzalen *et al.* 1998) and prey plasmid pACT2 by Staub O.

pNLX3-xPAPCc
cDNA for the cytoplasmic domain of xPAPC (residues 715-979) was amplified by PCR and cloned into the pNLX3 using *Bam*HI/*Pst*I sites in frame with LexA BD domain.
pNLX3-hPcdh8c
cDNA for the cytoplasmic domain of hPcdh8 (human Pcdh8) was amplified by PCR and cloned into pNLX3 using *Eco*RI/*Sal*I sites in frame with Lex BD domain.

Point mutant constructs pNLX3-xPAPCcS741A, pNLX3-xPAPCcT947A, pNLX-xPAPCcS955A, pNLX3-xPAPCcS741E, pNLX3-xPAPCcS955E were generated by PCR site-directed mutagenesis with pNLX-xPAPCc as template.
Deletion construct pNLX3-xPAPCcΔ16aa was generated by PCR mediated mutagenesis with pNLX3-xPAPCc as template.

pACT2-xSpry2
xSpry2 cDNA was amplified by PCR and cloned into pACT2 using *Eco*RI/*Xho*I sites in frame with Gal4 AD domain.
pACT2-xSpred1
xSpred1 cDNA was amplified by PCR and cloned into pACT2 using *Bam*HI/*Bgl*II sites in frame with Gal4 AD domain.
pACT2-dSpry
dSpry cDNA was amplified by PCR and cloned into pACT2 using *Eco*RI/*Xho*I sites in frame with Gal4 AD domain.
pACT2-hSpry1

hSpry1 cDNA was amplified by PCR and cloned into pACT2 using *Eco*RI/*Xho*I sites in frame with Gal4 AD domain.
pACT2-hSpry2
hSpry2 cDNA was amplified by PCR and cloned into pACT2 using *Eco*RI/*Xho*I sites in frame with Gal4 AD domain.
pACT2-xDsh
xDsh cDNA was subcloned from pCS2-xDsh-myc into pACT2 in frame with Gal AD domain.
pACT2-x14-3-3ε
pMyc-x14-3-3ε was provided by Kumagai A (Kumagai and Dunphy 1999). x14-3-3ε cDNA was subcloned from pMyc-x14-3-3ε into pACT2 in frame with Gal AD domain.

3.1.9.2 Plasmids for GST pull-down assay

pGEX6p2-xPAPCc
cDNA for the cytoplasmic domain of xPAPC was amplified by PCR and cloned into the pGEX6p2 using *Sal*I/*Not*I sites.
pGEX6p2-xAXPCc
cDNA for the cytoplasmic domain of xAXPC (residues 838-1016) was amplified by PCR and cloned into the pGEX6p2 using *Sal*I/*Not*I sites.

3.1.9.3 Plasmids for expression in *Xenopus* embryos

pCS2-xPAPC, pCS2-M-PAPC, pCS2-xFz7, pCS2-xDsh-GFP, pCS2-Flag and pCS2MT were from AG Steinbeisser. pCS2-xPKC-GFP was provided by Amaya E (Sivak *et al.* 2005).
pCS2-xPAPCc-Flag
cDNA for the cytoplasmic domain of xPAPC was amplified by PCR and cloned into the pCS2-Flag using *Xho*I/*Xba*I sites with the Flag tag at the C-terminal of xPAPCc.
pCS2-xPAPCc-S741A/S955A-Flag
It was generated by PCR site-directed mutagenesis with pCS2-xPAPCc-Flag as template.
pCS2-xAXPCc-Flag
cDNA for the cytoplasmic domain of xAXPC was amplified by PCR and cloned into the pCS2-Flag using *Xho*I/*Xba*I sites with the Flag tag at the C-terminal of xAXPCc.
pCS2MT-xp120 and pCS2HA-xARVCF
These constrcuts are used for expression of Myc-tagged xp120 and HA-tagged xARVCF catenin, respectively. They were provided by McCrea PD (Fang *et al.* 2004).
pCS2MT-xSpry1
It is used for expression of Myc-tagged xSpry1 and provided by Nishida E (Hanafusa *et al.* 2002).
pCS2MT-xTubulin
xTubulin cDNA was amplified by RT-PCR with embryo RNA as template and cloned into pCS2MT using *Xho*I/*Xba*I sites.
pCS2-xSpry1-GFP
xSpry1 cDNA was amplified by PCR and cloned into the pCS2-EGFP-C1 using *Bgl*II/*Xba*I sites.
pCS2MT-xCK2β
xCK2β cDNA was amplified by PCR and cloned into the pCS2MT using *Eco*RI/*Xho*I sites with the 6xMyc tag at the N-terminal of xCK2β.
pCS2-xCK2α and pCS2-xCK2β
These constructs are used for expression of untagged xCK2α and xCK2β, respectively. They were provided by Dominguez I (Dominguez *et al.* 2004).

3.2 Molecular biology methods

3.2.1 Maintenance of bacterial strains

Strains were stored as glycerol stocks (LB-medium, 25% (v/v) glycerol) at –70°C.

An aliquot of the stock was crossed out on LB-plate containing the appropriate antibiotics and incubated overnight (o/n) at 37°C. Plates were stored up to 6 weeks at 4°C.

3.2.2 Preparation of competent bacteria

Calcium chlorid-method

A single colony was inoculated into 2 ml LB medium and incubated o/n on a shaker at 37ºC. 1 ml o/n culture was inoculated into 400 ml of LB medium and incubated on a shaker at 37ºC for 3-4 h until OD_{600}=0.4-0.6. The culture was transferred to sterile centrifuge tubes and centrifuged 5000 rpm (Rotor JA-14), 10 min at 4°C. The supernatant was poured off and the cells were kept on ice. Then the cell pellet was resuspended in 100 ml of ice cold sterile 50 mM $CaCl_2$ and incubated for 15 min on ice. After centrifugation 6000 rpm (Rotor JA-14), 10 min at 4°C the cells were resuspended in 20 ml of ice cold 50 mM $CaCl_2$ containing 10% Glycerol. Aliquot of 100 µl were incubated in micorcentrifuge tubes for 2 h on ice. Subsequently, the suspension was frozen in liquid nitrogen and stored at –70ºC.

3.2.3 Transformation of *E. coli*

To 100 µl of competent DH5α cells either 50-100 ng of plasmid DNA or 10 µl of ligation mixture were added and incubated for 20 min on ice. After a heat shock (1.5 min, 42°C) and successive incubation on ice (2 min), 800 µl of LB-medium was added to the bacteria and incubated at 37°C for 60 min with gently shaking. Cells were plated on LB plates containing the appropriate antibiotics. Plates were incubated at 37°C o/n.

3.2.4 Plasmid Minipreparation

JetQuick Mini Kit was used for preparation of small scales of plasmid DNA according to the manufacture's protocol.

3.2.5 Plasmid Midipreparation

JETStar Plasmid Midi Kit was used for preparation of plasmid DNA that will be used for making RNA.

3.2.6 Enzymatic modification of DNA

3.2.6.1 Digestion of DNA by restriction endonucleases

DNA was incubated with the recommended amount of appropriate enzymes in the recommended buffer for 2 h at recommended temperature according to the manufacturer's protocol. The DNA was purified between the two digestions using the JetQuick PCR Purification Kit.

3.2.6.2 Generation of blunt-end DNA fragments

A reaction mixture was made containing DNA, 1 × T4 DNA polymerase reaction buffer and 20 µM of each dNTP. Then 1 unit of T4 DNA polymerase was added and incubated at 15°C for 30 min. Then the reaction was stopped by heating at 75°C for 10 min.

3.2.6.3 Dephosphorylation of plasmid DNA

1 unit SAP (scrimps alkine phosphatase) per 100 ng plasmid DNA and SAP buffer were added to DNA. The reaction was incubated at 37°C for 2 h and terminated by incubation at 70°C for 10 min. The plasmid DNA was used for ligation without further purification.

3.2.6.4 Ligation of DNA fragments

Ligation of DNA fragments was performed by mixing 50 ng vector DNA with fivefold to eightfold molar excess of insert DNA. 1 µl of T4 DNA ligase (5 weiss unit/µl) and 2 µl of 10x ligation buffer were added and the reaction mix was brought to a final volume of 20 µl. The reaction was incubated for 2h at RT. The reaction mixture was used directly for transformation without any further purification.

3.2.7 DNA electrophoresis

DNA fragments were separated in horizontal electrophoresis cambers using agarose gels. Depending on the size of DNA fragments, agarose gels were prepared by heating 0.9-2 % (w/v) agarose in 1x TBE buffer. After agarose was dissolved completely, ethidium bromide was added. The gel was covered with 1x TBE buffer and the DNA samples were mixed with sample buffer and pipetted in the sample pockets. The gel was run at constant voltage (10 V/cm gel length) until the bromphenol blue dye had reached the end of the gel. Finally gels were documented using a UV-light imaging system.

3.2.8 DNA purification

3.2.8.1 Purification of DNA fragments

For purification of DNA fragments the JetQuick PCR Purification Kit was used according to the manufacture's protocol.

3.2.8.2 Extraction of DNA fragments from agarose gels

The JetQuick Gel Extraction Kit was used for isolation and purification of DNA fragments from agarose gels. Ethidium bromide-stained gels were illuminated with UV-light and the appropriate DNA band was excised from the gel with a clean scalpel and transferred into an Eppendorf tube. The DNA fragment was purified following the manufacture's protocol.

3.2.9 *In vitro* transcription of CAP-mRNA

For injection into *Xenopus* embryos, mRNAs were transcripted from linearized plasmids using the MEGAscript Kit. Plasmids were linearized with the appropriate restriction enzyme to generate a free 3´ terminus at the end of the coding region. Linearized DNA was precipitated by adding 0.05 volumes of 0.5 M EDTA (pH8.0), 0.1 volumes of 3 M NaAC and 2 volumes of Ethanol at -20°C for 15 min and resuspended in ddH_2O to final concentration of 0.5-1 µg/µl. The prepared DNA was used as template for transcription using the MEGAscript Kit following the manufacturer's protocol. RNAs were purified by precipitation with NH_4AC and extracted with phenol-chloroform. The purified RNAs were analyzed by running agarose gels.

3.2.10 Determination of DNA and RNA concentration

The concentration of the isolated DNA or RNA and the ratio of absorbance at 260 nm to 280 nm (A260/A280 ratio) were measured with the NanoDrop ND-1000 spectrophotometer. A ratio of A260/A280 between 1.8 and 2 monitored a sufficient purity of the DNA or RNA preparation.

3.2.11 Polymerase Chain Reaction

Prepare components as below:

Component	Final Concentration
Template	10-100 ng plamid DNA or cDNA
Primer forward	0.1–0.5 µM
Primer reverse	0.1–0.5 µM
10x Reaction buffer	1x
Magnesium	1.0–3.0 mM
dNTP mix	200 µM each dNTP
Thermostable DNA polymerase	1 unit/100 µl reaction

PCR was carried out using an automated thermal cycler. The following standard protocol was adjusted to each specific application:
3 min 95°C (initial denaturation)
30 cycles:
1 min 95°C (denaturation)
1 min 46-70°C (annealing)
1.5 min/kb 72°C (extension)
10 min 72°C (final extension)

PCR products were either separated by agarose gel electrophoresis, excised and subsequently purified with the QIAquick Gel Extraction kit or directly purified with the PCR Purification Kit. Purified PCR products were ready to use for downstream work.

3.2.12 Mutagenesis of plasmids

Site-specific base changes in DNA constructs were introduced using inverse PCR. Complementary oligonucleotides containing the desired sequence change and the flanking regions were used to amplify the complete plasmid sequence. Non-mutated plasmid template was then digested with *Dpn*I, an enzyme recognizing sequence with methylated residues that are not present in the newly synthesized PCR product. The PCR product was phosphorylated at 5´ ends, self-ligated and transformed in *E. coli*. The mutagenized vector was isolated and analyzed by DNA sequencing.

3.2.13 DNA Sequencing

DNA sequencing was performed using the Big Dye Terminator Cycle Sequencing kit and the facility in Institute of Human Genetics, University of Heidelberg.

3.3 Embryological methods

3.3.1 Preparation of *Xenopus laevis* embryos

Various doses (350-500 IU, depending on the condition of frogs) of chorionic gonadotropin dissolved in ddH_2O were subcutaneously injected to the dorsal lymph sac of healthy female frogs. Generally the injected frogs were kept at RT waterbath o/n and began spawning eggs the next morning.

Testes used for *in vitro* fertilization were dissected out from adult male frogs and maintained in 1x MBSH at 4°C, which are viable of fertilization for at least two weeks.

For *in vitro* fertilization, female frogs were gently squeezed to lay eggs into a large petri dish and excess liquid was removed. Subsequently a small piece of testis was cut into fine pieces with scissors, suspended in 0.5-1 ml 1x MBSH and transferred onto the eggs. The eggs were gently mixed well with the sperm suspension, spread to a single layer on the bottom of petri dish. Then plenty volume of H_2O was added to cover the fertilized eggs. About 30 min later, fertilization rates can be determined by observing cortical rotation. Embryos were dejellyed with 2% cysteine (adjusted to pH8.0 with NaOH), washed intensively with water and cultured in 1x or 0.1x MBSH depending on the desired stages.

3.3.2 Microinjection and manipulation of *Xenopus* embryos

3.3.2.1 Micorinjection

Place a needle into the holder on the micromanipulator. Cut off the end of the needle using forceps under the microscope. Dilute the RNA or DNA in Gurdons buffer. Use a volume of approximately 5 nL per injection for embryos at the 1-4-cell stages. In general, an injection pressure of 10 psi and an injection time period of 1 sec are used. Transfer embryos to be injected into plastic dishes covered with 1% agarose (in 1x MBSH) and the injection was performed in 1x MBSH. Drive the needle tip through surface of the embryo, give pressure to the needle and inject the RNA or DNA into the animal blastomeres at 4-cell stage. After injection, embryos were cultured in plastic dishes containing 1x or 0.1 X MBSH at temperature between 12 to 24°C depending on the stage and time of harvest of the embryos.

3.3.2.2 Explantation of animal caps

Explantation of animal caps were carried out in plastic dishes covered with 1% agarose (in 1x MBSH) when the embryos develop to stage 8 to 9. Grasp the membrane with the very tips of one pair of forceps in the vegetal region while bracing the embryo against the side of the other forceps.

With the other forceps, grasp the membrane close to the place where the first one penetrates; hold the membrane and pull away to remove it. After the removal of vitelline membrane, roll the embryo animal pole up and gently push it back into shape in order to maintain a good blastocoel. Excise the cap tissue with the forceps.

For activin treatment, transfer the caps into wells filled with 0.5x MBSH containing activin. After incubation for 2h at RT, the caps were taken out and cultured in plastic dishes filled with 0.5x MBSH till stage 20.

For confocal microscopy, fix the caps in MEMFA solution in the dark at RT for 1h and then kept at 4°C till confocal microscopy.

3.3.3 RT-PCR (Reverse transcription PCR)

3.3.3.1 Isolation of RNA from embryos or explants

Embryos or explants were collected at proper stages in 1.5 ml tubes and 100 µl Trizol was added to homogenize. Then 900 µl Trizol was added and mixed. Keep for 5 min at RT. Then 200 µl chloroform was added and spin 20 min at 4°C. Take the upper phase and add isopropanol, mix and keep for 10 min at RT. Spin 20 min at 4°C. Wash the pellet with 70% ethanol twice. Dissolve in 20µl Nuclease-free H_2O.

3.3.3.2 Reverse Transcription (RT)

Add 500 ng RNA and 1µl random primer $d(N)_6$ (0.2 µg/µl), fill up to 5.5 µl with H_2O. Keep for 5min at 70°C. Then add 4 µl Mix (2 µl 5x RT buffer, 1 µl 10 mM dNTPs, 0.3 µl RNase inhibitor, 0.7 µl H_2O), mix and keep for 5 min at 25°C. Add 0.5 µl reverse transcriptase, 1.5 h at 42°C and 10 min at 70°C.

3.3.3.3 PCR

Take 1 µl cDNA for 10 µl PCR reaction. The primers were:

ODC Forward: GTCAATGATGGAGTGTATGGATC
Reverse: TCCATTCCGCTCTCCTGAGCAC

Xnr3 Forward: TGAATCCACTTGTGCAGTTCC
Reverse: GACAGTCTGTGTTACATGTCC

95°C 1min, 65°C 1min, 72°C 1min

20 cycles for ODC and 28 cycles for Xnr3

3.4 Protein biochemical methods

3.4.1 Determination of protein concentration

To determine the total protein concentration of e.g. cell lysates, BCA protein assay kit (Pierce) was used following the manufacturer's protocol.

3.4.2 SDS-polyacrylamide gel electrophoresis

Separation of proteins was performed by means of the discontinuous SDS-polyacrylamide gel electrophoresis (SDS-PAGE). The size of the running and stacking gel was as follows:

Separation gel: height ~8 cm, thickness 1 mm

10 or 12%(v/v) acrylamide

Stacking gel: height ~2 cm, thickness 1 mm

5% (v/v) acrylamide

10 or 15-well combs

After complete polymerization of the gel, the chamber was assembled as described by the manufacture's protocol. Samples were loaded in the pockets and the gel was run at constant current at 10 mA for the stacking gel and then for the separation gel at 20 mA. The gel run was stopped when the bromphenol blue dye had reached the end of the gel. Gels were then either stained or subjected to Western Blotting.

3.4.3 Western Blot

3.4.3.1 Electrophoretic transfer

Proteins were transferred from the SDS-gel onto a nitrocellulose membrane (Amersham) using wet transfer method. Proteins were transferred on ice at 400 mA for 90 min. The prestained protein marker was used as molecular weight marker and to monitor the transfer.

3.4.3.2 Immunological detection of proteins on nitrocellulose membranes

After electrophoretic transfer, the membranes were removed from the sandwich and placed in plastic dishes. Membranes were washed once in PBS-T and then incubated in blocking buffer for 30 min at RT with gently shaking. Afterwards, the primary antibody was added in an appropriate dilution and incubated either for 1 h at RT or o/n at 4°C. The primary antibody was removed and the membrane was washed 3x 10 min with PBS-T. The appropriate secondary antibody was then applied for 1 h at RT. The membrane was washed again 3x 10 min with PBS-T. The antibody

bound to the membrane was detected by using the enhanced chemiluminescence detection reagent. The membrane was incubated for 2-3 min in detection reagent. Then the solution was removed and the blot was dried and placed between two saran warp foils. The membrane was exposed to X-ray film (Biomax-MR, Kodak) for several time periods and the films were developed in a dark room in an automatic developing machine.

3.4.4 Coomassie staining of polyacrylamide gels

The coomassie staining of polyacrylamide gels was performed with the Imperial Protein Stain kit (Pierce) following the manufacturer's protocol.

3.4.5 Co-immunoprecipitation

Xenopus embryos were injected with 500 pg mRNA encoding differently tagged proteins at 2–4 cells stage. The embryos were grown until gastrula stage and protein was extracted in NP-40 lysis buffer. The embryo extract was incubated for 2 h with 4 µg of Ab against the tag like Flag, Myc or HA, or mouse IgG as a control. The samples were centrifuged and 30 µl of protein G beads (Pierce) was added to the supernatant. The beads were incubated with the protein extract for 2-3 h, centrifuged and washed four times with NP-40 lysis buffer. The beads were dissolved in 2x SDS-PAGE loading buffer and boiled for 5 min. The immunoprecipitates were separated on 10% SDS–PAGE and subjected to Western blotting.

3.4.6 GST pull-down assay

3.4.6.1 Expression of GST fusion protein

1. Transform recombinant GST expression vector into *E. coli* strain BL21. Inoculate single recombinant colony into 4 ml 2xYTA (or 40ul o/n culture to 4 ml medium, 100 fold dilution).
2. Grow to OD_{600} of 0.6-0.8 with vigorous agitation at 37ºC (3-5h).
3. Divide into 4 tubes and add 10 µl 100 mM IPTG (1 mM final concentration) into 3 tubes.
4. Continue incubation for additional 2h, 4h and 6h, respectively.
5. Harvest cells by centrifuging 1ml culture.
6. Resuspend each pellet in 40 µl 1x SDS loading buffer, heat at 100ºC for 3 min and spin.
7. Load 20 µl sample and run 10% SDS-PAGE.
8. Stain gel with Coomassie Brilliant Blue to check which colony express GST-fusion protein.

3.4.6.2 Batch purification of GST fusion protein

1. Inoculate positive colony in 20 ml 2xYTA medium, 37ºC o/n.
2. Dilute into 500 ml 2xYTA medium, 37ºC till OD_{600} = 0.8.
3. Induce by adding 100 mM IPTG to final concentration of 1mM.
4. Incubate for additional 3h at 30ºC.
5. Spin and resuspend in 20 ml PBS lysis buffer (20 mg lysozyme, 40 µl 0.5M EDTA, 200 µl 100 mM PMSF, 200 U DNase I in PBS), stir at RT for 30 min.
6. Opitional: the cells can be disrupted by sonication.
7. Add Triton X-100 to 1% and DTT to 15 mM, mix.
8. Spin at 13,000 rpm at 4ºC for 30 min.
9. Take 1.33 ml Glutathione Sepharose 4B (Amersham Pharmacia Biotech, Freiburg), spin and wash with 10 ml PBS twice and resuspend to 1ml in PBS.
10. Mix the supernatant from 8. with 1ml beads from 9., 4ºC for 1h.
11. Spin and wash 3-4 times with 10 ml ice-cold PBS (+ 1 mM PMSF and 15 mM DTT).
12. The beads with the bound GST or GST fusion protein are kept for 4ºC and ready for use with GST pull-down. For long-term storage, add 10% glycerin to the beads and keep at -20ºC.

3.4.6.3 GST pull-down of embryo extracts

1. Gastrulation stage *Xenopus* embryos were homogenized in buffer H (50 mM Tris, pH 7.5, 250 mM KCl, 5 mM EDTA, 1 mM dithiothreitol, 0.1% Triton X-100) with protease inhibitors. 100 embryos/ml buffer H.
2. The extracts were centrifuged at 13,000 rpm at 4°C for 30 min. The supernatant was taken and centrifuge again at 13,000 rpm at 4°C for 30 min.
3. The supernatant was cleared by incubation with GST Sepharose beads o/n at 4°C.
4. After centrifugation at 13,000 rpm at 4°C for 30 min, the precleared supernatant was incubated o/n with GST-xPAPCc, GST-xAXPCc or GST Sepharose beads at 4°C.
5. The beads were washed three times with buffer H. The bound proteins were released by boiling in SDS loading buffer and resolved by 10% SDS-PAGE.
6. For mass spectrometry, the gels were subjected to coomassie staining with the Imperial Protein Stain kit. The bands of interest were excised from the gels and sent for mass spectrometry protein identification in Center for Molecular Biology (ZMBH), University of Heidelberg.

3.5 Yeast methods

3.5.1 Preparation of frozen competent L40 yeast cells

1. Grow L40 stain in appropriate media (YPAD) 30° o/n. Approximately 1ml for every 100ml intended to inoculate the next day (i.e. 2.5 ml o/n to inoculate 250ml). For a yeast strain with a selectable plasmid, grow in appropriate selection media about 20 ml for every 100ml intended to inoculate the next day. Some yeast strains in selection media may take 2-3 days to reach saturation. Grow yeast just to the point of saturation (OD_{600} =1.0).

2. Inoculate 250ml YPAD- this will be enough for about every seventy-five 100ul aliquots of frozen competent cells. Scale up as desired. Let them grow to log phase (OD_{600} ~0.7). For a strain with a selectable marker inoculate to OD_{600} ~0.3 so it goes through one doubling time. Too many doubling times lead to loss of selection marker.

3. Spin down cells (6,000g for 10 min) and wash in 0.4 volumes of starting volume (i.e 40 ml for 100 ml culture) of 100 mM LioAC.

4. Spin down cells again and wash in a 0.2 volumes starting volume with 100 mM LioAC.

5. Spin down a final time and resuspend cells in 100mM LioAC with 15% glycerol to a final volume of 0.03 of starting volume.

6. Aliquot 100 µl shots in microfuge tubes and put cells into a cardboard box and allow to freeze slowly in –80°C, unlike *E. coli* competent cells, flash freezing in liquid nitrogen will severely reduce their competency.

3.5.2 Transformation of frozen yeast cells

1. Spin down 100 µl frozen competent cells from –80°C (or made fresh) 1 minute at ~14,000 rpm. Use one tube per single or double transformation.

2. Aspirate supernatant and add the following in order.

50% PEG	240 µl
1M LiAc	36 µl
ssDNA	79 µl
plasmid DNA	5 µl (about 200 ng)
Total	360 µl

A master mix may be made, by leaving out plasmid DNA and mixing the other three ingredients, vortex lightly to mix before aliquotting. If doing a double transformation use 3 µl of each of the plasmid DNA and reduce the amount of ssDNA to 78 µl per transformation to keep the DNA/PEG-LiAc ratio the same.

3. Resuspend the yeast cells in the mixture by vortexing well to remove any clumps.
4. Incubate on rocker in 30°C for 30 min at 150rpm.
5. Heat shock in 42°C water bath for 15 min.
6. Spin down at 14,000 rpm for 1 min., aspirate off the supernatant.
7. Resuspend cells in 200 µl ddH_2O and plate all cells on appropriate selection media plates.
8. Incubate plates in 30°C for 2-4 days until colonies appear.

3.5.3 Pre-transformation of L40 with xPAPCc bait plasmid

1. According to method in **3.5.2**, transform xPAPCc bait plasmid, pNLX3-xPAPCc, into L40 and plate on SD-Trp plate.
2. Inoculate the positive clones in 5 ml SD-Trp media and cultured at 30° till saturation (OD_{600} >1.0).
3. Pellet the yeast cells by spinning the culture at 1000g for 5 min at RT.
4. Resuspend the pellet with 1ml of cold ddH_2O and add 150 µl of fresh-made NaOH/ β -ME buffer.
5. Vortex the cells for 30 seconds and incubate on ice for 15 min.
6. Vortex again and add 150 µl of 55% TCA (in water). Vortex and place on ice for 10 min.
7. Collect the protein extracts by centrifugation at 12,000g for 10 min at 4°C. Remove the supernatant and centrifuge again to remove any residual supernatant.
8. Resuspend the pellet in 300 µl of SU buffer. Add 1-2 µl of Tris-HCl (pH 8.0) if the solution turns yellow. Vortex to resuspend the protein pellet. Heat at 65°C for 3 min prior to loading 30-40 µl sample for SDS/PAGE.
9. Analyze by standard western blot method using antibody against LexA. The positive clones that express LexA-bait fusion protein are called L40-xPAPCc.

3.5.4 Check auto-activation of LacZ reporter gene in L40-xPAPCc

1. Streak L40-xPAPCc strain on SD-Trp+X-Gal plates and incubate at 30°C for 2-4 days.
2. Check whether the colonies turn blue to see whether xPAPCx can activate LacZ by itself.

3.5.5 Optimization of 3-AT concentration to prevent His3 leak in L40-xPAPCc

1. Streak L40-xPAPCc strain on SD-Trp/-His plates containing 0, 2.5, 5, 7.5, 10, 12.5, 15 mM 3-AT and incubate at 30°C for a week.
2. Use the lowest concentration of 3-AT that allows small colonies (< 1 mm) to grow after a week.

3.5.6 Amplification of *Xenopus laevis* oocyte MatchMaker cDNA library

Titer of cDNA library

1. Take *E. coli* frozen glycerol stock (transformed with cDNA library), do not thaw it. Just scratch with a sterile needle or tip at the surface of the frozen bacteria and thaw it in a sterile Ep tube.
2. Take 2 µl thawed bacteria into 1 ml LB media and transfer to plastic cuvette.
3. Measure OD_{600}. 1 $OD_{600} = 10^{6-8}$ viable cells per ml. Assuming an average of 10^7 cells/OD/ml, calculate the approximate concentration of viable cells in the 1 ml dilution.
4. Based on the estimated average concentration dilute 5 x10^6 cells in 25 ml LB media (200 cfu/ µl). Mix by inverting. From that, plate 1 µl, 0.1 µl on LB/Amp plates, respectively. Incubate o/n at 37°C. (25 ml dilution will be used later to amplify the library and is used here to have similar conditions).
5. Count colonies on plates. With this number it is possible to calculate the titer of the cDNA library.

Amplification of library

6. Prewarm 100 pieces of 15 cm LB/Amp plates at 37°C.
7. As before, scratch bacterial stock with a needle or tip and transfer into 1 ml LB media. Measure OD_{600}. Calculate number of viable cells based on estimated titer.
8. Dilute 5 x 10^6 cells in 25 ml LB media. Mix well by inverting. Plate 200 µl (4 x 10^4 cfu/ plate) on each 15 cm LB/Amp plate. Spread bacteria with rounded glassrod. Mix the dilution always before plating the next plate. Plate a small aliquot on small plate (as above) to calculate the number of total colonies. Incubate o/n at 37°C.
- Plate more colonies than there are independent clones in the library (2x -3x).
- Usually about 100 large plates are required to plate 3-4 x10^6 colonies.
9. Add 6 ml LB/Amp media per plate and scrape colonies as completely as possible. Add 2 ml LB/Amp media per plate to wash and collect all media together into sterile flasks (about 800 ml). It takes about 4h.
10. 37°C, 200 rpm for 2h.
11. Take out 1 ml x 8 to make glycerol stocks and freeze at -80°C.
12. Spin the bacteria by centrifugation at 6000 rpm for 15 min at 4°C.
13. Freeze two thirds of the pellet at -80°C.
14. Suspend one third of the pellet in 40 ml P1 buffer (Qiagen).
15. Make 2 Maxi preps (Qiagen).
16. Yield is approximately 500 µg DNA/ Maxi prep.

3.5.7 Transformation of L40-xPAPCc with cDNA library

1. Inoculate single colony of L40-xPAPCc in 10 ml SD-Trp (in 50 ml sterile flask) and grow for 8h at 30°C at 250 rpm.

2. Inoculate all culture from above in 100 ml SD-Trp (in 500 ml sterile flask) and grow o/n at 30°C at 250 rpm.

3. Prepare a 1:10 dilution of the o/n culture in water by diluting 100 µl culture in 900 µl water, prepare a blank by diluting 100 µl SD-Trp in 900 µl water.

4. Measure the OD_{600} of the 1:10 dilution and calculate the OD of the undiluted culture by multiplying with 10.

5. Calculate the amount of culture needed for 30 OD units. Aliquot this amount of the o/n culture into 50 ml Falcon tubes and spin down at 700 g for 5 min

6. Resuspend the pellet in 200 ml 2x YPAD (pre-warmed to 30°C) in a 1L flask and remove 1 ml aliquot.

7. Centrifuge the 1 ml aliquot at 2500 g for 5 min, discard the supernatant and resuspend the pellet in water.

8. Measure the OD_{600} against a water blank, the OD_{600} should be around 0.15 (15 OD units in 100 ml = OD 0.15).

9. Grow the cells at 30°C at 250 rpm for 3-5h to OD_{600} of 0.6 (two cell divisions).

10. Thaw 1 ml single stranded carrier DNA, boil for 5 min, place immediately on ice. Repeat once more and carrier DNA is now ready for use.

11. Prepare the LiOAc/TE mix:

LiOAc/TE mix	10 ml
1 M LiOAc	1 ml
10x TE pH 7.5	1 ml
ddH2O	8 ml

12. Prepare the PEG/LiOAc master mix:

PEG/LiOAc mix	15 ml
1 M LiOAc	1.5 ml
10x TE pH 7.5	1.5 ml
50% PEG	12 ml

13. Divide the 200 ml culture into four 50 ml Falcon tubes.

14. Centrifuge at 700g for 5 min.

15. Resuspend each pellet in 30 ml of sterile water by vortexing.

16. Centrifuge at 700g for 5 min.

17. Remove the supernatant, resuspend each pellet in 1 ml LiOAc/TE mix and transfer to Ep tube.

18. Centrifuge at 700g for 5 min.

19. Remove the supernatant and resuspend each pellet in 600 µl of LiOAc/TE mix.

20. Set up four 50 ml Falcon tubes and add 10 µg of the cDNA library to each tube.

21. Add 200 µl carrier DNA to each tube.

22. Add 600 µl yeast cells from step 19 to each tube.

23. Vortex briefly to mix.

24. Add 2.5 ml PEG mix to each tube.

25. Vortex for 1 min to thoroughly mix all components.

26. Incubate at 30°C for 45 min at 100 rpm.

27. Add 160 µl DMSO to each tube, mix immediately by shaking.

28. Incubate at 42°C for 20 min (Mix occasionally).

29. Pellet cells at 700 g for 5 min.

30. Resuspend each pellet in 3 ml 2x YPAD.

31. Let the cells recover at 30°C for 90 min at 100 rpm.

32. Pellet the cells at 700 g for 5 min.

33. Resuspend each pellet in 5 ml TE, pool into one tube (20 ml).

34. Plate 1 ml per 15 cm SD-Trp/-Leu/-His/+30 mM 3-AT plate (total 20 plates).

35. Use the remaining resuspended cells to prepare $1:10^3$ and $1:10^4$ dilutions in TE and plate on 10 cm SD-Trp/-Leu plates to calculate the transformation efficiency.

36. Seal all plates with parafilm and incubate at 30°C for 3-6 days (2-3 days for SD-Trp/-Leu plates).

37. Calculate the total number of transformants and the transformation efficiency from the number of colonies on SD-Trp/Leu plates:

Total number of transformants = number of colonies on SD-Trp/Leu plate x dilution factor x 20

Transformation efficiency = total number of colonies/40 µg (clones/µg DNA)

Total number of transformants should be greater than 2×10^6.

38. Pick all big colonies that grow on SD-Trp/-Leu/-His/+30 mM 3-AT plates and restreak them on fresh SD-Trp/-Leu/-His/+30 mM 3-AT plates to make master plates.

3.5.8 X-Gal colony-lift filter assay

1. Print 50 lines in each filter and autoclave the filters. Use forceps to make each filter cling to the agar of each SD-Trp/-Leu/-His/+30 mM 3-AT plate.

2. Streak each colony from master plates on each line of the filter (50 colonies per plate) and let them grow at 30°C for 2–4 days.

3. Prepare Z buffer/X-gal solution.

4. For each plate of clonies to be assayed, presoak a sterile Whatman No. 5 or VWR grade 410 filter by placing it in 5 ml of Z buffer/X-gal solution in a clean 15 cm plate.

5. Use forceps to pick up the filter on which cells grow and immerse it completely in liquid nitrogen for 10 seconds.

6. Remove the filter from the liquid nitrogen and let it thaw at RT to permeabilize the cells.

7. Put the presoaked filter in a clean 15 cm plate, then carefully place the filter (colonies facing up) on the presoaked filter. Avoid trapping air bubbles under or between the filters.

8. Seal the plate and incubate the filters at 30°C and check every hour for the appearance of blue colonies. Prolonged incubation (more than 8h) may give false positives.

3.5.9 Plasmid recovery from yeast and retransformation into *E. coli*

1. For each positive clone in X-Gal filter assay (turn blue), inoculate it in 5 ml of SD-Leu media and grow o/n at 30°C at 250 rpm till saturation.

2. Centrifuge 4000 g for 5 min.

3. Resuspend in 250 µl of P1 buffer of Qiagen Miniprep Kit and add about 100 µl of 400-500 µm acid-washed glass beads (Sigma G8772).

4. Add 250 µl of P2 buffer and vortex for 5 min. Incubate for another 5 min.

5. Add 350 µl of P3 buffer and proceed as in the Kit protocol.

6. Wash the column twice with nuclease removal buffer (PB buffer) and once with wash buffer.

7. Elute the plasmid DNA with 30 µl elution buffer heated at 50°C.

8. Thaw the KC8 electrocompetent cells on ice.

9. Add 40 µl of KC8 cells to the prechilled electroporation cuvette.

10. Add 2-4 µl of eluted plasmid DNA to the cells and mix well by gently tapping the tube.

11. Perform the electroporation according to the manufacturer´s instructions.

12. After shocking, immediately add 1 ml of LB media.

13. Transfer the cells to a 15-ml tube and incubate at 37°C for 1h with vigorous shaking (250 rpm). Do not reduce incubation time.

14. Pellet cells by centrifugation at 2500 rpm for 5 min at RT and resuspend pellet in 100 µl of M9 media and spread on M9/Amp agar plates for nutritional selection.

15. Incubate plates at 37°C for 36-48 h and isolate plasmid from 3 randomly selected KC8 transformants.

16. Digest isolated prey plasmids with *Eco*RI/*Xho*I to check the size of the insert to know whether each colony contain more than one prey plasmid.

3.5.10 Confirmation of positive interactions

1. Use primer pACT2-U2 and pACT2-D2 to do sequencing of each prey plasmid.
2. Do BLAST with the prey sequences.
3. Select prey plasmids encoding potential interacting proteins to confirm positive interactions.
4. Cotransform frozen L40 cells with prey plasmid and bait pNLX3-xPAPCc plasmid and plate on SD-Trp/-Leu plates to make sure that both plasmids are contransformed into L40.
5. After incubation at 30°C for 2-3 days, a lot of colonies should appear.
6. Randomly pick up 2-3 colonies from each plate and streak them as a line on SD-Trp/-Leu or SD-Trp/-Leu/-His/+15 mM 3-AT/+X-Gal plates respectively.
7. Incubate SD-Trp/-Leu plates at 30°C for 2-3 days to make sure that the colonies grow. Incubate SD-Trp/-Leu/-His/+15 mM 3-AT/+X-Gal plates at 30°C for 4-6 days. If blue colonies grow, the interaction is interpreted as positive.

4. Result

4.1 Prediction and test of xPAPCc interacting proteins

4.1.1 Prediction of xPAPCc interacting proteins by sequence-based approach

In general proteins contain one or more modular domains such as kinases, phosphatases, and phoshopeptide-binding domains, as well as characteristic short sequence motifs that direct post-translational modifications such as phosphorylation, or mediate binding to specific modular domains. Therefore, to predict protein protein interactions, it is important to identify modular domains and sequence motifs from primary sequence of protein. Various bioinformatics programs have been used extensively to predict successfully modular domains in proteins and recently a web-accessible program Scansite has been developed to facilitate the prediction of short protein sequence motifs, which is more difficult than prediction of domains (Obenauer and Yaffe 2004). Here I used Scansite program (http://scansite.mit.edu/) to scan the protein sequence of xPAPC for predicted domains and motifs. As shows in Fig. 10, several cadherin domains are predicted to be present in the extracellular domain of xPAPC as expected. In terms of intracellular domain, which is the focus of the present study, no modular domains are predicted. However, several motifs are predicted that are likely to be phosphorylated by specific protein kinases including PKC, casein kinase, GSK3 kinase or bind to domains including 14-3-3 domains and SH3 domains.

The 14-3-3 proteins bind phosphoserine/threonine chiefly in the context of two short sequence motifs: mode 1 R-S-x-pS/T-x-P or mode 2 R-x-Y/F-x-pS/T-x-P, where x is any amino acid and pS/T is phosphoserine/threonine (Muslin et al 1996). In xPAPCc, three mode 1 14-3-3 binding motifs are predicted (Fig. 10): S741 RLLSTP (consistent surrounding sequences are shown in red and phosphoserine/threonine is shown underlined), T947 RSATLS, S955 RSSSRY. Previous studies have shown that individual members of 14-3-3 proteins have important functions in early *Xenopus* development (Wu and Muslin 2002; Lau *et al.* 2006). Specially, it was shown that there are two aPKC phosphorylation sites in xPar-1, which are essential for 14-3-3ε binding and for proper gastrulation movements. Binding of 14-3-3ε to xPar-1 induces relocation of xPar-1 from the plasma membranes to the cytoplasm and therefore regulates xPar-1 function in gastrulation (Kusakabe and Nishida 2004). So it is likely that the interaction of 14-3-3 and xPAPCc also play a role in regulation of xPAPC function in gastrulation movements.

To verify the predicted interaction of *Xenopus* 14-3-3 with xPAPCc, cDNA encoding *Xenopus* 14-3-3ε or 14-3-3ζ was cloned into pCS2-MT and cDNA encoding xPAPCc was cloned into

pCS2-Flag. Sense RNA was in vitro transcripted from the plasmid and co-injected into 4 stage *Xenopus* embryos for Co-IP experiments. It was found that x14-3-3ε or x14-3-3ζ could not be co-immunoprecipitated with xPAPCc (results not shown). To further check the interaction of 14-3-3 and xPAPCc, yeast two-hybrid assay was carried and it was also found that 14-3-3ε could not interact with xPAPCc (results not shown). In conclusion, no experimental data support the predicted interaction of xPAPCc with 14-3-3, at least in the case of 14-3-3ε and 14-3-3ζ isoforms, although it is possible that other isoforms of 14-3-3 not tested here could interact with xPAPCc.

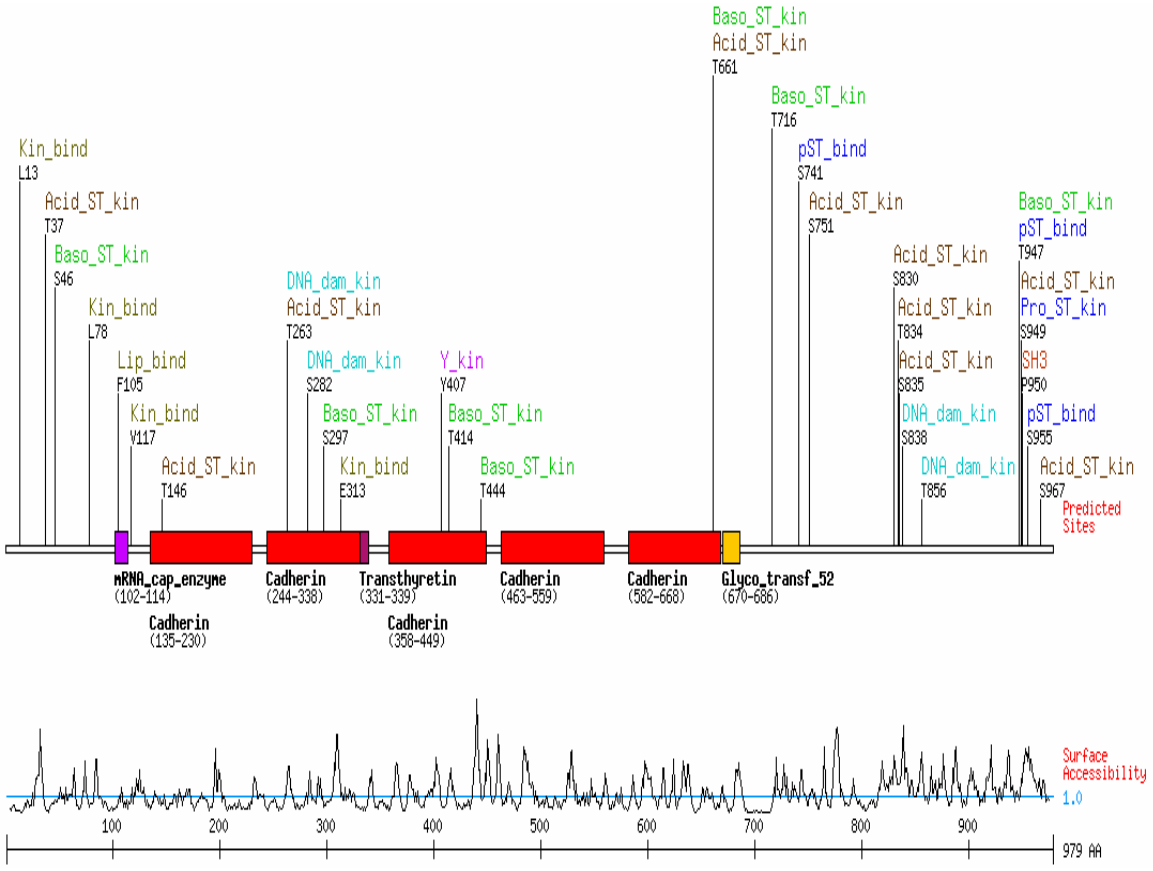

Figure 10. Predicted domains and motifs present in xPAPC by Scansite. The stringency level for prediction is set as medium. 1-692 aa of xPAPC is extracellular domain, 693-714 aa is transmembrane domain and 715-979 is intracellular domain.

4.1.2 Prediction of xPAPC interacting proteins by function-based approach

Another empirical approach to predict proteins that interact with the target protein is to check biomedical literature and find proteins that share a similar function and expression patterns with those of target protein. It is based on the assumption that two physiologically interacting proteins

should have overlapping function and expression patterns. As described in **2.2.7**, β-catenin can interact with C-terminal region of classic cadherins but not that of protocadherin and mediate the signaling of classic cadherins. Interestingly, p120 catenin subfamily like p120 and ARVCF bind the juxtamembrane region of classic cadherin and mediate Rho GTPase activity. In *Xenopus*, p120 and ARVCF are enriched in the animal hemisphere in early gastrula stage and they are essential for CE movements (Paulson *et al.* 2000). Considering that xPAPC also regulates Rho activity, is required for CE movements, and is expressed in dorsal marginal zone at gastrula, it is tempting to speculate that p120 catenin subfamily interact with the juxtamembrane region of xPAPC and mediate the signaling function of xPAPC. Therefore, sense RNA was in vitro transcripted from the Myc-tagged p120 or HA-tagged ARVCF constructs and co-injected with Flag-xPAPCc mRNA into 4 stage *Xenopus* embryos for Co-IP experiments. The results (not shown here) showed that p120 or ARVCF did not associate with xPAPCc. In conclusion, it is unlikely that p120 catenin subfamily members interact with xPAPC and mediate the signaling of xPAPC to modulate gastrulation movements.

4.2 GST pull-down assay to identify xPAPC interacting proteins

While prediction approach failed to find xPAPC interacting proteins, GST pull-down approach was taken to identify the interacting proteins.

4.2.1 Cloning and expression of GST-xPAPCc fusion constructs

Because the present study aims to identify interacting proteins of cytoplasmic domain of xPAPC, the construct of this domain fused with GST is necessary for the production of the recombinant protein in *E. coli*. Therefore, cDNA encoding xPAPCc was amplified by PCR and cloned into GST vector pGEX6p2 by *Sal*I/*Not*I to create pGEX-xPAPCc.

To overcome the degradation problem, the *E. coli* strain BL21, which lacks the intrinsic proteases encoded by the *omp*T and *lon* genes, was used to express the pGEX constructs. BL21 cells were transformed with pGEX6p2 or pGEX-xPAPCc and tested for GST fusion protein expression (Fig. 11). A single band of approximately 26 KDa was observed in Lane 5, corresponding well to the expected size of GST. In contrast, several bands of different sizes were observed in Lane 3. While two strong bands appeared at approximately 55 KDa representing full-length GST-xPAPCc fusion protein, several weak bands likely representing degraded GST-xPAPCc protein were observed between 55 KDa and 26 KDa. To reduce the production of these truncated proteins, lysozyme digestion method was used instead of sonication method with the hope that less protein degradation will happened and more full-length GST-xPAPCc protein will be produced. However, as sown in Lane 4, no big difference was achieved compared with Lane 3. By western blot using GST antibody, all these bands appeared between 55 and 26 KDa gave positive signal (results not shown), meaning that all these bands represent truncated GST-xPAPCc proteins but not contaminated proteins from *E. coli* during the purification.

Based on all these data it is persumed that there are several codons present in xPAPCc sequence that are very rare in prokaryotes but frequently used in eukaryotes (considering that even invertebrate has no PAPC homolog), which may lead to the occurrence of truncated products due to premature translation termination. In other words, these truncated GST-xPAPCc proteins are likely a result of inefficient translation rather than proteolytic degradation.

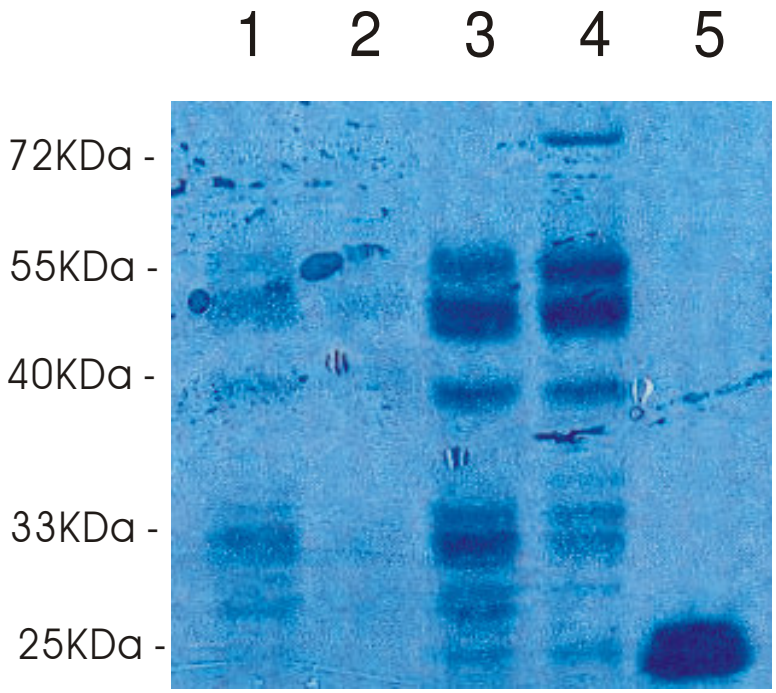

Figure 11. Expression and purification of GST-xPAPCc fusion protein in BL21. BL21 transformed with pGEX-xPAPCc or pGEX6p2 were induced to express recombinant protein with 1 M IPTG for 3h at 30ºC. Whole cell lysate from induced cultures was either sonicated or lysozyme-digested and subjected to GST purification beads. Start elution (E1) from lysozyme-digested samples (Lane 4), E1 from sonicated samples (Lane 3), middle elution (E2) from sonicated samples (Lane 2) and GST purification beads after elution (Lane 1) as well as E1 from sonicated pGEX6p2 samples (Lane 5) were analysed by SDS-PAGE and Coomassie staining.

4.2.2 GST pull-down assay

Since the majority of purified proteins are full-length GST-xPAPCc fusion protein, GST pull-down assay was carried to identify proteins associated with xPAPCc. To make a better control, cytoplasmic domain of xAXPC was fused with GST to make GST-xAXPCc fusion protein and also used in GST-pulldown to identify those proteins present in embryos that specially associated with xPAPCc. By several preliminary GST pull-down experiments using sensitive silver staining of SDS-PAGE gels, several special bands appeared in GST-xPAPCc pull-down lanes but not in GST-xAXPCc or GST pull-down lanes. To prepare these xPAPCc binding proteins for analysis by mass spectrometry, large scale GST pull-down was performed with lysates made from embryos in gastrulation stage and proteins associated with GST-xPAPCc were analysed by coomassie staining of SDS-PAGE gels (Fig.12).

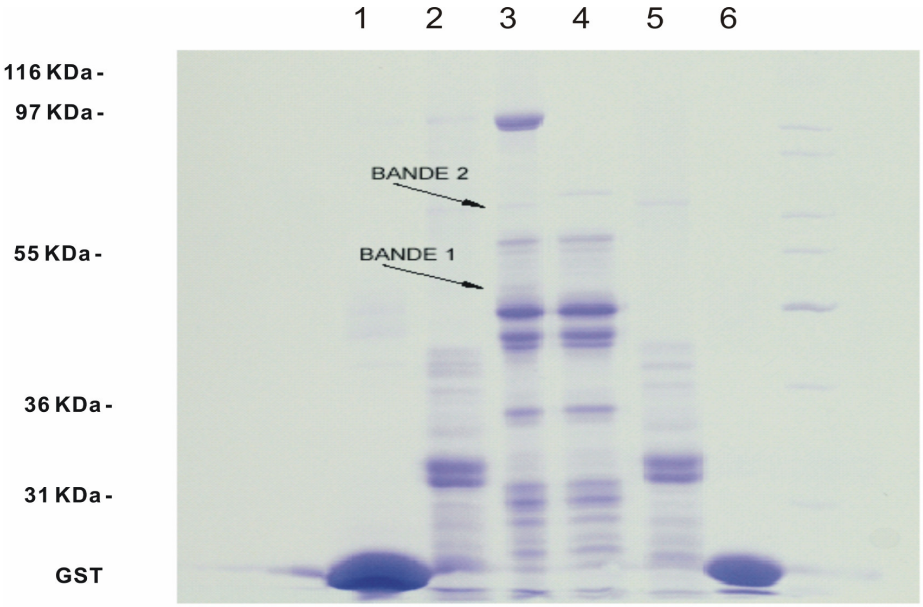

Figure 12. xPAPCc associated proteins pulled-down from gastrulation-stage *X. laevis* embryos. Proteins from embryo extracts that bound to xPAPCc were affinity-purified with GST-xPAPCc and resolved by SDS-PAGE and coomassie staining. Two proteins with molecular masses of 70 and 50 KDa were pulled down by GST-xPAPCc but not by GST-xAXPCc or GST beads. The two bands were excised from the gel and identified by MALDI time-of-flight mass spectrometry. Lane 1: GST beads + 100 embryo extracts, 2: GST-xAXPCc beads + 100 embryo extracts, 3: GST-xPAPCc beads + 100 embryo extracts, 4: GST-xPAPCc beads + buffer H, 5: GST-xAXPCc beads + buffer H, 6: GST beads + buffer H.

Mass spectrometry analysis revealed that the 50 KDa band corresponded to β-tubulin protein while the 70 KDa band corresponded to fragment of vitellogenin A2 precursor (molecular weight 203 KDa). Vitellogenin A2 precursor is the major egg-yolk proteins that are sources of nutrients during early embryo development and its involvement in gastrulation movements has never been reported. Therefore this band may be derived from embryo extracts contaminated with yolk and was excluded for further study.

Microtubules, an important component of the cytoskeleton, are polymers of α- and β-tubulin dimers. Microtubules serve as structural components within cells and are involved in many cellular processes including mitosis, cytokinesis, and vesicular transport. Therefore, it is possible that the binding of xPAPCc to tubulin may be involved in the transport of xPAPC to special membrane area to regulate planar cellular polarity. So it is important to verify the interaction of xPAPCc and β-tubulin by other methods. Unfortunately, their interaction was tested as negative by Co-IP and yeast two-hybrid methods (results not shown).

In conclusion, no interaction partners of xPAPCc were identified by GST pull-down approach.

4.3 Yeast two-hybrid screen

The yeast two-hybrid assay is a powerful tool for the study of protein-protein interactions (Fields and Song 1989). Fusion protein consisting of the DNA-binding domain and the target protein ("bait") is used to screen a cDNA library fused to the activation domain. In yeast cells where interaction between the coexpressed bait protein and a library encoded target protein occurs, reporter genes under the control of a promoter with binding sites for the reconstituted transcription factor are activated. For the Gal4-based Matchmaker *Xenopus laevis* oocytes cDNA library employed in this study, interacting clones will express HIS3 that allows positive metabolic selection, and β-galactosidase that can be detected by blue staining when tested with X-Gal. To identify potential interaction partners of xPAPCc, cDNA fusion construct encoding the xPAPCc together with the yeast transcription factor LexA DNA binding domain (LexA-BD) was generated and used to screen the oocytes cDNA library fused to the Gal4 activation domain (Gal4-AD).

4.3.1 Cloning of yeast two-hybrid bait vector

cDNA encoding xPAPCc was PCR amplified with pCS2-fl-PAPC(-UTR) as template and *Bam*HI and *Pst* I sites were introduced into the 5´and 3´ends of the PCR product, respectively. The PCR product and vector pNLX3 were cut with *Bam*HI/*Pst*I, ligated and transformed into E. coli. Recombinant plasmids were purified from 4 random clones and three of them had correct size of insert after digestion with *Bam*HI/*Pst*I (Fig.13). After sequencing we verified that we got correct pNLX3-xPAPCc bait vector.

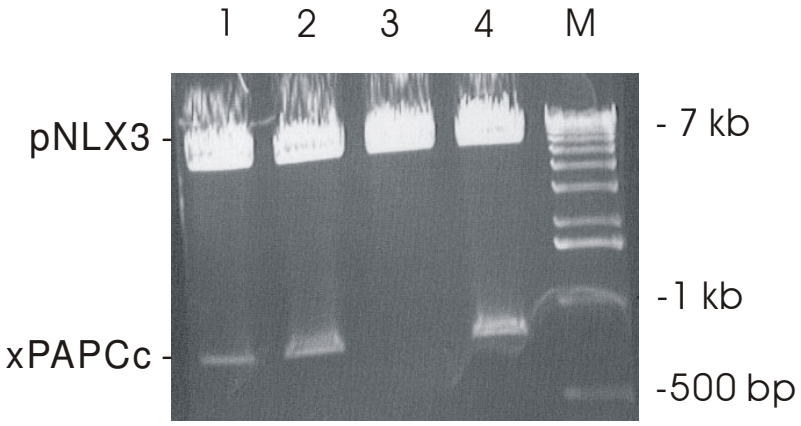

Figure 13. Restriction analysis of recombinant bait vector. Recombinant pNLX3-xPAPCc bait vectors were cut by *Bam*HI/*Pst*I to check the insert. 1-4: four randomly selected clones. M: 1 Kb DNA ladder.

4.3.2 Expression of bait fusion protein in yeast strain L40

Because the plasmid pNLX3 has *TRP1* marker, pNLX3-xPAPCc bait vector and pNLX3 empty vector (as control) were transformed into L40 and positive clones were selected on SD medium lacking thryptophan. Three randomly selected pNLX3-xPAPCc clones and two pNLX3 clones were analyzed for expression of LexA-BD-xPAPCc fusion protein or LexA-BD protein by western blot with antibody against LexA-BD. Clone 3 has a strong expression of bait fusion protein, therefore it is named as L40-xPAPCc and used for further analysis.

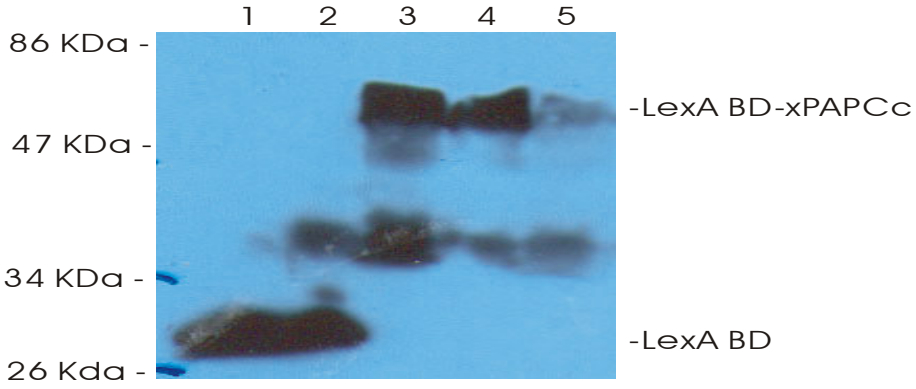

Figure 14. Expression of LexA-BD-xPAPCc in L40. Whole cell lysates were made from L40 clones transformed with different vector and proteins were separated by 12% SDS-PAGE and subjected to western blot by LexA-BD antibody. 1-2: two clones transformed with pNLX3, 3-5: three clones transformed with pNLX3-xPAPCc.

4.3.3 Test of auto-activation of *LacZ* reporter gene in L40-xPAPCc

Some bait proteins are not suitable for yeast two-hybrid assay since they have transcriptional activation function, which means that they can activate reporter genes even without interacting with prey proteins. To show whether this is the case for xPAPCc, L40-xPAPCc strain was streaked on SD-Trp/+X-Gal plate and after incubation for 4 days, the clones did not turn blue. So we can conclude that xPAPCc can not activatate *LacZ* by itself and is suitable for further yeast two-hybrid assay.

4.3.4 Optimization of 3-AT concentration to prevent *His3* leak in L40-xPAPCc

Besides *LacZ*, another reporter gene for positive interaction is *His3*. That means when bait and prey protein interact, the yeast can grow on media lacking His. However, in some instance, yeast transformed with bait plasmids can lead to background growth on media lacking His. 3-AT is a competitive inhibitor of yeast His3 protein (His3p) and used to inhibit low levels of His3p expression, and thus to suppress background growth.

To optimize the concentration of 3-AT to inhibit background growth of L40-xPAPCc on media lacking His, L40-xPAPCc strain was streaked on SD-Trp/-His plates containing a series of 3-AT concentration and incubated for a week. It was observed that L40-xPAPCc grew on plates containing 0, 2.5, 5, 7.5, 10 and 12.5 mM 3-AT, but not on plates containing 15 mM 3-AT. So the optimal 3-AT concentration to inhibit background growth is 15 mM. Since the stronger bait and prey proteins interact, the more His3p will be produced. Therefore, higher concentration of 3-AT in selection media is better to select strong two-hybrid interaction. So media containing 30 mM 3-AT will be used for library screening of strong interaction partners of xPAPCc.

4.3.5 Amplification of *Xenopus laevis* oocyte MatchMaker cDNA library

Since the premade library is provided as *E. coli* transformants, not as purified DNA, I should amplify the library to produce enough plasmid DNA to screen the library in yeast.
By counting colonies on plates the titer of the library was calculated as: 2x 10^8 cfu/ml. Amplification of library was achieved by plating total of 4x 10^6 cfu on 100 pieces of 15 cm LB/Amp plates. 800 ug plasmid DNA was purified from one third of bacteria pellet collected from the plates. This amount of DNA is enough for library screening.

Since the cDNAs were cloned into pACT2 vector by *Eco*RI/*Xho*I, the quality of purified plasmid DNA was checked by digestion with *Eco*RI/*Xho*I.

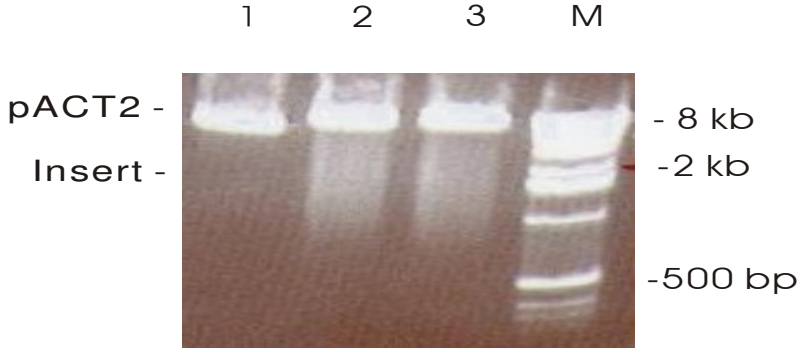

Figure 15. Restriction analysis of plasmid DNA purified from library culture. 1. 400 ng pACT2 vector, 2-3: 400 ng purified plasmid DNA, M: 1 Kb DNA ladder.

As shown in Fig.15, while the empty pACT2 vector has no insert (line 1), purified plasmid DNA has cDNA insert with a range of size from 700 bp to 4 kb and the majority of the insert is about 2 kb (line 2 and 3). This is in accordance with the product information of cDNA library provided by Clontech. Thus it is concluded that the plasmid DNA purified from library culture is good enough for subsequent library screening.

4.3.6 Library screening with xPAPCc bait plasmid

Xenopus laevis oocyte cDNA library was transformed into L40 harboring xPAPCc bait plasmid. Transformation efficiency was calculated by plating dilutions of transformants on SD-Trp/Leu plates. About 100 colonies grew on SD-Trp/Leu plates when 10^4 dilution was plated, which means that totally 10^6 clones were screened in this assay. After 6 days of incubation, totally 261 big clones (≥ 1mm) grew on 20 pieces of SD-Trp/-Leu/-His/+30 mM 3-AT plates. These 261 clones represent potential interacting partners of xPAPCc and therefore subjected to further X-Gal colony-life filter assay. 77 clones showed strong blue staining while the left showed weak or no blue staining. Therefore these 77 clones are considered as positive clones that harbor prey plasmids that might interact with xPAPCc.

4.3.7 Analysis of positive clones

Since many clones may contain the same insert, to sort clones to eliminate duplicates, a simple method is to amplify the inserts by PCR with yeast cells as template and characterize PCR product by digestion with a frequent-cutter restriction enzyme like *Alu*I. However, in my hand, PCR with yeast cells as template was not so consistent, sometimes inserts can be amplified and sometimes it failed. Therefore, DNA was extracted from each positive yeast clone and retransformed into the *E. coli* strain KC8, which carries a leucine deficiency that can be complemented by the *LEU2* marker present on the library vector pACT2, thereby selecting only for this plasmid while separating it from the bait vector also present in the DNA preparation. The isolated prey plasmids were subjected to *Eco*RI/*Xho*I digestion to check the size of the insert and then sequenced from both direction with primer pACT2-U2 and pACT2-D2. Sequences were analysed by BLAST and the proteins encoded by these 77 positive clones were shown in Table 1.

Most of the clones encode DNA or RNA binding proteins like transcription factor, especially those with zinc finger (ZF) domain, hnRNP, Rad52 and tRNA-ribosyltransferase 1, proteasome subunits like cathepsin, which are commonly encountered false positives in yeast two-hybrid screens (http://www.fccc.edu/research/labs/golemis/main_false.html). Some clones encode Wnt11, granulin, fibronectin and nidogen-2 that are known to be localized in extracellular matrix and are therefore unlikely to interact with cytoplasmic xPAPCc in a physiological context. Two clones encode claudin4L2 and RGS12 (regulator of G protein signaling 12) proteins that are not in frame with the activation domain and are also excluded for further analysis. Several clones encode sequences that have no homolog perhaps due to the fact that the genome of *Xenopus laevis* is not completely sequenced yet. The left clones are striking in that most of them encode

serine/threonine protein kinases that include Nemo-like kinase (NLK, 5 clones), casein kinsase II beta subunit (CK2β, 2 clones), polo-like kinase 1 (Plk1, 1 clone), STE20-like TAO kinase 1 (1 clone), while several clones encode sprouty1 (1 clone), neutral sphingomyelinase II (1 clone), homolog of X.tropicalis LOC549360 (1 clone) and putative protein LOC431845 (2 clones). These serine/threonin protein kinases are known to play important roles in signaling. Sprouty is well established to be potent regulator of FGF signaling and recently was implicated in regulation of PCP signaling in *Xenopus*. Neutral sphingomyelinase II catalyzes the hydrolysis of sphingomyelin to form ceramide and phosphocholine and ceramide mediates numerous cellular functions. Homolog of *X. tropicalis* LOC549360 is a protein composed of 593 aa and has 3 LIM domains, indicating it may act as an adaptor in signaling. Putative protein LOC431845 is predicted as a 725 aa transmembrane protein conserved in worm, mice and human. The putative transmembrane domain is 378-395 aa. The DNA sequence in the prey plasmid encodes 425-725 aa. So it is physiologically relevant that its cytoplasmic domain interact with xPAPCc.

To confirm the interaction of these encoded prey proteins with xPAPCc, the corresponding prey plasmid and pNLX3-xPAPCc or pNLX3 (as negative control) were cotransformed into L40 and selected on SD-Trp/-Leu plates to guarantee the presence of both prey and bait plasmids in L40 and 2-3 colonies from each plate were streaked on selective SD-Trp/-Leu/-His/+15 mM 3-AT/+X-Gal plates for observation of growth and colony color (results shown in right two column of Table 1). If the colony did not grow, or grow but the colony is white, then the interaction is negative (marked as -). If the colony grows and turns light blue, then the interaction is weak (marked as +). If the colony turns blue, then the interaction is medium (marked as ++). If the colony turns dark blue, then the interaction is strong (marked as +++).

The interaction of NLK, CK2β, STE20-like TAO kinase 1, sprouty1, neutral sphingomyelinase II, homolog of X.tropicalis LOC549360 and LOC431845 with xPAPCc are verified since only in the presence of pNLX3-xPAPCc but not pNLX3 that these transformed clones can grow on selective media and turn blue, indicating the activation of reporter genes as a result of their interaction. However, the interaction of Plk1 with xPAPCc was not verified since yeast cotransformed with plasmids encoding these two proteins can not grow on selective media.

In conclusion, by yeast two-hybrid screen several interacting partners of xPAPCc were successfully identified, providing the basis for further characterization of their physical and functional interaction.

Table 1. Prey proteins encoded by 77 positive clones isolated in yeast two-hybrid

Clone No.	Insert size (kb)	Prey protein	Growth on selective plate	Verified interaction
2	1.5	No homolog	-	
3	3+1.6	Brachyury and Tbx related protein (Brat)	-	
4	1.2	Hairy2 (transcription factor)	+	
5	1+0.9	IMAGE4970961, DNA polymerase delta p38 subunit	+	
6	2.4	Polo-like kinase 1	-	-
8	1	LOC494658,hnRNP	+	
9	1.2+0.4	Fibronection	+	
10	2.5	Rad52 (DNA repair)	+	
12	1.2	No homolog		
25	1.6+1.4	No homolog		
27	1.2+0.4	Fibronection		
29	2	Sprouty1	+++	+++
30	2.2+0.7	LOC495003, nidogen-2	+	
32	1.9+0.8	MGC79044, Q6PCB6-LOC58489 protein	+++	+++
54	1.6+0.7	NLK	+++	+++
62	3	Homolog of X.tropicalis LOC549360,3 LIM domains	+++	+++
65	1.6+0.7	NLK	+++	+++
68	1.3	No homolog		
139	1.6+0.7	NLK		
142	1.5	queuine tRNA-ribosyltransferase 1	+++	
148	2.1	tudor repeat associator with PCTAIRE2 (TRAP), 3 tudor RNA binding domains	-	
151	2.5	L08474, ubiquitin-like fusion protein, Ub&ZF domain	+	+
154	3	chondroitin sulfate glucuronyltransferase	+	+
155	1.6+1.5	No homolog		
164	3	chondroitin sulfate glucuronyltransferase	+	+
166	1.2+0.4	Fibronection	+	
167	4	IMAGE4970961, DNA polymerase delta p38 subunit		
172	2.8	IMAGE5516170, Smarcd1(transcription factor)		
183	2.2+0.7	LOC495003, nidogen-2		
185	1.2	LOC495091, Secernin 2,dipeptidase activity	++	++
187	0.8+0.7	LOC431845 (ZF domain)		
188	1.5	queuine tRNA-ribosyltransferase 1		
202	2.8	IMAGE5516170, Smarcd1(transcription factor)		
203	1.8	Cathepsin B	+++	
204	1.5	queuine tRNA-ribosyltransferase 1		
205	1.2	Glutamine synthetase	+	+
206	0.6	CK2β	+++	+++
207		hnRNP		
208	3	Granulin (growth factor)	+++	
209	1.6+0.7	Homolog of X.tropicalis MGC147329(ZF domain)		
211	2.2+0.7	LOC495003, nidogen-2		
212	3	Granulin (growth factor)		
213	1.8	Cathepsin B		
214	1.2	Hairy2 (transcription factor)		
215		hnRNP		
216	0.7+0.6	hnRNP		
222	1.6+1	No homolog		
223		hnRNP		
224	1.5	queuine tRNA-ribosyltransferase 1		

226	1.8	Cathepsin B		
227	1	claudin4L2, not in frame	+++	
228	1.5	queuine tRNA-ribosyltransferase 1		
229	1.6	Wnt11	+++	
231	1.6+0.7	NLK		
232	2.5	Rad52 (DNA repair)		
233	1.6+0.7	NLK		
234		Homolog of X.tropicalis LOC548850, RNA binding motif protein 7	+++	
235	0.9+0.6	No homolog	+++	+++
237	0.6	CK2β	+++	+++
238	1.5	DAZ-like protein (involved in germ cell)	+++	
239	3	Granulin (growth factor)	++	
241	2.6	MGC79044, Q6PCB6-LOC58489 protein	++	++
243	0.8+0.7	LOC431845	+++	+++
244	1.5	MGC115457,neutral sphingomyelinase II	+++	+++
245	3	Granulin (growth factor)	++	
247	1.2	Glutamine synthetase	+	+
249	1.8	No homolog	+++	
250		No homolog		
252		hnRNP		
253	0.9	MGC115737, RGS12, not in frame	+	
254	1.5	queuine tRNA-ribosyltransferase 1		
255	0.8+0.7	LOC431845	+++	+++
256	1.5	queuine tRNA-ribosyltransferase 1		
257	2.3	MGC80412,STE20-like kinase,TAO kinase 1	+++	+++
258	1.2	Hairy2(transcription factor)		
260	1.9+0.8	MGC79044, Q6PCB6-LOC58489 protein	+++	+++
261	1.6+1.3	No homolog	+++	+++

4.4 Physical and functional interaction of xPAPC and xSpry1

One positive clone from yeast two-hybrid screen encodes xSpry1. Sequencing analysis revealed that this clone contained partial sequence of xSpry1 cDNA and the ORF of xSpry1 was in frame with that of the ACT2 vector. Moreover, the partial sequence of xSpry1 in this clone would encode a protein corresponding to 173-319 aa of xSpry1, meaning that the C-terminal half of xSpry1 is enough to interact with xPAPCc. The function of Spry is mostly studied in *Drosophila* and mammal cells, where it acts to inbibit FGF signaling in a negative feedback as described in **2.2.2**. Spry is induced by FGF signaling and then blocks FGF signaling at several levels. In *Xenopus*, only recently it is shown that Spry can inhibit PCP signaling although the mechanism is unknown (Sivak *et al.* 2005). Given the fact that xPAPC can enhance PCP siganling, it is of great interest to address the interaction of xPAPCc and xSpry1 in details.

4.4.1 Physical interaction of xPAPC and xSpry1

First I need to use different methods to demonstrate that xPAPCc and xSpry1 interact specially both *in vitro* and *in vivo*.

4.4.1.1 Interaction of xPAPC and xSpry1 revealed by yeast two-hybrid

In general, protein protein interaction depends on posttranslational modification. To further verify the specific interaction of xPAPCc and xSpry1, I noticed that there are 3 phosphoserine/threonine binding motifs in xPAPCc as shown in **4.1** and demonstrated in Fig.16. Therefore, I examine whether phosphorylation of these motifs are important for the interaction of xPAPCc and xSpry1. As shown in Fig. 17, S741 to A741 mutation weakened the interaction; T947 to A947 had no impact on interaction; while S955 to A955 mutation abolished the interaction. On the other hand, phosphorylation-mimic mutants including S741 to E741 and S955 to E955 interact with xSpry1. These results strongly suggest that the interaction of xPAPCc and xSpry1 is phosphorylation-dependent.

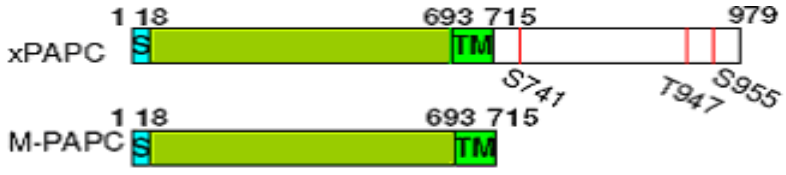

Figure 16. Schematic representation of *Xenopus* PAPC structure. The signal peptide is marked in blue and the transmembrane domain in green. 3 predicted 14-3-3 binding sites S741, T947 and S955 (Scansite 2.0) are marked in red. M-PAPC lacks the cytoplasmic domain.

Spry proteins constitute a large family of highly conserved members. To examine whether the interaction of xPAPCc and xSpry1 is conserved, I made prey vectors that express *Drosophila* Sprouty (dSpry), xSpry2 or xSpred1 (*Xenopus* Sprouty-related protein 1) and found that xPAPCc can interact with dSpry, xSpry2 but not with xSpred1, thus demonstrating that the interaction of xPAPCc and Spry is highly specific. Importantly, I found that xDsh can not bind xPAPCc (Fig.17).

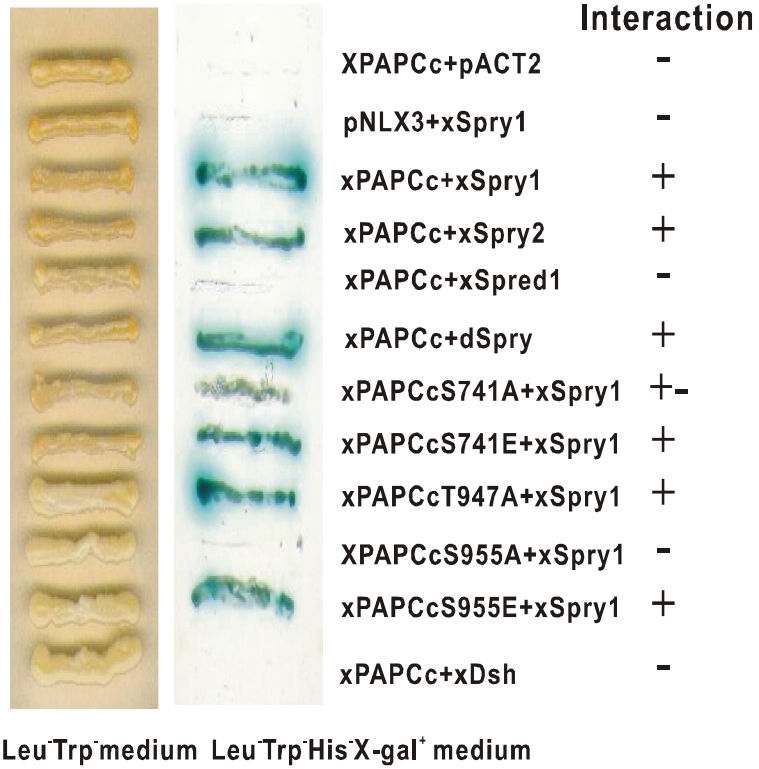

Figure 17. Interaction of xPAPCc and Spry revealed by yeast two-hybrid assay. cDNAs were cloned into bait vector pNLX3 or prey vector pACT2 and co-transformed into yeast strain L40 and selected on SD-Trp/-Leu plates at 30°C for 2-3 days to make sure that both bait and prey vectors are transformed. One representative colony from each co-transformation was picked and streaked onto Leu^-Trp^- medium (SD-Trp/-Leu plates, left panel) or $Leu^-Trp^-His^-X\text{-}gal^+$ medium (SD-Trp/-Leu/-His/+15 mM 3-AT/+X-Gal plates, right panel) and incubated at 30°C for 4-6 days. Blue colonies grow on $Leu^-Trp^-His^-X\text{-}gal^+$ medium when bait and prey proteins interact.

4.4.1.2 Interaction of homologues of PAPC and Sprouty

Since xPAPCc can bind xSpry1, xSpry2 and dSpry, it is interesting to characterize whether the interaction of PAPCc and Sprouty is also conserved in human. hPcdh8 is claimed as the homolog of xPAPC (Yamamoto *et al.* 2000), so I made bait construct of pNLX3-hPcdh8c (cytoplasmic domain of hPcdh8) and checked their interaction with human or *Xenopus* Sprouty. The cytoplasmic domain of PAPC from all four vertebrate species including mouse, *Xenopus*, zebrafish and human contain a very conserved 16-amino acid invariant region KDSGKGDSDFNDSDSD (Yamamoto *et al.* 2000), to see whether this region is important for the

interaction of PAPC with Sprouty, I made deletion construct pNLX3-xPAPCcΔ16aa. The results are summarized in Table 2. hPcdh8c could bind hSpry1 weakly but not bind hSpry2, suggesting the interaction of cytoplasmic domain of PAPC and Sprouty is not well conserved. Also supporting this is that the deletion of conserved 16-amino acid region did not abrogate the interaction of xPAPCc with xSpry1 or xSpry2. It is very interesting that xPAPCc can interact with hSpry1 but not hSpry2. In contrast, hPcdh8c could bind xSpry2 strongly while bind xSpry1 weakly. These results suggest that there are some specificity in the interaction of different members of PAPC and Sprouty.

Table 2. Interaction of PAPC homologs with Sprouty homologs by yeast two-hybrid assay.

Bait	Prey	Interaction
xPAPCcΔ16aa	xSpry1	+
xPAPCcΔ16aa	xSpry2	+
hPcdh8c	hSpry1	weak
hPcdh8c	hSpry2	-
xPAPCc	hSpry1	+
xPAPCc	hSpry2	-
hPcdh8c	xSpry1	weak
hPcdh8c	xSpry2	+

4.4.1.3 Association of xPAPC and xSpry1 revealed by Co-IP

It has been documented that xPAPC is expressed in the dorsal marginal zone at stage 9.5 and the expression expands to about 180º of the marginal zone at stage 10.5 (Kim *et al.* 1998); while expression of xSpry1 was first localized to the dorsal marginal zone during gastrula stages, but later expanded laterally and ventrally (Sivak *et al.* 2005), thus xPAPC and xSpry1 share similar expression patterns in early gastrulation stage (Fig. 18) and have great chance to interact during gastrulation.

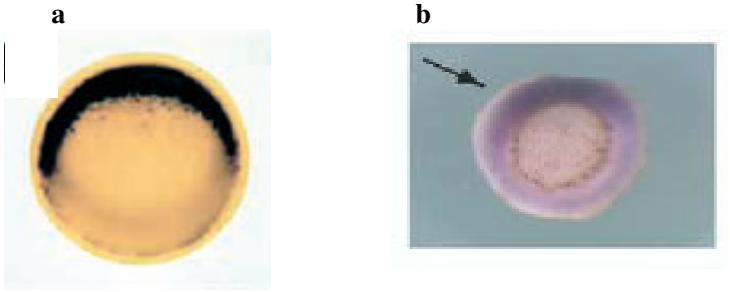

Figure 18. Expression Patterns of xPAPC and xSpry1 Overlap in early gastrulation. a. xPAPC is expressed in dorsal marginal zone at stage 10.5, later its expression expanded laterally and ventrally. **b.** xSpry1 is also expressed in dorsal marginal zone at stage 10.5, and later expanded laterally and ventrally (modified from Kim *et al.* 1998; Sivak *et al.* 2005).

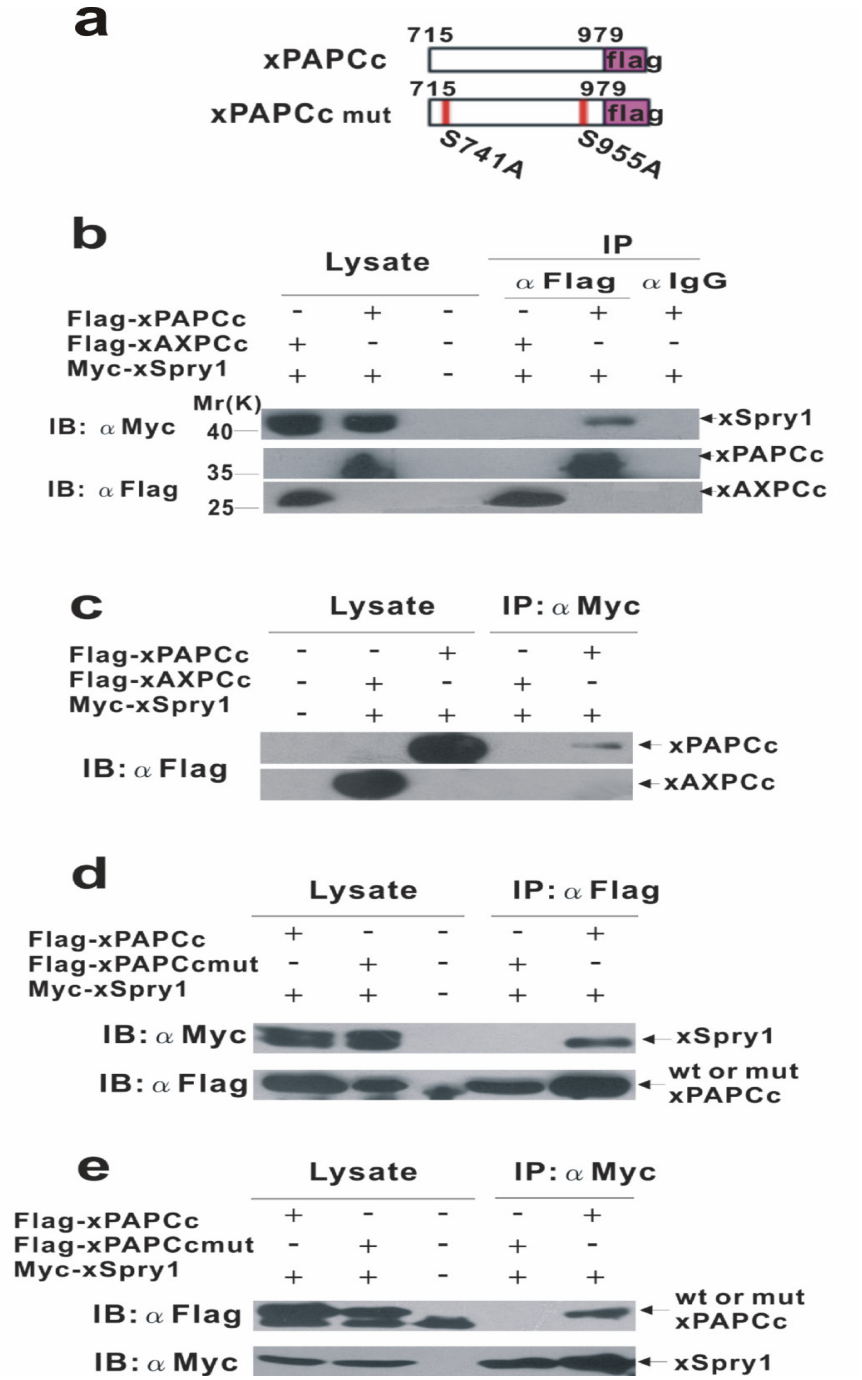

Figure 19. xPAPC associates with xSpry1 in embryos. a. Schematic representation of Flag-tagged xPAPCc constructs and the mutant form xPAPCcmut in which both serine residues in 741 and 955 are mutated to alanine. **b-e.** 4-cell-stage embryos were injected with Flag-xPAPCc, Flag-xPAPCcmut (S741A/S955A) or Flag-xAXPCc mRNA (500 pg) together with Myc-xSpry1 mRNA (500 pg) and grown up to gastrula stages. Embryo lysates were collected and subjected to Co-IP and western blot with Myc or Flag Ab.

Co-immunoprecipitation is a commonly used technique to check protein protein interaction. In Co-IP the target antigen precipitated by the corresponding Ab “co-precipitates” a binding partner from lysate, which is detected by Ab against the partner. Therefore Co-IP assay was performed to demonstrate the interaction of xPAPCc and xSpry1 *in vivo*. To this aim I made

Flag-tagged xPAPCc or xPAPCc with mutations in the two phosphorylation sites implicated in the interaction with xSpry1 in yeast (Fig.19a). As a control, I made Flag-tagged xAXPCc construct. Myc-xSpry1 was Co-IPed with Flag-xPAPCc by Flag Ab but not the preimmune serum and furthermore, Myc-xSpry1 was not Co-IPed with Flag-xAXPCc (Fig.19b). In a reciprocal experiment, Myc Ab specifically Co-IPed Flag-xPAPCc but not Flag-xAXPCc (Fig.19c). To further confirm the interaction is specific and phosphorylation-dependent, I tested the interaction between xSpry1 and mutant xPAPCc. Myc-xSpry1 was Co-IPed with Flag-xPAPCc but not with Flag-xAXPCc-S741A/S955A (Fig.19d). In a reciprocal experiment, Myc Ab specifically Co-IPed Flag-xPAPCc but not Flag-xPAPCc-S741A/S955A (Fig.19e). These data indicate that xPAPC interacts with xSpry1 in *Xenopus* embryos.

4.4.1.4 Physical interaction of xPAPC and xSpry1 *in vivo*

To further demonstrate the *in vivo* interaction of xPAPC and xSpry1, I propose that xPAPC should recruit xSpry1 to membrane since xPAPC is a membrane protein. When xSpry1-GFP mRNA was injected into embryos, a large part of xSpry1 appeared on the membrane, but there were some left in cytoplasm (Fig.20a). This may be due to endogenous FGF signaling in the cells of animal caps because it has been shown in mammal cells that FGF can induce membrane recruitment of Sprouty (Hanafusa *et al.* 2002). When xPAPC mRNA was coinjected, almost all of xSpry1 went to membrane (Fig.20b). Nevertheless, when M-PAPC mRNA was coinjected, the situation was similar to xSpry1 injected alone (Fig.20c). This indicates that cytoplasmic domain of xPAPC is needed to recruit xSpry1 to membrane.

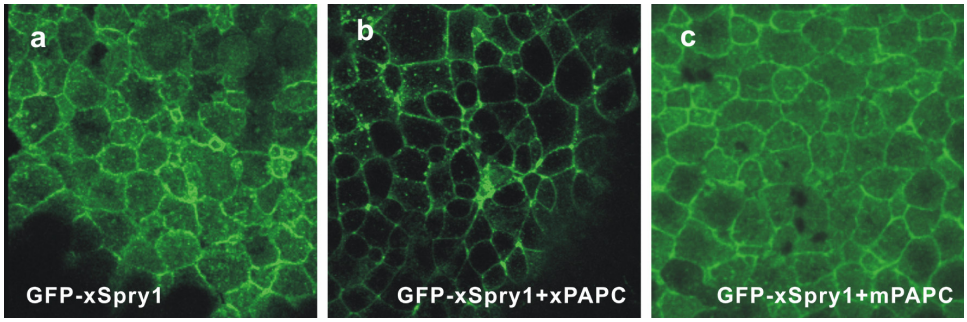

Figure 20. Membrane recruitment of GFP-xSpry1 by xPAPC in animal cap cells. 400 pg GFP-xSpry1 mRNA was injected alone (**a**) or with 600 pg xPAPC mRNA (**b**) or 600 pg M-PAPC mRNA (**c**) into 4-cell-stage embryos. At late blastula stages (stage 9) animal caps were excised and the localization of GFP-xSpry1 was determined by confocal microscopy.

4.4.2 Functional interaction of xPAPC and xSpry1

Having established that xPAPCc physically associates with xSpry1, I next address the biological significance of the interaction between xPAPC and xSpry1. It is interesting to note that xSpry1 and xSpry2 has been suggested recently as an inhibitor of PCP pathway (Sivak *et al.* 2005). In view that xPAPC can regulate gastrulation movement by functionally interacting with PCP pathway (Medina *et al.* 2004; Unterseher *et al.* 2004), I proposed a working model that xPAPC could modulate gastrulation movements by specifically antagonizing xSpry1.

4.4.2.1 xPAPC antagonizes xSpry1 in CE movements

As a first step to address the functional antagonism between xPAPC and xSpry1 in modulation of gastrulation movements, the animal cap explant assay was employed since PCP pathway is essential for coordinated CE movements which lead to elongation of activin-induced explants. xSpry1 inhibited animal caps elongation at dose of 100pg but not 30pg mRNA (Fig. 21b-c). But when suboptimal amounts of xPAPC MO were injected together with 30pg xSpry1 mRNA, the animal caps could not elongate while this amount of xPAPC MO had no effect when injected alone (Fig.21d-e). Gain of xSpry1 and loss of xPAPC can inhibit elongation respectively as described in Introduction. But importantly here I demonstrate that low gain of xSpry1 and low loss of xPAPC synergize to inhibit elongation (Fig.21f, Table 3), indicating that endogenous xPAPC can relieve the inhibitory effect of xSpry1 on animal caps elongation. In other words, xPAPC and xSpry1 antagonize each other in CE movements.

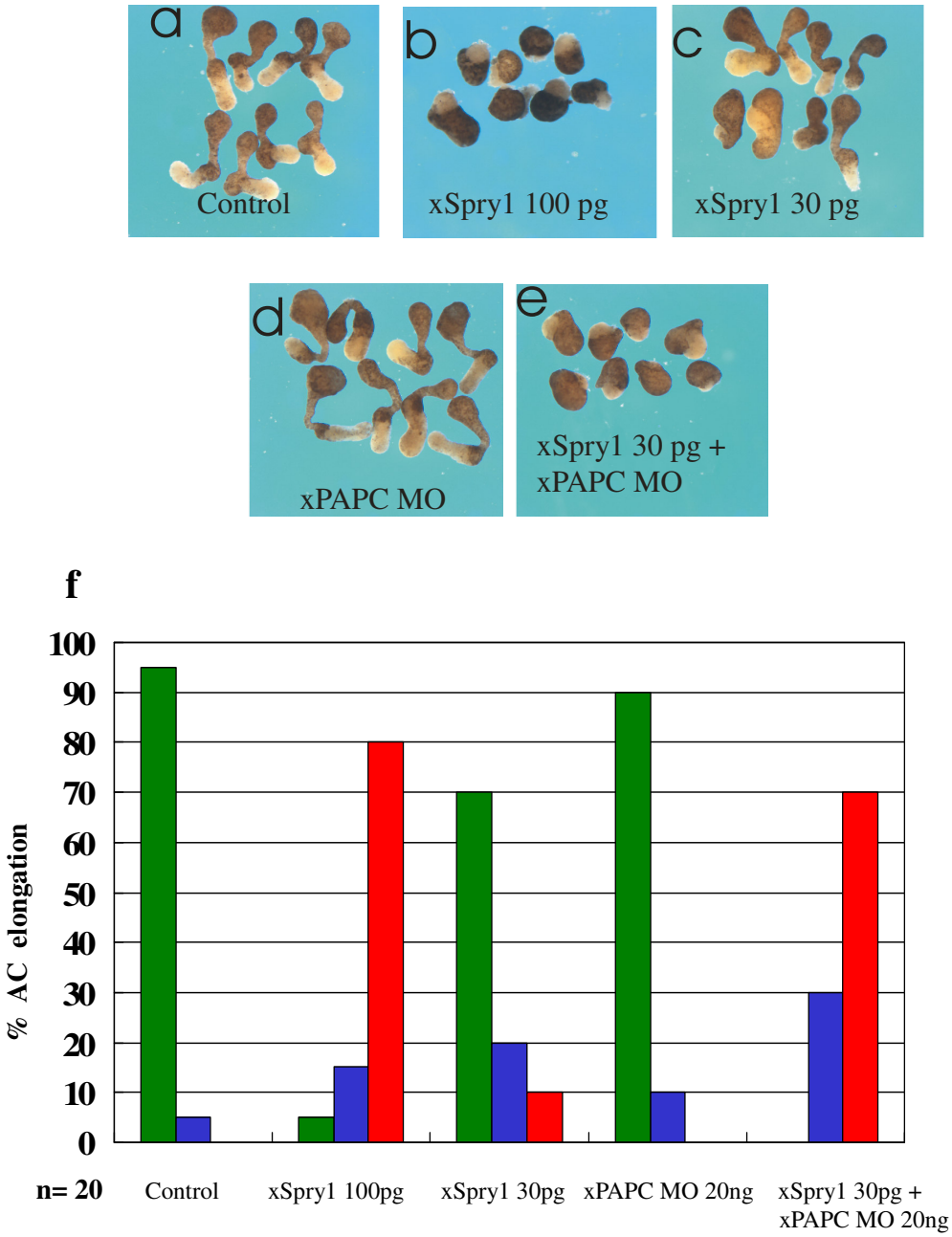

Figure 21. xPAPC antagonizes xSpry1 to promote CE movements. Synthetic mRNAs or MO were injected into 4 blastomeres of 4-cell stage embryos. At stage 8.5 animal caps (AC) were explanted, exposed to activin protein for 3 hours and cultured to stage 20. Activin-treated AC from control embryos (**a**) elongated. AC from embryos injected with 100 pg xSpry1 mRNA per blastomere (**b**) did not elongate. AC from embryos injected with 30 pg xSpry1 mRNA (**c**), or 20 ng xPAPC MO (**d**) elongated. However, AC from embryos coinjected with 30 pg xSpry1 mRNA and 20 ng xPAPC MO (**e**) did not elongate. **f.** Total No. of AC that showed full elongation (green),partial elongation (blue) or no elongation (red) from group **a-e** done in two independent experiments (n=10 each).

Table 3. Loss of xPAPC and gain of xSpry1 synergize to inhibit CE movements

Exp	mRNA or MO (/blastomere)	Full elongation (%)	Partial elongation (%)	No elongation (%)	n
1	Control	100	0	0	10
	xSpry1 (100 pg)	10	10	80	10
	xSpry1 (30 pg)	60	20	20	10
	xPAPC MO (20 ng)	90	10	0	10
	xSpry1 (30 pg) + xPAPC MO (20 ng)	0	20	80	10
2	Control	90	10	0	10
	xSpry1 (100 pg)	0	20	80	10
	xSpry1 (30 pg)	80	20	0	10
	xPAPC MO (20 ng)	90	10	0	10
	xSpry1 (30 pg) + xPAPC MO (20 ng)	0	40	60	10

4.4.2.2 xPAPC antagonizes xSpry1 in recruitment of PCP components

To elucidate at which level of PCP pathway xPAPC and xSpry1 interact, I examined their effects on the translocation of xDsh to plasma membrane by xFz7, a hallmark of PCP pathway activation (Wallingford *et al.* 2000). The recruitment of Dsh to the membrane by xFz7 (Fig.22c) was inhibited by xSpry1 (Fig.22d) while xPAPC and xPAPCc but neither M-PAPC nor xPAPCcmut rescued the recruitment (Fig.22e-h). It is important to note that xPAPC can not recruitment Dsh to membrane by itself (Fig.22b). This is in accordance with previous yeast two-hybrid assay showing that the cytoplasmic domain of xPAPC can not interact with Dsh (Fig.17). Thus xPAPC is not sufficient for Dsh translocation but can enhance Dsh recruitment by antagonizing xSpry1 with its cytoplasmic domain.

PKCδ has been characterized as a new player in PCP pathway by regulating Dsh translocation (Kinoshita *et al.* 2003), therefore we determined the interaction of xPAPC and xSpry1 at the level of PKCδ translocation. xSpry1 inhibited Fz7-mediated PKCδ translocation (Fig.22l). xPAPC and xPAPCc but neither M-PAPC nor xPAPCcmut rescued PKCδ translocation (Fig.22m-p) although xPAPC itself could not activate PKCδ translocation (Fig.22j). These results demonstrate that xPAPC and xSpry1 act antagonistically in PCP pathway downstream of Fz7 and upstream of PKCδ and Dsh to modulate CE movements and the interaction of cytoplasmic domain of xPAPC with xSpry1 is required since mutant form of xPAPCc that did not interact with xSpry1 failed to promote membrane recruitment of Dsh and PKCδ.

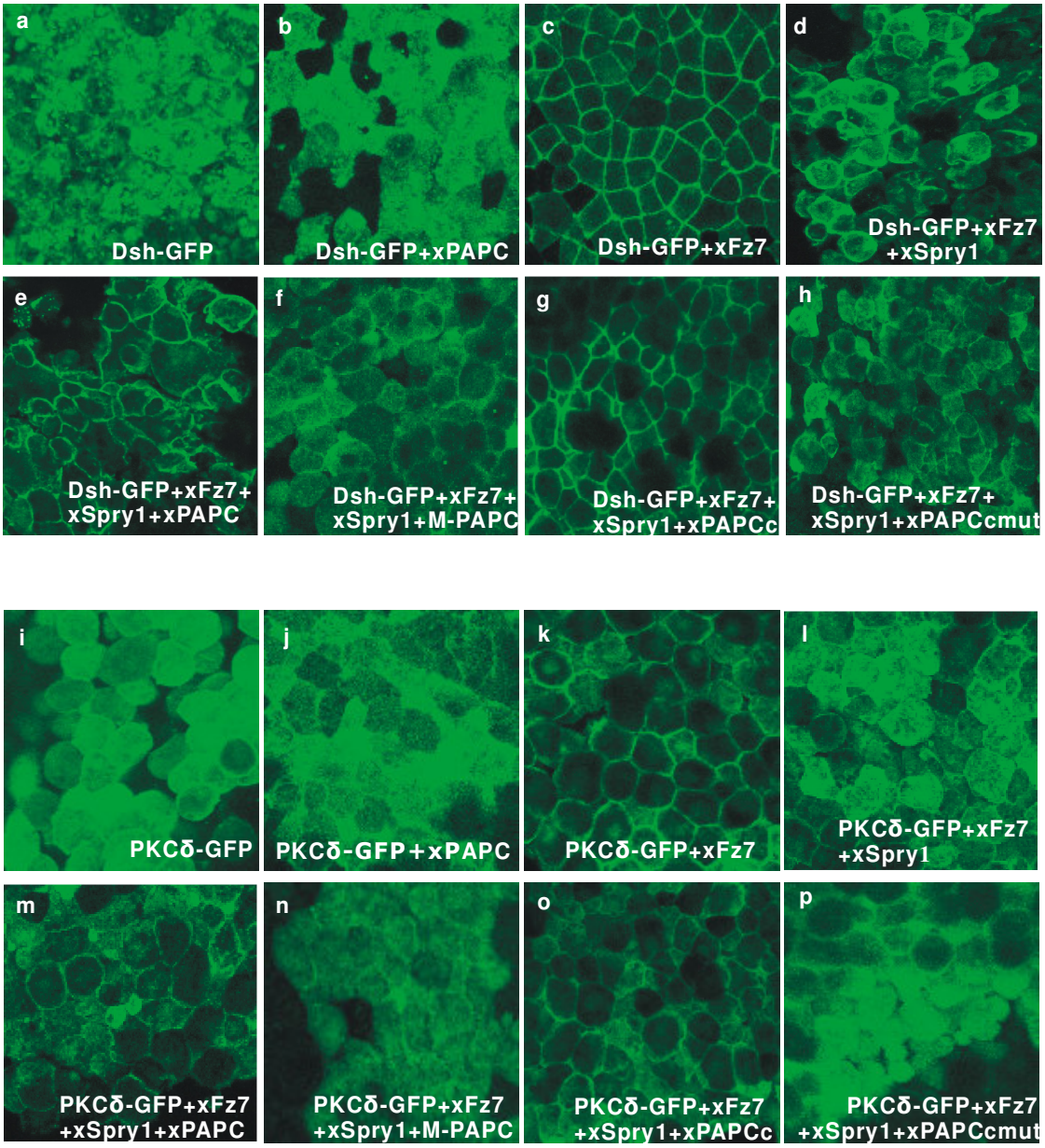

Figure 22. xPAPC antagonizes xSpry1 to promote membrane recruitment of PCP components Dsh and PKCδ. mRNAs were injected at the 4-cell stage, caps were excised at stage 9 and the localisation of Dsh-GFP or PKCδ-GFP was analysed by confocal microscopy. Dsh-GFP mRNA (300 pg) or PKCδ-GFP mRNA (300 pg) was injected alone (**a, i**) or with mRNAs encoding Fz7 (300 pg) (**c,k**) or PAPC (800 pg) (**b, j**). xSpry1 mRNA (1 ng) was co-injected with Dsh-GFP or PKCδ, and Fz7 (**d,l**). In addition to Dsh-GFP or PKCδ in combination with Fz7 and xSpry1, mRNAs for xPAPC (800 pg) (**e,m**),M-PAPC (800 pg) (**f,n**), xPAPCc (800 pg) (**g,o**) or xPAPCcmut (800 pg) (**h,p**) were injected.

4.4.2.3 xPAPC antagonizes xSpry1 in tissue separation

Our lab has shown previously that xPAPC can regulate tissue separation during gastrulation by modulation of Rho and JNK activities (Medina *et al.* 2004). In view that xPAPC and xSpry1 antagonizes each other in PCP pathway to regulate CE movements as described above, I addressed whether this antagonism also occurs in the regulation of tissue separation.

As described in **2.1.2**, tissue separation will lead to the formation of Brachet´s cleft and xPAPC is indispensable for the cleft formation since loss of xPAPC function by MO perturbs the cleft formation. Therefore I examined whether xSpry1 can inhibit cleft formation. Cleft develops normally in control embryo (Fig.23a). In xSpry1-injected embryo, the anterior part of cleft, which is formed during vegetal rotation, was not impaired. But the posterior part of cleft is invisible (Fig.23b). It has been reported that injection of xPAPC MO in embryos would cause defects in the posterior but not anterior part of cleft (Medina *et al.* 2004). Thus gain of xSpry1 has the same phenotype as loss of xPAPC in terms of cleft formation, indicating that xSpry1 and xPAPC antagonize each other in tissue separation.

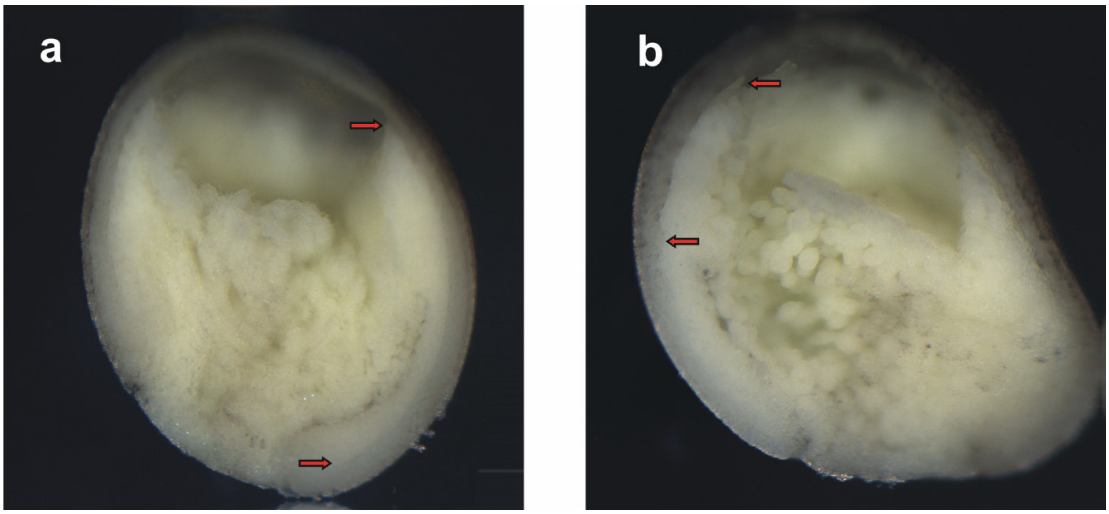

Figure 23. xSpry1 perturbs Brachet´s cleft formation. Brachet´s cleft formation was analyzed in embryos at stage 10.5 that were fractured sagittally through the dorsal midline. The length of Brachet´s cleft from the anterior (up) to the posterior (down) end was indicated by red arrows. **a.** In control embryos Brachet´s cleft develops normally. **b.** In xSpry1 mRNA (600 pg) injected embryos no posterior cleft develops.

Next I examined the antagonism of xPAPC and xSpry1 in tissue separation by employing an *in vitro* separation assay using animal cap explants. As shown in Fig.24a, embryos were injected into the animal pole with synthetic mRNA or MO, cells were removed from the inner layer of the animal cap at early gastrula stages and positioned on the inner surface of blastocoel roof (BCR) from uninjected embryos. After 45 min, if the animal caps stay on the BCR surface, they show tissue separation behaviour. If they sink into the BCR, then they do not show tissue separation.

a.

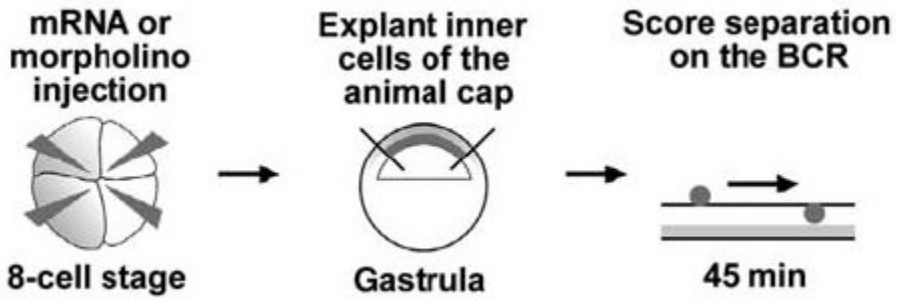

b. Fz7+xPAPC

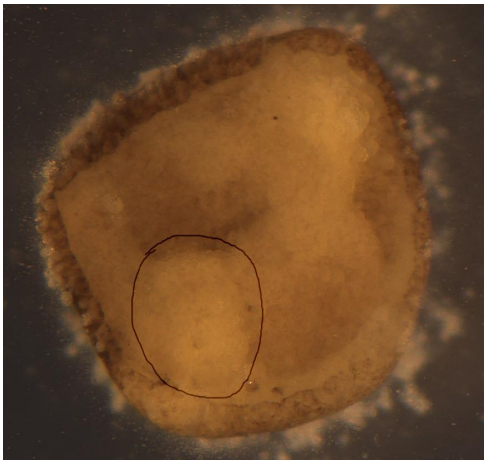

c. Fz7+xPAPC+xSpry1

Figure 24. xPAPC antagonizes xSpry1 to promote tissue separation in synergism with Fz7. a. Scheme demonstrating the blastocoel roof assay for analysis of tissue separation behaviour. **b.** Animal caps coinjected with Fz7 and xPAPC show separation behaviour. **c.** Animal caps coinjected with Fz7, xPAPC and xSpry1 mRNAs do not show separation behaviour.

Explants from embryos injected with Fz7 and xPAPC mRNA remained on the surface of BCR (Fig.24b), indicating they showed tissue separation. In contrast, explants from embryos injected with Fz7, xPAPC and xSpry1 mRNA sank and merged with BCR, showing clearly that xSpry1 could inhibit tissue separation induced by Fz7 and xPAPC.

All together, by Brachet´s cleft formation analysis as well as *in vitro* BCR assay, it is demonstrated that the antagonism between xPAPC and xSpry1 also exists in another morphogenetic process, i.e. tissue separation.

4.5 Physical and functional interaction of xPAPC and xCK2

Sequencing analysis revealed that two positive clones isolated from yeast two-hybrid screen contained partial sequence of xCK2β cDNA and the ORFs of xCK2β were in frame with that of the ACT2 vector. Moreover, the partial sequence of xCK2b in both clones would encode a protein corresponding to 100-215 aa of xCK2β, meaning that the C-terminal half of xCK2β is sufficient to interact with xPAPCc. The regulatory CK2β subunit alone has no known catalytic activity, but it does associate with the catalytic CK2α subunit to generate a stable holoenzyme complex CK2. Several studies suggest that the regulatory subunit modulates the ability of CK2α to interact with and to phosphorylate substrate proteins (Meggio *et al.* 1992). Thus, CK2β appears as a crucial mediator of cellular functions of CK2, which plays important roles in *Xenopus* early embryonic development by regulating Wnt/β-catenin signaling (Dominguez *et al.* 2004; Dominguez *et al.* 2005). Therefore I examined the physical and functional interaction between xPAPCc and xCK2.

4.5.1 Physical interaction of xPAPC and xCK2β

It is important to prove that xPAPCc and xCK2β interact specially both *in vitro* and *in vivo*.

4.5.1.1 Interaction of xPAPC and xCK2β revealed by yeast two-hybrid

Since two phosphoserine/threonine binding motifs in xPAPCc, i.e. S741 and S955 have impact on the interaction of xPAPCc with xSpry1, I checked whether these motifs also affect the interaction of xPAPCc and xCK2β. As shown in Fig. 25, S741 to A741 mutation and T947 to A947 mutation had no impact on interaction; while S955 to A955 mutation abolished the interaction. On the other hand, S955 to E955 phosphorylation-mimic mutant interacted with xCK2β. These results strongly suggest that the interaction of xPAPCc and xCK2β is phosphorylation-dependent.

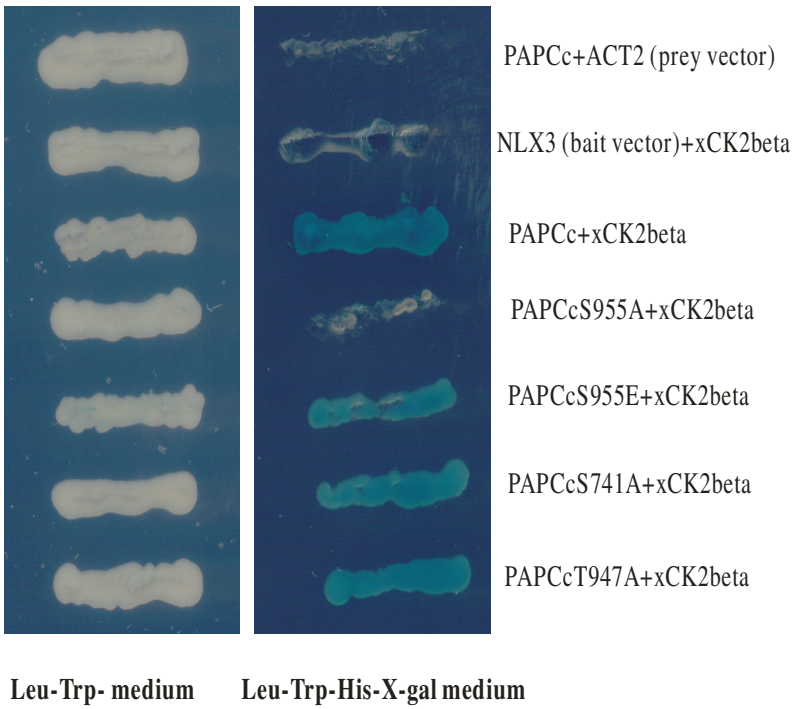

Figure 25. Interaction of xPAPCc and xCK2β revealed by yeast two-hybrid assay. cDNAs were cloned into bait vector pNLX3 or prey vector pACT2 and co-transformed into yeast strain L40 and selected on SD-Trp/-Leu plates at 30°C for 2-3 days to make sure that both bait and prey vectors are transformed. One representative colony from each co-transformation was picked and streaked onto Leu^-Trp^- medium (SD-Trp/-Leu plates, left panel) or $Leu^-Trp^-His^-X\text{-}gal^+$ medium (SD-Trp/-Leu/-His/+15 mM 3-AT/+X-Gal plates, right panel) and incubated at 30°C for 4-6 days. Blue colonies grow on $Leu^-Trp^-His^-X\text{-}gal^+$ medium when bait and prey proteins interact.

4.5.1.2 Physical interaction of xPAPC and xCK2β *in vivo*

Both CK2α and CK2β mRNA are provided maternally, encoding proteins that are present in the upper two thirds of the embryo (Animal and Medial sections) and nearly absent from the vegetal third in early development stages (Dominguez *et al.* 2004). xPAPC is expressed in the dorsal marginal zone at stage 9.5 and the expression expands to about 180º of the marginal zone at stage 10.5 (Kim *et al.* 1998). Thus xPAPC and xCK2β have chance to interact in gastrulation stage. Co-IP assay was performed to demonstrate the interaction of xPAPCc and xCK2β *in vivo*. As shown in Fig.26, Myc-xCK2β was Co-IPed with Flag-xPAPCc but not Flag-xAXPCc by Flag Ab although the band is very weak. In a reciprocal experiment, the Myc Ab failed to pull-down Flag-xPAPCc. This may be due to the weak interaction between xPAPCc and xCK2β (see the weak band in the up-right side of Fig.26). Since xPAPCc is tagged with 1x Flag epitope while xCK2β is tagged with 6x Myc epitope, it is reasonable to suppose that Myc Ab could detect low amount of 6xMyc-xCK2β that was Co-IPed with xPAPCc by Flag Ab. In contrast, Flag Ab could not

detect low amount of Flag-xPAPCc that was Co-IPed with xCK2β by Myc Ab. Taken together these results demonstrate that xPAPCc interacts specially with xCK2β in *Xenopus* embryos.

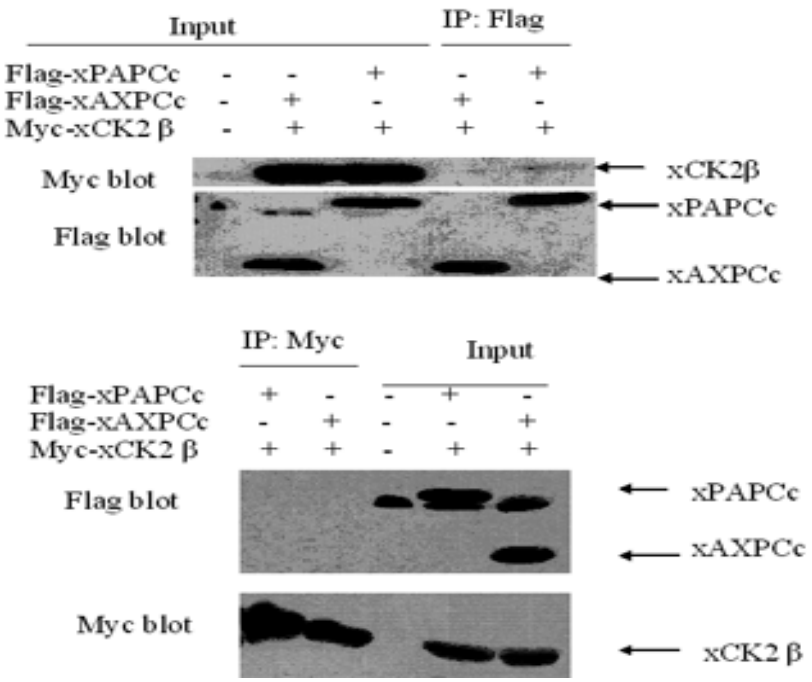

Figure 26. xPAPC associates with xCK2β in embryos. 4-cell-stage embryos were injected with Flag-xPAPCc or Flag-xAXPCc mRNA (500 pg) together with Myc-xCK2β mRNA (500 pg) and grown up to gastrula stage. Embryo lysates were collected and subjected to Co-IP and western blot with Myc or Flag Ab.

To further demonstrate the *in vivo* interaction of xPAPC and xCK2β, I investigated whether xPAPC could recruit xCK2β to cell membrane since xPAPC is a membrane protein. When xCK2β-GFP mRNA was injected into embryos, most of CK2β appeared in cytoplasm (Fig.27a). When xPAPC mRNA was coinjected, most of CK2β appreared in membrane (Fig.27b). However, when M-PAPC mRNA was coinjected, most of CK2β appreared in cytoplasm (Fig.27c). This indicates that cytoplasmic domain of xPAPC is indispensable for membrane recruitment of CK2β.

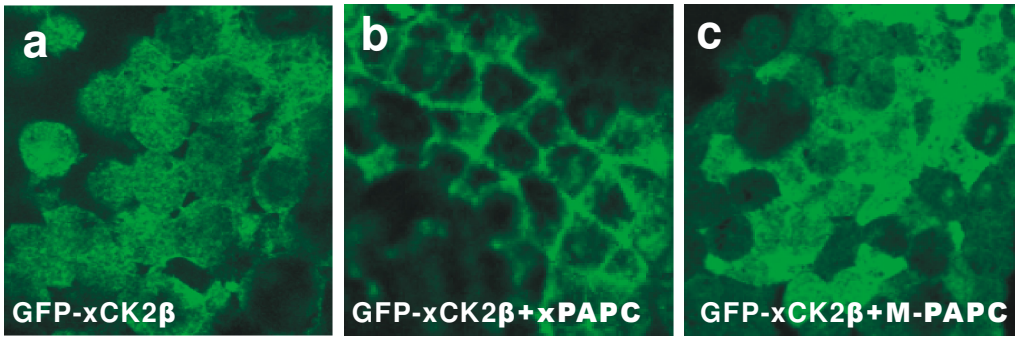

Figure 27. Membrane recruitment of GFP-xCK2β by xPAPC in animal cap cells. 400 pg GFP-xCK2β mRNA was injected alone (**a**) or with 600 pg xPAPC mRNA (**b**) or 600 pg M-PAPC mRNA (**c**) into 4-cell-stage embryos. At late blastula stage (stage 9) animal caps were excised and the localization of GFP-xCK2β was determined by confocal microscopy.

4.5.2 Functional interaction of xPAPC and xCK2

After proving that xPAPCc physically associates with xCK2β, I next address the biological significance of the interaction between xPAPC and xCK2β. Since xCK2β functions with xCK2α to promote dorsal axis formation in *Xenopus* embryos (Dominguez *et al.* 2004), I examined the impact of xPAPCc on the dorsal axis formation induced by CK2α/β complex and found that xPAPCc can antagonize xCK2α/β-induced dorsal axis formation.

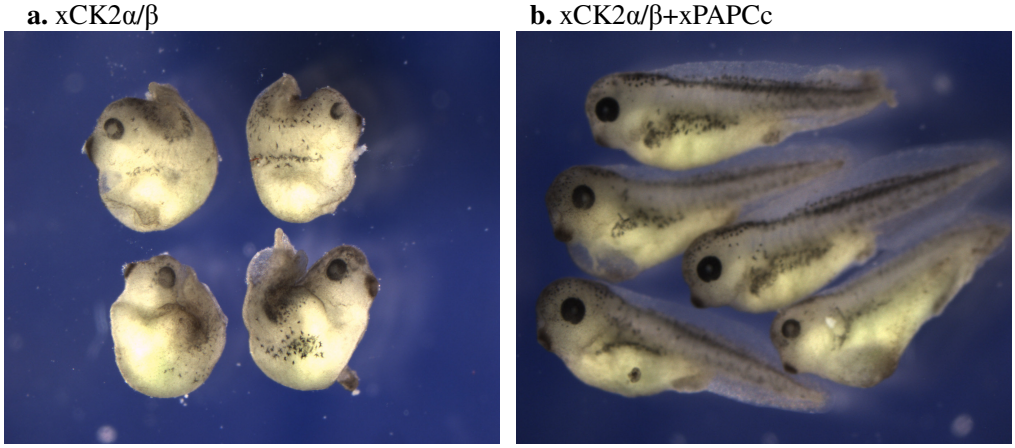

Figure 28. xPAPCc antagnozes xCK2α/β-induced ectopic axis formation. Embryos were injected ventrally at the 4-cell stage with (**a.**) 600 pg xCK2α/400 pg xCK2β mRNAs or (**b.**) 600 pg xCK2α/400 pg xCK2β and 500 pg xPAPCc mRNAs and develop till stage 38. Duplicated dorsal structures were seen in **a.** but were absent in **b.**

Coinjection of xCK2α/β mRNAs into ventral region of *Xenopus* embryos at the 4-cell stage induced ectopic axis formation (Fig.28a), as reported earlier (Dominguez *et al.* 2004). Interestingly, injection of xPAPCc mRNAs greatly inhibited the ectopic axis formation induced

by xCK2α/β (Fig.28b), suggesting that xPAPC may regulate Wnt/β-catenin signaling.

Therefore, the impact of xPAPC on CK2-induced Wnt target gene Xnr3 was investigated. Consistent with previous report (Dominguez *et al.* 2004), CK2 induced strong expression of Xnr3 in animal caps (Fig.29 lane 3). Co-injection of xPAPC at different doses inhibited Xnr3 expression (Fig.29 lane 4 and 5). Moreover, co-injection of xPAPCc but neither M-PAPC nor xAXPCc inhibited Xnr3 expression significantly (compare lane 5-8 of Fig.29). These results demonstrate that cytoplasmic domain of xPAPC that interacts with CK2β is crucial to antagonize CK2-induced Wnt/β-catenin signaling.

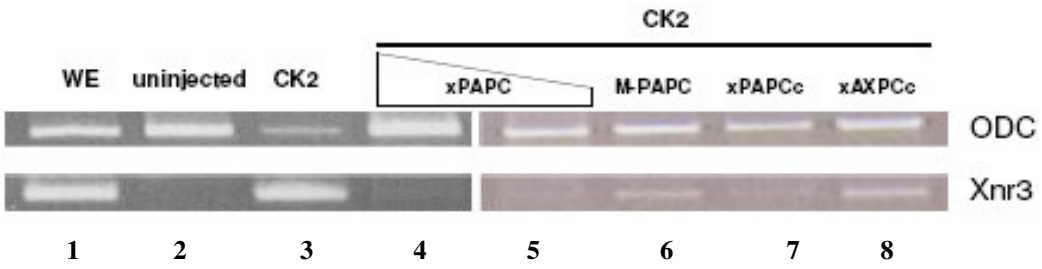

Figure 29. xPAPCc antagonizes xCK2α/β-induced β-catenin/TCF target gene Xnr3. Embryos were injected at the 4-cell stage with 800 pg xCK2α/600 pg xCK2β mRNAs **(3)** or plus 800 pg xPAPC **(4)**, 300 pg xPAPC **(5)**, 300 pg M-PAPC **(6)**, 300 pg xPAPCc **(7)**, 300pg xAXPCc **(8)**. At stage 8 animal caps were explanted and cultured to stage 10 for analysis of Xnr3 and control ODC expression by RT-PCR. Whole embryos **(**WE**,1)** and uninjected animal caps **(2)** are positive and negative controls.

5. Discussion

In the vertebrate embryo morphogenetic movements which establish the basic body plan are regulated by β-catenin-independent Wnt-signaling (Keller 2002). A growing number of proteins from different classes have been identified and characterized to contribute to these processes (see **2.2**). Among them is xPAPC. xPAPC has signaling functions which are essential for CE movements and tissue separation during gastrulation. PAPC modulates the activities of the Rho GTPase and JNK, which are effectors of PCP pathway (Medina *et al.* 2004; Unterseher *et al.* 2004). Importantly, the signaling activities of xPAPC reside in its cytoplasmic domain. How xPAPC is connected to β-catenin-independent Wnt-signaling is not clear yet. In other words, what is the link between PAPC signaling and PCP pathway? It is likely that cytoplasmic proteins that interact with cytoplasmic domain of xPAPC (xPAPCc) may provide the link. But until now no proteins have been reported as interacting partners of xPAPCc. So in this study, 3 different approaches were employed to isolate the interacting partners of xPAPCc. Then the physical and functional interactions of these identified partners with xPAPCc were characterized in detail.

5.1 Comparasion of different approaches to identify xPAPCc interacting partners

A variety of methods have been developed to detect protein protein interaction since protein-protein interactions are engaged in nearly all biological processes. Each method has its own advantages and limitations, especially with regard to the sensitivity and specificity of the methods. Co-IP is considered to be the gold standard assay for protein-protein interactions, especially when it is performed with endogenous proteins. However, this method can only verify interactions between suspected interaction partners and is not a screening approach. Yeast two-hybrid method has high sensitivity but is subjected to a notorious high false-positive rate. On the other hand, the intrinsic nature of particular proteins will dictate, to a large extent, which approaches are suitable for identification of their interacting partners. For instance, if an interaction is likely to depend on posttranslational modifications that occur only in eukaryotes, GST pull-down will not be appropriate. If a protein such as transcription factor can auto-activate transcription of reporter genes, it is not suitable for yeast two-hybrid assay. Moreover, if a protein interacts simultaneously with multiple partners in a complex fashion, yeast two-hybrid may fail to identify these partners. Therefore it is best to combine different approaches to isolate and identify interacting partners of a particular protein. Based on these considerations, three complementary approaches were utilized in my study with the aim to isolate interacting partners of xPAPCc.

5.1.1 Candidate approach

A simple but risky method to identify protein protein interaction is to make prediction based on the structure and function characteristics of the studied proteins. By use of bioinformatics program Scansite, 14-3-3 was predicted to be a putative protein that interacts with xPAPCc via 3 motifs present on xPAPCc. Considering that 14-3-3 proteins have important functions in early *Xenopus* development (Wu and Muslin 2002; Lau *et al.* 2006), especially in the modulation of gastrulation movements (Kusakabe and Nishida 2004), I examined the interaction between 14-3-3ε or 14-3-3ζ isoforms and xPAPCc by Co-IP method and got negative results. Since the interaction between 14-3-3 and 14-3-3 binding motifs present on the studied proteins is direct and phosphorylation of 14-3-3 binding motifs occurs in yeast, yeast two-hybrid assay is suitable to check the direct interaction of 14-3-3 and xPAPCc. Therefore I made prey plasmid expressing 14-3-3ε and cotransformed it into yeast with bait plasmid expressing xPAPCc, no blue colonies grew in selection medium, indicating that 14-3-3ε could not interact with xAPCc. In fact 14-3-3 has been identified as interacting partners of a variety of bait proteins using yeast two-hybrid screen (Godde *et al.* 2006; Pulina *et al.* 2006; Rong *et al.* 2007) The failure to verify the interaction of 14-3-3 and xPAPCc is also in accordance with the fact I did not isolate 14-3-3 in yeast two-hybrid screen with xPAPCc as the bait (Table 1). Taken together, the predicted interaction between 14-3-3 and xPAPCc was not verified by experimental methods and 14-3-3 is unlikely to be engaged in the modulation of xPAPC signaling activities.

On the other hand, by comparison of the structure, function and expression patterns of xPAPC and p120 catenin subfamily including p120 and ARVCF (see **2.2.7.1.2**), I assume that p120 and/or ARVCF associate with the juxtamembrane region of xPAPC and mediate the signaling activities of xPAPC, thereby modulating morphogenetic movements during gastrulation. By Co-IP method I failed to detect the association of p120 or ARVCF with xPAPCc. Therefore on one hand xPAPC can not bind to β-catenin due to the absence of β-catenin binding site at the C-terminal region. On the other hand, it is not associated with p120 catenin subfamily at the juxtamembrane region. In this aspect xPAPC is completely different from classic cadherins, which can associate with both β-catenin and p120 at the C-terminal and juxtamembrane region, respectively. Thus it is suggested that even xPAPC and classic cadherins share conserved extracellular EC domains that mediate cell adhesion, the signaling mechanisms mediated by their cytoplasmic domain diverge during evolution to fulfill their different biological functions.

5.1.2 GST pull-down approach

To isolate proteins present in gastrulation stage embryos that associate with xPAPCc, a recombinant protein of xPAPCc fused to GST (GST-xPAPCc) was expressed in *E. coli* and purified by glutathione-Sepharose affinity chromatography. GST pull-down experiments with lysates from gastrulation stage embryos using glutathione- Sepharose bound GST-xPAPCc revealed two proteins that associates with GST-xPAPCc specifically. Analysis of the isolated proteins by mass spectrometry revealed that these two proteins are β-tubulin and fragment of vitellogenin A2 precursor.

Vitellogenin A2 precursor is enriched in the egg yolk to provide nutrients necessary for early embryo development. Thus it is unlikely to associate with xPAPC which is expressed in mesoderm. Most likely the protein band contaning fragment of vitellogenin A2 precursor is derived from embryo extracts contaminated with yolk. Based on all these considerations, vitellogenin A2 precursor was excluded for further characterization of the interaction with xPAPCc.

β-tubulin is an important component of microtubules that play crucial roles in a variety of cellular processes such as mitosis, cytokinesis, and vesicular transport. With the association of β-tubulin and xPAPCc revealed by GST pull-down, it is tempting to assume that the biding of xPAPCc to tubulin may be involved in the transport of xPAPC to special membrane area to regulate planar cellular polarity. Therefore both Co-IP and yeast two-hybrid experiments were carried out to verify the interaction of xPAPCc and β-tubulin and the results showed no interaction. Thus the conclusion is drawn that β-tubulin could not bind xPAPCc.

In summary, GST pull-down approach failed to isolate any interesting interacting partners of xPAPCc. In retrospect, at least two factors account for this.

One is that GST-xPAPCc fusion protein is not well expressed in *E. coli*. No matter whether sonication or lysozyme digestion method was used and despite the addition of protease inhibitors during the purification of GST-xPAPCc fusion protein, a series of truncated proteins sized between 55 KDa (corresponding to full-length GST-xPAPCc fusion protein) and 26 KDa (corresponding to GST protein alone) were observed (Fig.11). Moreover, all these bands gave positive signal when subjected to western blot using GST antibody, indicating clearly that they are truncated GST-xPAPCc proteins but not proteins from *E coli* associated nonspecially to GST-

xPAPCc. Given the fact that PAPC molecule only exist in vertebrate, it is likely that several codons are present in xPAPCc sequence that are rarely used in E coli. As a result, premature translation termination will happen and truncated GST-xPAPCc proteins be synthesized. These truncated GST-PAPCc proteins may act as dominant negative to greatly reduce the efficiency of the capture of xPAPCc associated proteins by full-length GST-xPAPCc.

Another important factor is that the interaction of xPAPCc with its binding partners may depend on posttranslational modifications of xPAPCc. For example, the interaction of xPAPCc with two partners xSpry1 and xCK2β isolated by yeast two-hybrid screening depends on phosphorylation of the serine residues present on xPAPCc (see **4.4.1** and **4.5.1**). GST-xPAPCc protein expressed in *E. coli* may lack these posttranslational modifications and unable to pull-down those interacting partners that depend on posttranslational modifications to bind xPAPCc.

All together, GST pull-down proved to be unsuitable to isolate xPAPCc interacting partners.

5.1.3 Yeast two-hybrid approach

While the previous two approaches failed to isolate xPAPC interacting partners, yeast two-hybrid approach successfully isolated several proteins that bind xPAPCc. At least two of them, i.e. xSpry1 and xCK2β were verified to specially interact with xPAPCc both physically and functionally.

cDNA encoding xPAPCc was PCR amplified and subcloned into pNLX3 vector to make bait vector for yeast two-hybrid screen. pNLX3 vector is derived from plasmid pBMT 116, which contains LexA DNA-binding (BD) domain and *Trp1* marker gene. pNLX3 contains SV40 nuclear localization sequence (NLS) inserted at the carboxy-terminus of LexA-BD domain (Iouzalen *et al.* 1998). The addition of NLS in pNLX3 vector may lead to better recruitment of bait protein to nucleus and stronger transcription of the report genes induced by the interaction of bait and prey proteins in nucleus. Indeed, it was reported that the addition of NLS in the LexA-XRalB fusion protein improved the detection of binding between XRalB and RLIP76 (Iouzalen *et al.* 1998). Therefore the use of pNLX3 bait vector in my yeast-two-hybrid screen may increase the chance to isolate weak interacting partners of xPAPCc. More importantly, xPAPCc-LexA-BD fusion protein was expressed well in yeast strain L40 (Fig.14) and could not activate reporter genes transcription in the absence of prey protein.

With respect to the library, although it was provided as *E coli* transformations instead of purified DNA, after library amplification and DNA purification I got DNA with high quality and quantity. When subject to digestion, the majority of the plasmids released fragment of about 2 kb (Fig.15), indicating that the complexities of the library was not lost much during the amplification. All these facts guarantee that yeast two-hybrid system I adopted is very suitable to isolate xPAPCc interacting partners.

Technically, to achieve high transformation efficiency of library plasmids, I did not do simultaneous cotransformation of pNLX3-xPAPCc bait and library plasmids into L40; instead, I did sequential transformation by pre-transforming bait plasmid into L40 to get L40-xPAPCc and then transforming library plasmids into L40-xPAPCc. In this way, I got a few million transformants that nearly saturate screening.

One major drawback of two-hybrid screen is the high false-positive rate, which I also encountered in my screening. Generally these false-positives can be categorized as “biological” and “technical” false-positives (Vidalain *et al.* 2004). “Biological” false-positives mean that protein protein interactions occur in yeast cells, but not in vivo in the organism of study, because the two proteins have different tempospatial expression patterns. In my screen, positive clones that encode Wnt11, granulin, fibronectin or nidogen-2 can be classified in this category since these proteins are localized and function in extracellular matrix and have no physiological context to interact with cytoplasmic xPAPCc. “Technical” false-positives mean that protein protein interactions are detected due to technical limitations of the system. Many DNA or RNA binding proteins encoded by library plasmids will lead to the activation of reporter transcription even without specific interaction with the bait protein. These proteins were isolated in my screen including transcription factors, hnRNP, DNA repair protein Rad52 etc. (Table 1). All these false-positives are hard to avoid and one has to distinguish them from true positives by putting in a lot of efforts.

The quality of the cDNA library is also very important for the successful isolation of interacting proteins. I used commercial *Xenopus laevis* oocyte cDNA library from Clonetech. In retrospect, only one clone encoding xSpry1 was isolated from the screen. Moreover I failed to isolate any clones encoding xSpry2, although by yeast two-hybrid assay it was shown that xSpry2 interacts with xPAPCc. The reasons are not clear but one factor may be the *Xenopus* oocyte cDNA library. In theory, mRNA encoding every gene should be present in *Xenopus* oocytes and the

corresponding cDNA should be represented in oocyte cDNA library. Nevertheless, these mRNAs are in a wide range of abundance. As a result, high-abundance mRNAs have more clones while low-abundance mRNAs have less or even no clones in the cDNA library. The expression of xSpry1 and xSpry2 are strongly induced in MBT, their maternal expression is very low (Sivak *et al.* 2005). This may lead to their low or no representation in the library. In contrast, mRNAs for both α and β subunits of CK2 are abundant in *Xenopus* oocyte (Wilhelm *et al.* 1995). CK2β is expressed in oocyte and negatively regulates *Xenopus* oocyte maturation (Chen *et al.* 1997). NLK mRNA is also abundant in *Xenopus* oocyte (Hyodo-Miura *et al.* 2002). These may explain why 2 clones encoding CK2β and 5 clones encoding NLK were isolated from screening *Xenopus* oocyte library.

Besides Spry1 and CK2β, other potential interacting partners of xPAPCc isolated from yeast two-hybrid screen are NLK (5 clones), TAO kinase 1 (one clone) and neutral sphingomyelinase II (one clone). All these five clones contained full sequence of xNLK cDNA including partial 5´UTR of xNLK. The ORF of xNLK (encoding a protein of 447 aa) was in frame with that of the ACT2 vector. One clone contained 3´partial sequence of xTAO kinase 1 cDNA and the ORF of xTAO kinase was in frame with that of the vector. The encoded protein would correspond to 577-897 aa of xTAO1. One clone contained 3´partial sequence of neutral sphingomyelinase II cDNA that was in frame with the vector. The encoded protein would correspond to 339-660 aa of neutral sphingomyelinase II. For these putative xPAPCc interacting partners, xNLK but not xTAO1 nor neutral sphingomyelinase II is implicated in the regulation of early embryo development. However, it is noteworthy that both NLK and xTAO1 are serine/threonine kinase and they may be implicated in the phosphorylation of xPAPCc, which is important for the interaction of xPAPCc with xSpry1 and xCK2β to modulate Wnt signaling. Therefore, it is important to verify the interaction of xPAPCc with xNLK and xTAO1 by Co-IP assay and examine whether xPAPCc is a substrate of xNLK and/or xTAO1 kinases.

NLK plays important regulatory roles in both canonical and non-canonical Wnt signaling. NLK phosphorylates TCF/LEF factors and inhibits the interaction of the β-catenin/TCF complex with DNA, therefore suppresses axis duplication induced by β-catenin in *Xenopus* embryos (Ishitani *et al.* 1999). Moreover, it was shown that NLK is activated by the non-canonical Wnt5a/Ca^{2+} pathway and antagonizes canonical Wnt/β-catenin signaling (Ishitani *et al.* 2003). In contrast, in zebrafish, NLK functions as a positive regulator of canonical Wnt signaling. In cooperation with Wnt8, NLK is essential for mesoderm formation and patterning of the midbrain. Furthermore, the

strong enhancement of the *slb/wnt11* phenotype by NLK MO indicates that NLK interacts with non-canonical Wnt signaling to regulate cell movements during gastrulation (Thorpe and Moon 2004). It has to be emphasized that in this study it is not clear whether NLK acts downstream of a non-canonical Wnt since NLK morphants do not show any obvious defects in CE movements. Instead, it is possible that NLK acts through canonical Wnt to regulate CE movements indirectly. For example, in zebrafish, maternal β-catenin signaling activates Stat3, which is required for CE movements (Yamashita *et al.* 2002). Maternal β-catenin signaling is also necessary to regulate gastrulation movements in *Xenopus*, probably through activation of *Xnr3* (Kuhl *et al.* 2001). Thus, Loss of NLK may lead to defects in the regulation of some canonical Wnt targets, which then cooperate with loss of Wnt11 to impair CE movements (Thorpe and Moon 2004). Whatever the various role of NLK plays in the regulation of Wnt signaling, given that xPAPC is also involved in the regulation of both canonical and non-canonical Wnt signaling, it is intriguing to further characterize the functional interaction of xPAPC and NLK in the regulation of Wnt signaling.

5.2 xPAPC modulates non-canonical Wnt signaling by antagonizing xSprouty

Yeast two-hybrid assay and Co-IP experiments consistently demonstrate that xPAPCc interacts with xSpry1 in a phosphorylation-dependent manner (Fig. 17 and 19). Moreover, xPAPC but not M-PAPC lacking cytoplasmic domian can recruit xSpry1 to cell membrane in animal caps. More stringent treatment is necessary to extract membrane bound proteins like xPAPC from embryos, which would also disrupt the association of xPAPC and its interacting partners. This may explain why I failed to detect the interaction of Flag-tagged full-length xPAPC and Myc-tagged xSpry1 in embryos by Co-IP (results not shown). Therefore, I made no further experiments to demonstrate that xPAPC and xSpry1 interact endogenously in embryos. Nevertheless, based on the lines of evidence shown above, it is concluded that xPAPCc and xSpry1 interact physically both *in vitro* and *in vivo*.

There is only one Sprouty member in *Drosophila* (dSpry), while there are four Sprouty genes in vertebrates (Spry1-4). By yeast two-hybrid assay, xPAPCc was shown to interact with xSpry2, dSpry, hSpry1 (human Spry1) but not hSpry2. Sprouty-related proteins with an EVH1 domain (Spreds) harbor a conserved N-terminal EVH1 domain and a C-terminal Spry domain and inhibit Ras/MAPK pathway similar to Sproutys (Bundschu *et al.* 2006). Since xPAPCc interacts with the C-terminal half of xSpry1 and Sprouty and Spred are similar in C-terminus, it is tempting to examine whether xPAPCc also interacts with Spreds. However, this was not the case by yeast two-hybrid assay (Fig.17). Thus xPAPCc binds to Sproutys specially.

To examine which domains of xPAPCc mediate the interaction with xSpry1, I made error-prone PCR-based mutagenesis of xPAPCc bait vector and did yeast two-hybrid with xSpry1 prey vector to find which mutations will abolish the interaction. Unfortunately the results were unsatisfactory. Therefore I made deletion constructs of xPAPCc bait vector. Construct that contain C-terminal half of xPAPCc (818-979 aa) interacts with xSpry1, in accordance with that S741 to A741 mutation weakened but did not abolish the interaction with xSpry1. xPAPCcΔ818-833 with the delection of the conserved 16-amino acid region interacts with xSpry1/2 (Table 2). This indicates that C-terminal region from 833 to 979 aa is important for the interaction (this is in agreement with that mutation of S955 to A955 abolished the interaction). Further experiments are needed to narrow down which region of 833-979 aa is responsible for the interaction with xSpry1/2.

The deletion of conserved 16 aa region did not impact the interaction of xPAPCc with xSpry1/2, suggesting that the interaction of PAPC with Sprouty is not conserved in vertebrates. Indeed, by yeast two-hybrid assay, hPcdh8c (cytoplasmic domain of human Pcdh8, homolog of xPAPC) binds hSpry1 weakly but does not bind hSpry2. Intriguingly, hPcdh8c binds xSpry1 weakly but xSpry2 strongly. In contrast, xPAPCc binds hSpry1 but does not bind hSpry2. The reasons are not clear but these results indicate that some specificity exists in the interaction between different members of PAPC and Sprouty families.

The finding that xPAPCc associates with xSpry1 provided the basis to further explore the physiological implication of their physical interaction. Earlier reports have shown that cytoplasmic domain of xPAPC is indispensable to promote caps elongation induced by low dose of activin (Kim *et al.* 1998), while xSpry1 can inhibit caps elongation induced by activin (Sivak *et al.* 2005). Indeed I found that injection of 100 pg of xSpry1 mRNA or 60 ng of xPAPC MO inhibited animal caps elongation (Fig.21b and results not shown). These results showed clearly that gain of xSpry1 or loss of xPAPC inhibits CE movements. When suboptimal amount of xSpry1 mRNA or xPAPC MO was injected, the caps elongation was not impaired (Fig.21c and d). But when suboptimal amount of xSpry1 mRNA and xPAPC MO were injected together, the caps elongation was impaired greatly (Fig.21e). Thus it is demonstrated that endogenous xPAPC can attenuate the inhibitory effect of xSpry1 on CE movements. In other words, low gain of xSpry1 and low loss of xPAPC synergize to inhibit CE movements (Table 3). These results indicate that xPAPC and xSpry1 modulate CE movements in an antagonistic manner.

Explanted dorsal marginal zones (DMZ), so called Keller explants, express both xPAPC and xSpry1 and display CE movements. Elongation was inhibited by overexpression of xSpry1 but partially rescued by co-expression of xPAPC (Köster unpublished). Thus the antagonism between xPAPC and xSpry1 was also seen in DMZ. Altogether these results demonstrate that xPAPC and xSpry1 have antagonistic activities which contribute to the regulation of CE movements.

PCP pathway regulates CE movements in *Xenopus* (see **3.2.1.4**). One hallmark of active PCP signaling is the membrane translocation of Dsh. Therefore the Dsh translocation in animal caps cells is used as a readout to examine the antagonism between xPAPC and xSpry1 in PCP signaling. It was shown that xSpry1 inhibits Dsh translocation, which may explained that it inhibits animal caps elongation as described above. Importantly, xPAPCc can antagonize xSpry1 to rescue Dsh translocation to membrane. M-PAPC or xPAPCcmut that could not interact with

xSpry1 is unable to antagonize xSpry1 in Dsh translocation. But xPAPCc that could interact with xSpry1 is able to antagonize xSpry1 in Dsh translocation (Fig.22c-h). It is important to note that xPAPC alone is not sufficient to recruit Dsh to membrane (Fig.22b). This is in agreement with yeast two-hybrid assay that xPAPCc can not bind Dsh (Fig.17). These results demonstrate that xPAPC is not able to drive PCP signaling but can antagonize xSpry1 to enhance Dsh translocation and PCP signaling induced by Wnt/Fz. Significantly, the ability of cytoplasmic domain of xPAPC to interact with xSpry1 is indispensable for the antagonism of xSpry1.

Next I further characterized at which step of PCP pathway that the antagonism between xPAPC and xSpry1 occurs. PKCδ acts upstream of Dsh in PCP pathway to regulate CE movements. Fz7 induces PKCδ membrane translocation, which then mediates Dsh membrane translocation and activation. Loss of PKCδ by MO inhibits Dsh translocation and PCP pathway activation (Kinoshita *et al.* 2003). On the other hand, xSpry1 can inhibit FGF-induced PKCδ membrane translocation in animal caps (Sivak *et al.* 2005). Therefore I checked whether xSpry1 also inhibit PKCδ translocation induced by Fz7. As shown in Fig.22l, xSpry1 inhibits PKCδ translocation. Furthermore, xPAPC or xPAPCc but neither M-PAPC nor xPAPCcmut can partially rescue the inhibition, demonstrating that the cytoplasm domain of xPAPC is necessary to interact and antagonize xSpry1 in PKCδ translocation and PCP signaling (Fig.22m-p). Similarly, xPAPC alone can not induce PKCδ translocation (Fig.22j). Taken together these results suggest that xPAPC and xSpry1 act antagonistically in the PCP pathway downstream of Fz7 and upstream of PKCδ and Dsh. The cytoplasmic domain of xPAPC which interacts with xSpry1 is essential to promote membrane translocation of PCP components since the mutations that abolish the interaction with xSpry1 also impair the ability of xPAPCc to antagonize xSpry1. It has to be emphasized that Frizzled is necessary for the translocation of PKCδ and Dsh, while xPAPC has only modulatory effects on their translocation since xPAPC alone is not sufficient to promote their translocation.

Tissue separation is another important morphogenetic process during *Xenopus* gastrulation. It is interesting that tissue separation is regulated by Fz7 through Wnt/Ca^{2+} pathway (Winklbauer *et al.* 2001). Recently it was reported that xPAPC could interact with Fz7 by their ectodomains and synergize with Fz7 to promote tissue separation (Medina *et al.* 2004). Since tissue separation involves Ca^{2+} signaling (Winklbauer *et al.* 2001) and xSpry1 can inhibit Ca^{2+} signaling induced by FGF (Sivak *et al.* 2005), it is rational to assume that xSpry1 inhibits tissue separation and xPAPC antagonizes xSpry1 to promote tissue separation in synergism with Fz7. By analysis of Brachet´s cleft formation, it was found that xSpry1 impaired the formation of the posterior part of

the cleft (Fig.23), which is exactly the same phenotype of loss of xPAPC (Medina *et al.* 2004). This provides the first clue up to date that xSpry1 has inhibitory effect on tissue separation and this effect can be antagonized by xPAPC. By employing an *in vitro* separation assay, the antagonism between xSpry1 and xPAPC in tissue separation was confirmed (Fig.24).

These results evidently demonstrate that the functional interactions of xPAPC and xSpry1 occur not only in the regulation of PCP pathway (CE movements) but also in the regulation of Wnt/Ca^{2+} pathway (tissue separation).

Both xSpry1 and xSpry2 are shown to inhibit CE movements in animal caps assay and inhibit PKCδ translocation induced by FGF (Sivak *et al.* 2005). In the present study I only characterized the functional interactions between xPAPC and xSpry1 but not xSpry2. Nevertheless, based on the similar inhibitory effects of xSpry1 and xSpry2 on CE movements during gastrulation and that xPAPCc can interact physically with both xSpry1 and xSpry2 (Fig.17), it is reasonable to propose the model that xPAPC antagonizes both xSpry1 and xSpry2 to promote CE movements via PCP signaling and tissue separation via Wnt/Ca^{2+} signaling (Fig.30).

A growing body of evidence indicates that Fz acts as GPCR (Wang and Malbon 2003). Upon binding to Wnt ligands, Fz is activated and in turn activates heterotrimetric G proteins. Gβγ subunits activate PLC, resulting in the release of IP3 and DAG. IP3 catalyzes intracellular Ca^{2+} release and the activation of PKCα, both of which are implicated as key regulators of tissue separation (Winklbauer *et al.* 2001). On the other hand, phorbol ester PMA (phorbol 12–myristate 13–acetate, a DAG analog) can activate PKCδ, which in turn leads to Dsh translocation and JNK activation to modulate CE movements (Kinoshita *et al.* 2003). By mechanisms still unclear, xSproutys inhibit both PKC activation by DAG and Ca^{2+} release, block both PCP pathway and Wnt/Ca^{2+} pathway. As a result, morphogenesis including CE movements and tissue separation do not happen at this stage. When gastrulation begins, xPAPC is expressed in dorsal margin zone. Perhaps resulting from the interaction with Fz7 mediated by extracelluar domains (Medina *et al.* 2004), xPAPC is localized in the vicinity of membrane microenvironment that Fz7 and xSproutys reside. Thus cytoplasmic domain of xPAPC gets access to binding and sequestering xSproutys. As a result, the inhibitory effects of xSproutys are released. Consequently, PCP signaling and Wnt/Ca^{2+} signaling are activated, allowing morphogenesis like CE movements and tissue separation to proceed (Fig.30).

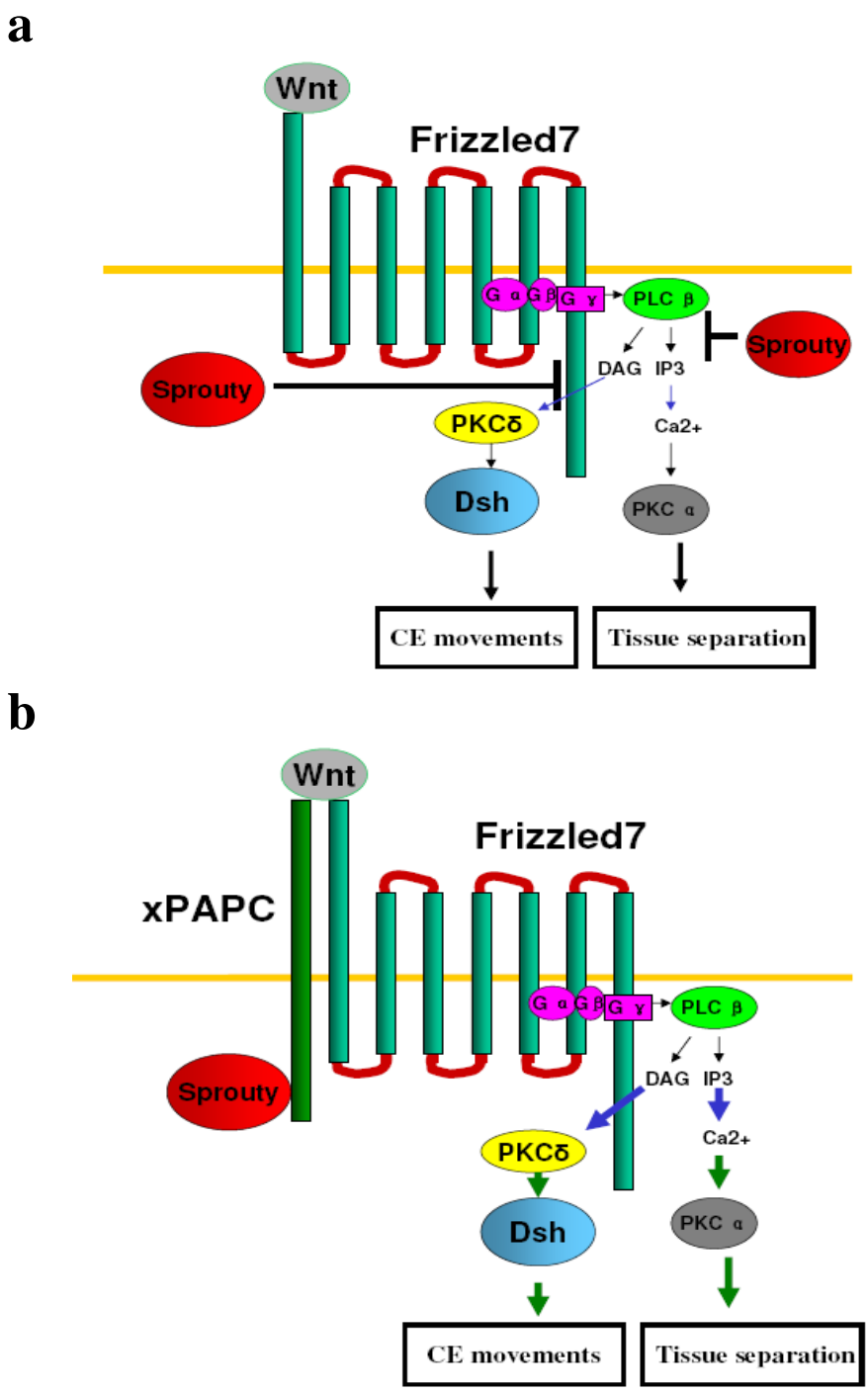

Figure 30. xPAPC antagonizes Sprouty and modulates morphogenesis during *Xenopus* gastrulation. Wnt ligands binding to Fz7 leads to the activation of G proteins. The Gβγ subunits activate PLCβ to release IP3 and DAG. DAG activates PKCδ, which then activates Dsh and downstream PCP signaling to regulate CE movements. IP3 activates Ca^{2+} signaling and PKCα, which is implicated in tissue separation. **a**. Sprouty inhibits PKCδ activation and Ca^{2+} signaling, thereby blocking CE movements and tissue separation. **b**. xPAPC interacts with Fz7 via ectodomains and sequesters Sprouty. The inhibitory effects of Sprouty on PCP and Ca^{2+} signaling are released, leading to CE movements and tissue separation.

5.3 xPAPC modulates canonical Wnt signaling by antagonizing xCK2

CK2β, the regulatory subunit of the holoenzyme CK2, was shown to interact with xPAPCc by yeast two-hybrid and Co-IP assays. Furthermore, xPAPC but not M-PAPC can recruit xCK2β to cell membrane in animal caps, demonstrating their *in vivo* interaction.

When injected ventrally, xCK2 induces a visible second axis (Dominguez *et al.* 2004). Surprisingly, xPAPCc can inhibit xCK2-induced second axis formation (Fig.28). Correlating with its ability to induce second axis, xCK2 can induce Wnt target genes like Xnr3 and Xsiamois (Dominguez *et al.* 2004). xPAPC or xPAPCc but niether M-PAPC nor xAXPCc can inhibit xCK2-induced Xnr3 transcription in animal cap explants (Fig.29). Moreover, loss of xPAPC by PAPC MO can enhance Xnr3 transcription in animal cap explants (Köster unpublished). Taken together, these data indicate that xPAPC can inhibit canonical Wnt signaling by sequestration of CK2β.

If the antagonism between xPAPC and xCK2 is true, what are the underlying mechanisms? To address this question, it is important to know the structure of CK2.

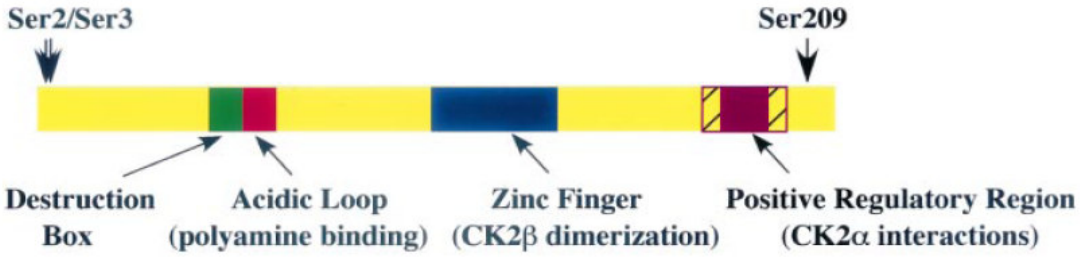

Figure 31. Structure of the regulatory CK2β subunit. Notable elements within its 215 amino acid are shown as: sequence (Arg47-Asp55) resembling a destruction box (shown in green), an acidic loop (Asp55-Asp64) involved in polyamine binding (shown in red), a zinc finger (Cys109-Cys140) mediating CK2β dimerization (shown in blue) and a positive regulatory domain involved in interacting with the catalytic CK2α subunit (shown in magenta). This positive regulatory domain has been desfined as a sequence encompassing Asn181-Ala203 (indicated by hatched bars). Contacts between CK2α and a sequence (Arg186-Gln198) within this positive regulatory region of CK2β (solid magenta bar) have been identified in the high-resolution structure of CK2 (modified from Litchfield 2003).

Protein kinase CK2 is distributed ubiquitously in eukaryotic organisms, where it exist in tetrameric complexes consisting of two catalytic subunits CK2α and two regulatory subunits CK2β. The amino acid sequence of CK2β is even more highly conserved between species than that of the catalytic subunits. In fact, its entire 215-amino acid sequence is identical between birds and mammals, with these sequences differing from that of *Xenopus laevis* by only a single conservative amino acid substitution (Litchfield 2003). Importantly, the zinc finger Cys109-

Cys140 containing four cysteine residues mediates dimerization of CK2β subunits (Fig.31). This dimerizazion of CK2β takes place in the absence of the catalytic subunits. Moreover, the failure of dimerization-incompetent mutants of CK2β to form complexes with catalytic subunits of CK2 indicates that the formation of CK2β dimers is a prerequisite for the formation of complex with the catalytic subunits of CK2 (Canton *et al.* 2001). On the other hand, C-terminal domain of CK2β is required for complex formation with the catalytic subunits of CK2 as shown in Fig.31 (Niefind *et al.* 2001). Earlier, by deletion of C-terminal 179-215 aa of xCK2β, it had been shown that C-terminal region of xCK2β is involved in the interaction with xCK2α (Hinrichs *et al.* 1995).

In my study I found that xPAPCc interact with C-terminal of CK2β (100-215 aa). Therefore it is highly possible that xPAPCc interaction will hinder the dimerization of CK2β and/or the interaction between Ck2β and CK2α, which will lead to the failure of functional CK2 complex formation. Indeed, injection of either CK2α or CK2β alone failed to induce second axis in *Xenopus*, demonstrating that CK2 complex formation is indispensable for CK2 function in vivo (Dominguez *et al.* 2004). In future it is important to narrow down the region of CK2β responsible for the interaction with xPAPCc so that I can check the competitive interaction between xPAPCc, CK2β or CK2α with CK2β to examine whether xPAPCc would impair CK2 complex formation and if yes, at which step.

Another implication of xPAPC-CK2β interaction is that xPAPC may be a substrate of CK2. Several lines of evidence support this possibility. First, many interaction partners of CK2β are potential substrates of CK2, such as tumor suppressor protein Doc1, Fas-associated protein FAF1, fibroblast growth factor 2, p53, p21WAF1 and p27 KIP1 (Bolanos-Garcia *et al.* 2006). Secondly, CK2 is a serine/threonine kinase and the phospohrylation of S955 in xPAPC is implicated in the physical interaction of xPAPC with both xSpry1 and xCK2β. Thirdly, there are several predicted CK2 phosphorylation sites in xPAPCc. The next step would be to characterize whether xPAPCc is a substrate of CK2 by performing *in vitro* CK2 kinase assay and *in vivo* analysis.

5.4 xPAPC as a switch between canonical and non-canonical Wnt signaling

Based on the data on the functional interactions between xPAPCc and xSpry1 as well as between xPAPC and CK2β, I propose that xPAPC has dual functions in the regulation of Wnt pathway. On one hand, xPAPC promotes non-canonical Wnt signaling by antagonizing xSproutys (see **5.2,** Fig.30). On the other hand, xPAPC inhibits canonical Wnt signaling by antagonizing xCK2. In this aspect, it is interesting to mention the observed antagonisms between non-canonical and canonical Wnt signaling (Veeman *et al.* 2003). So it is possible for xPAPC to inhibit canonical Wnt signaling via two approaches. One is direct and involves the interaction with xCK2β. The other is indirect and involves the interaction with xSprouty.

It is interesting to note that a protein can regulate diverse signaling pathways by interacting with different proteins. Diversin is a typical example. Diversin was first identified as a binding partner of axin by yeast two-hybrid. Functionally it recruits CK1 and axin to form complex to promote β-catenin phosphorylation and degradation, therefore inhibiting canonical Wnt signaling (Schwarz-Romond *et al.* 2002). Recently, diversin was shown to interact with the DEP domain of Dsh and promote non-canonical Wnt signaling to modulate gastrulation movements in zebrafish (Moeller *et al.* 2006). Here I showed that xPAPC plays dual roles in the regulation of canonical and non-canonical Wnt siganling by interacting with CK2β and Sprouty, respectively. It is proposed that xPAPC acts as a switch from canonical Wnt to non-canonical Wnt signaling. Before gastrulation, canonical Wnt signaling is activated to induce the organizor and the specification of dorso-ventral polarity while non-canonical Wnt signaling is blocked by xSprouty. When embryos develop to gastrulation stage, xPAPC is expressed in dorsal margin zone. By simutaleous sequestration of xSprouty and CK2β, xPAPC promotes non-canonical Wnt signaling to modulate gastrulation movements while it inbibits canonical Wnt signaling to modify mesoderm specification (Fig. 32).

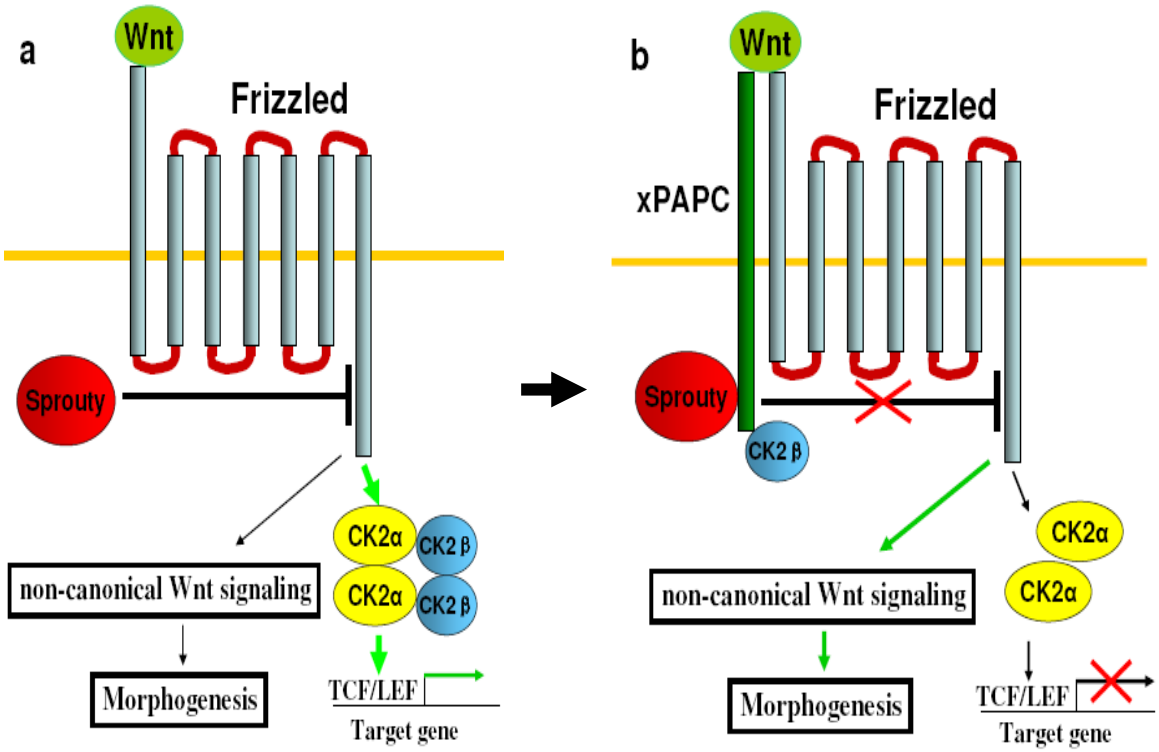

Figure 32. xPAPC acts as a switch from canonical to non-canonical Wnt signaling in *Xenopus* development. **a**. Before gastrulation, canonical Wnt signaling is transduced by CK2α/β to promote Wnt target gene transcription for patterning. Non-canonical Wnt signaling is blocked by xSprouty to prevent morphogenesis. **b**. With the advent of gastrulation, xPAPC sequesters xSprouty to promote non-canonical Wnt signaling. xPAPCc also sequesters CK2β to inhibit canonical Wnt signaling. Consequently, morphogenesis is favored while patterning is blocked (green and black represent activation and inactivation of signaling pathway, respectively).

5.5 Is xPAPC a co-receptor for non-canonical Wnt signaling?

5.5.1 Crosstalk of non-canonical Wnt and FGF signaling in the modulation of gastrulation morphogenesis

Although it is well established that FGF signaling is essential for mesoderm induction and patterning during vertebrate body axis formation, in fact FGF signaling is also implicated in the regulation of gastrulation movements. For example, bFGF induces migration, lamellipodia formation and polarization in gastrula stage cells (Wacker *et al.* 1998). FGF target genes including Xmc and NRH promote CE movements (Frazzetto *et al.* 2002; Sasai *et al.* 2004; Chung *et al.* 2005). Furthermore, xSproutys are induced by FGF signaling and selectively antagonize FGF-induced CE movements (Sivak *et al.* 2005). In conclusion, FGF signaling has both positive

effects (via activation of PKCδ or induction of Xmc and NRH) and negative effects (via induction of xSproutys) on morphogenesis like CE movements and tissue separation. Indeed, FGF signaling is also implicated in tissue separation (Wacker *et al.* 2000, Steinbeisser unpublished).

On the other hand, xPAPC modulates non-canonical Wnt signaling to promote CE movements and tissue separation (Kim *et al.* 1998; Medina *et al.* 2004; Unterseher *et al.* 2004). Therefore, the finding in the present study that xPAPC associates with and antagonizes xSproutys shed novel light on how non-canonical Wnt signaling and FGF signaling are fine-tuned by protocadherins to modulate morphogenesis. It is envisioned that in gastrula stage embryos, FGF signaling and non-canonical Wnt signaling crosstalk in a highly special tempo-spatial manner to decide when and where CE movements and tissue separation should proceed. In this way the highly orchestrated morphogenesis can be accomplished.

In this aspect it is really interesting to notice that another newly identified FGF target gene ANR5 (Ankyrin repeat domain protein 5) can associate with and cooperate with xPAPC to promote tissue separation (Chung *et al.* 2007), which means xPAPC can associate with two FGF target genes with opposite effects on morphogenesis. Thus it is imagined that in early stage FGF induces xSproutys to block gastrulation movements (Sivak *et al.* 2005), when xPAPC is induced by Nodal-related or β-catenin signaling (Wessely *et al.* 2004), FGF induces ARN5 to cooperate with xPAPC to antagonize xSproutys to permit gastrulation movements to ensue. This scenario demonstrates marvelously how signaling pathways are intertwined and fine-tuned to precisely control morphogenesis.

5.5.2 Mechanisms underlying inhibition of non-canonical Wnt pathway by xSpry1

Morphogenetic processes during *Xenopus* gastrulation including CE movements and tissue separation are considered to be regulated by PCP and Wnt/Ca^{2+} pathway, respectively (Wallingford *et al.* 2000; Winklbauer *et al.* 2001). It is interesting that xSpry1 can inhibit both CE movements and tissue separation (Fig.21, 23 and 24), indicating that xSpry1 has inhibitory effects on both PCP and Wnt/Ca^{2+} pathway. It has been reported that in *Xenopus* xSpry1 acts as inhibitors of FGF-induced PKCδ recruitment to membrane as well as FGF-induced Ca^{2+} signaling (Sivak *et al.* 2005). Nevertheless, in my present study, for the first time it was shown that xSpry1 inhibits Fz7-induced PKCδ recruitment to membrane (Fig.22), providing more direct link between xSpry1 and PCP pathway. On the other hand, for the first time it was demonstrated that xSpry1 inhibits tissue separation (Fig.23 and 24). Although I have no direct evidence that xSpry1

inhibits Wnt/Fz-induced Ca^{2+} release, it is strongly indicated that xSpry1 may play such as a role, given the fact that tissue separation is regulated by Wnt/Ca^{2+} signaling and xSpry1 inhibits tissue separation. So it is logical to conclude that xSpry1 acts as inhibitors of both PCP pathway and Wnt/Ca^{2+} pathway. But the detailed mechanisms are not clear yet.

To gain a better understanding of the functional antagonism between xPAPC and xSpry1, it is necessary to elucidate at which level that xSpry1 inhibit PCP and/or Wnt/Ca^{2+} pathway. If we compare Fig. 6 and Fig. 30, a similarity between FGF and Wnt/Fz induced PKCδ activation and Ca^{2+} release is visible. In both cases activation of PLC is involved. The difference is that FGF activates PLCγ while Wnt/Fz activates PLCβ. In both cases xSpry1 inhibits both PKCδ activation (driven by DAG) and Ca^{2+} release (driven by IP3), therefore I speculate that xSpry1 inhibits PLC activation, thus blocking the production of both DAG and IP3. To investigate how xSpry1 inhibits PLC activation, first we should know the modes of activation of PLC by FGF or Wnt/Fz signaling.

In terms of activation of PLCγ by FGF, as shown in Fig.33, the current mode is that FGF induces autophosphorylation of tyrosine at position 766 from a conserved region of all FGFRs. By the interaction of its SH2 domain with the phosphorylated Tyr 766, PLCγ is recruited to the vicinity of FGFR and is phosphorylated and activated by FGFR (Rhee 2001). Indeed, it was demonstrated that PLCγ1 is phosphorylated and associated with FGFR1 during *Xenopus* early development (Ryan and Gillespie 1994).

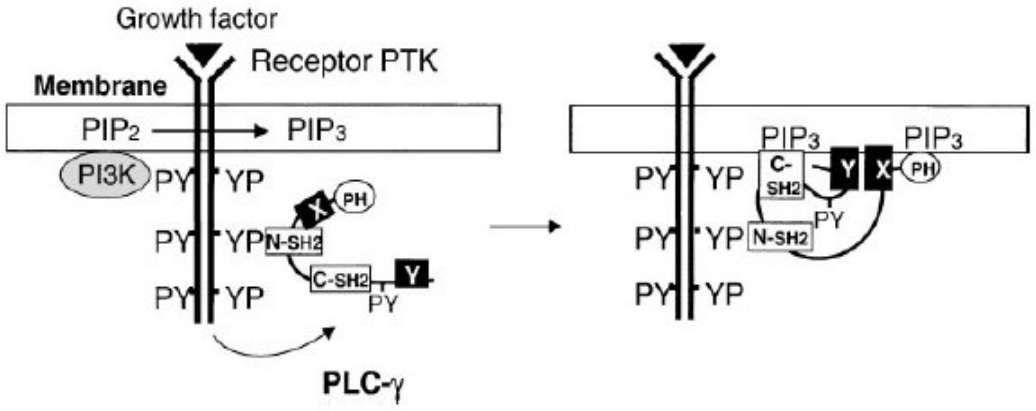

Figure 33. Growth factor receptor–induced PLCγ activation. Left. Growth factor like FGF triggers autophosphorylation of receptor PTK on tyrosine residues, serving as docking sites for SH2 domain–containing proteins including PtdIns 3-kinase (PI3K) and PLCγ. The receptor PTK phosphorylates and activates PLCγ and PI3K, the latter of which catalyzes the conversion of PIP2 to PIP3. **Right.** Phosphorylated PLCγ likely undergoes conformational changes and is maintained in proximity to the membrane through association both of its N-SH2 domain with the receptor PTK and of its PH or C-SH2 domains with PIP3 (modified from Rhee 2001).

So how xSproutys could inhibit PLCγ activation? It is interesting to note that Sprouty proteins contain no SH or PH domains, but they harbour Try residues and proline–arginine motifs that may mediate binding to SH2 and SH3, respectively. Indeed, Tyr 53 of Spry1 and Tyr 55 of Spry2 can interact with SH2 domain of adaptor protein Grb2 (Hanafusa *et al.* 2002). The proline–arginine motifs in Spry1 and Spry2 mediated their interaction with CIN85 SH3 domain (Haglund *et al.* 2005). Based on these data, I speculate that Tyr residues of Sprouty would bind to PLCγ SH2 domain in competition with Tyr residues of FGFR. As a result, PLCγ can not be recruited to the vicinity of FGFR for phosphorylation and activation. Therefore I cloned SH domains of *Xenopus* PLCγ1 (xPLCγ1 SH) into HA tagged vector and did Co-IP experiments in *Xenopus* embryos to check the interaction of HA-tagged xPLCγ1 and Myc-tagged Spry1. Unfortunately the results were negative, indicating that xSproutys do not associate with xPLCγ1. Till now only two isoforms of PLCγ are identified in human and rat while only one isoform is identified in *Xenopus laevis*. Although it is valuable to check the interaction of other xPLCγ isoforms with xSproutys, given the high conservation of xPLCγ protein sequences, it is unlikely that xSproutys inhibit PLCγ activation by competing with FGFR for binding PLCγ.

Although a variety of experiments support that Fz behaves as GPCR (Wang and Malbon, 2003), and genetic analysis in flies proves that heterotrimeric G proteins are required for Fz signaling (Katanaev *et al.* 2005), it is far from clear how G proteins mediate PLCβ activation induced by Fz. Mechanistically, the activation of PLCβ by G proteins are more complex than the activation of PLCγ by RTK. Compared to PLCγ no SH domains are present in PLCβ. Instead, activated Gα subunit interacts with C-terminal C2 domain of PLCβ and recruits PLCβ to membrane, where the membrane-anchored Gβγ dimer interact with PH and catalytic Y domains of PLCβ to enhance the membrane recruitment and activation of PLCβ (Rhee 2001). To make things more complex, there are many different kinds of Gα, β, γ subunits and they have different combinations. In the near future it is imperative to characterize which Gα, β, γ combinations would mediate PLCβ activation downstream of Fz. Without this knowledge, it is futile to elucidate the mechanisms by which xSproutys inhibit PLC activation downstram of Fz and G proteins.

5.5.3 xPAPC as a Co-receptor in non-canonical Wnt signaling

In canonical Wnt/β-catenin signaling, Wnt ligands binds to the extracellular domains of both LRP and Fz receptors, forming membrane-associated hetero-oligomers that interact with both Disheveled (via the intracellular portions of Fz) and Axin (via the intracellular domain of LRP) to activate downstream β-catenin pathway (Cong *et al.* 2004). Therefore LRP acts as a co-receptor

for Wnt. Binding to Wnt induces phosphorylation and/or conformational change of cytoplasmic domain of LRP so that LRP can recruit and sequester axin to the plasma membrane. As a result, axin-mediated β-catenin degradation is inhibited and stabilized β-catenin can drive Wnt signaling. Importantly, it was shown recently that Wnt induces sequential phosphorylaiton of LRP by GSK3 and CK1, and this dual phospohrylation is indispensable for axin recruitment and Wnt pathway activation (Davidson *et al.* 2005; Zeng *et al.* 2005). It is intriguing to parallelize the mode of action of LRP with that of xPAPC revealed in my present study. Indeed cytoplasmic domain of xPAPC undergoes phosphorylation at serine residues S741 and S955 in *Xenopus* embryos (Wang unpublished), and it was showed clearly that phosphorylation-deficient mutant of xPAPCc could not bind xSprouty and could not antagonize the inhibitory effect of xSprouty on non-canonical Wnt signaling. It is not examined yet whether PAPC can bind Wnt, but it has been shown that PAPC can bind to Fz via ectodomains. Therefore, the present finding that xPAPC sequesters xSproutys to promote PCP and Wnt/Ca^{2+} signaling provide support for the co-receptor model of non-canonical Wnt signaling.

It is known that Wnts are classified as canonical Wnts and non-canonical Wnts based on their preferential ability to activate β-catenin signaling. While Wnt1, Wnt3a and Wnt8 are considered as canonical Wnts, Wnt5a and Wnt 11 are considered as non-canonical Wnts (Kuhl *et al.* 2000). However, a series of evidence suggests that the distinction between these two Wnt subclasses is not so clear. For example, Wnt1 and Wnt3a stimulation can cause rapid activation of Rho in several mammalian cell lines (Kishida *et al.* 2004). In contrast, non-canonical Wnt5a can activate β-catenin in mammary epithelial cells (Civenni *et al.* 2003) and Wnt11 is required to activate β-catenin signaling for dorsal cell fate specification in the early *Xenopus* embryos (Tao *et al.* 2005). Besides ligands, Fz receptors also show diversity in signaling. Fz7 can activate both canonical and non-canonical Wnt signaling depending on the context in *Xenopus* (Djiane *et al.* 2000; Sumanas *et al.* 2000). In flies, Fz1 and Fz2 act redundantly in canonical Wnt signaling, while Fz1 has a specific nonredundant role in Fz/PCP pathway (Wu *et al.* 2004). Taken together, both Wnt ligands and Fz receptors show signaling diversity.

So what contribute to the Wnt/Fz signaling specifity? At least two possibilities exist. The first is that different receptor context dictates Wnt signaling output. In other words, signaling mediated by different Wnt or Fz family members is not intrinsically regulated by the Wnt or Fz proteins themselves but by co-receptor availability. For example, in the presence of LRP, Wnt and Fz will activate canonical Wnt signaing. In contrast, in the presence of Ror2, a receptor tyrosine kinase

interacting with both Wnt5a and rFz2, Wnt5a will activate non-canonical Wnt/JNK pathway (Oishi *et al.* 2003). It is possible that xPAPC can modulate Fz7 signaling specificity in a similar manner. In the present of LRP, Wnt/Fz7 may drive canonical Wnt signaling for axis formation. Upon gastrulation xPAPC is induced and acts to sequester xSproutys to promote non-canonical Wnt signaling mediated by Wnt/Fz7 for gastrulation morphogenesis.

Another possibility is that the association with other membrane proteins controls the subcellular Fz localization, therefore regulating the specificity of Wnt/Fz signaling. Indeed, in flies the Fz1 and Fz2 have different subcellular localizations in imaginal disc epithelia. Fz1 localizes preferentially to apical junctional complexes to activate Fz/PCP signaling, while interfereing with canonical Wnt signaling. The cytoplasmic tail of Fz2 can block apical accumulation of Fz2 and Fz2 is evenly distributed basolaterally to activate canonical Wnt signaling (Wu *et al.* 2004). More interestingly, in vertebrate it was found recently that atypical cadherin Flamingo contributes to Wnt11-induced Fz7 accumulation at cell contact sites to promote local PCP signaling (Witzel *et al.* 2006). Considering that xPAPC associates with Fz7 via ectodomains, it is interesting to examine whether xPAPC has impact on the subcellular localization of Fz7 to modulate non-canonical Wnt signaling specially.

It is necessary in the future to identify what kinases and characterize what upstream events lead to the phosphorylation of xPAPC and its subsequent sequestration of xSproutys. Is it Wnt dependent? Undoubtedly, answers to these questions will broaden our understanding of regulation of Wnt signaling specificity. A variety of mechanisms are currently known to regulate Wnt signaling. Nevertheless, by controlling co-receptor availability (synthesis and degradation), posttranslational modification, subcellular localization etc., a sophisticated tempo-spatial modulation of Wnt signaling will be achieved.

6. Reference

Reference List

Axelrod JD, Miller JR, Shulman JM, Moon RT, Perrimon N (1998) Differential recruitment of Dishevelled provides signaling specificity in the planar cell polarity and Wingless signaling pathways. *Genes Dev.* **12,** 2610-2622.

Bolanos-Garcia VM, Fernandez-Recio J, Allende JE, Blundell TL (2006) Identifying interaction motifs in CK2beta--a ubiquitous kinase regulatory subunit. *Trends Biochem.Sci* **31,** 654-661.

Bottcher RT, Niehrs C (2005) Fibroblast growth factor signaling during early vertebrate development. *Endocr.Rev.* **26,** 63-77.

Bradley RS, Espeseth A, Kintner C (1998) NF-protocadherin, a novel member of the cadherin superfamily, is required for Xenopus ectodermal differentiation. *Curr.Biol.* **8,** 325-334.

Bundschu K, Walter U, Schuh K (2006) The VASP-Spred-Sprouty domain puzzle. *J Biol.Chem.* **281,** 36477-36481.

Canton DA, Zhang C, Litchfield DW (2001) Assembly of protein kinase CK2: investigation of complex formation between catalytic and regulatory subunits using a zinc-finger-deficient mutant of CK2beta. *Biochem.J* **358,** 87-94.

Chen M, Li D, Krebs EG, Cooper JA (1997) The casein kinase II beta subunit binds to Mos and inhibits Mos activity. *Mol.Cell Biol.* **17,** 1904-1912.

Chen X, Gumbiner BM (2006) Paraxial protocadherin mediates cell sorting and tissue morphogenesis by regulating C-cadherin adhesion activity. *J Cell Biol.* **174,** 301-313.

Chen X, Kojima S, Borisy GG, Green KJ (2003) p120 catenin associates with kinesin and facilitates the transport of cadherin-catenin complexes to intercellular junctions. *J Cell Biol.* **163,** 547-557.

Choi SC, Han JK (2002) Xenopus Cdc42 regulates convergent extension movements during gastrulation through Wnt/Ca2+ signaling pathway. *Dev.Biol.* **244,** 342-357.

Chung HA, Hyodo-Miura J, Nagamune T, Ueno N (2005) FGF signal regulates gastrulation cell movements and morphology through its target NRH. *Dev.Biol.* **282,** 95-110.

Chung HA, Yamamoto TS, Ueno N (2007) ANR5, an FGF Target Gene Product, Regulates Gastrulation in Xenopus. *Curr.Biol.*

Civenni G, Holbro T, Hynes NE (2003) Wnt1 and Wnt5a induce cyclin D1 expression through ErbB1 transactivation in HC11 mammary epithelial cells. *EMBO Rep.* **4,** 166-171.

Cong F, Schweizer L, Varmus H (2004) Wnt signals across the plasma membrane to activate the beta-catenin pathway by forming oligomers containing its receptors, Frizzled and LRP. *Development* **131,** 5103-5115.

Curtin JA, Quint E, Tsipouri V, Arkell RM, Cattanach B, Copp AJ, Henderson DJ, Spurr N, Stanier P, Fisher EM, Nolan PM, Steel KP, Brown SD, Gray IC, Murdoch JN (2003) Mutation of Celsr1 disrupts planar polarity of inner ear hair cells and causes severe neural tube defects in the mouse. *Curr.Biol.* **13,** 1129-1133.

Davidson G, Wu W, Shen J, Bilic J, Fenger U, Stannek P, Glinka A, Niehrs C (2005) Casein kinase 1

gamma couples Wnt receptor activation to cytoplasmic signal transduction. *Nature* **438,** 867-872.

Davidson LA, Marsden M, Keller R, Desimone DW (2006) Integrin alpha5beta1 and fibronectin regulate polarized cell protrusions required for Xenopus convergence and extension. *Curr.Biol.* **16,** 833-844.

Djiane A, Riou J, Umbhauer M, Boucaut J, Shi D (2000) Role of frizzled 7 in the regulation of convergent extension movements during gastrulation in Xenopus laevis. *Development* **127,** 3091-3100.

Dominguez I, Mizuno J, Wu H, Imbrie GA, Symes K, Seldin DC (2005) A role for CK2alpha/beta in Xenopus early embryonic development. *Mol.Cell Biochem.* **274,** 125-131.

Dominguez I, Mizuno J, Wu H, Song DH, Symes K, Seldin DC (2004) Protein kinase CK2 is required for dorsal axis formation in Xenopus embryos. *Dev.Biol.* **274,** 110-124.

Fang X, Ji H, Kim SW, Park JI, Vaught TG, Anastasiadis PZ, Ciesiolka M, McCrea PD (2004) Vertebrate development requires ARVCF and p120 catenins and their interplay with RhoA and Rac. *J Cell Biol.* **165,** 87-98.

Faure S, Cau J, de Santa BP, Bigou S, Ge Q, Delsert C, Morin N (2005) Xenopus p21-activated kinase 5 regulates blastomeres' adhesive properties during convergent extension movements. *Dev.Biol.* **277,** 472-492.

Fields S, Song O (1989) A novel genetic system to detect protein-protein interactions. *Nature* **340,** 245-246.

Formstone CJ, Mason I (2005a) Combinatorial activity of Flamingo proteins directs convergence and extension within the early zebrafish embryo via the planar cell polarity pathway. *Dev.Biol.* **282,** 320-335.

Formstone CJ, Mason I (2005b) Expression of the Celsr/flamingo homologue, c-fmi1, in the early avian embryo indicates a conserved role in neural tube closure and additional roles in asymmetry and somitogenesis. *Dev.Dyn.* **232,** 408-413.

Franz CM, Ridley AJ (2004) p120 catenin associates with microtubules: inverse relationship between microtubule binding and Rho GTPase regulation. *J Biol.Chem.* **279,** 6588-6594.

Frazzetto G, Klingbeil P, Bouwmeester T (2002) Xenopus marginal coil (Xmc), a novel FGF inducible cytosolic coiled-coil protein regulating gastrulation movements. *Mech.Dev.* **113,** 3-14.

Godde NJ, D'Abaco GM, Paradiso L, Novak U (2006) Efficient ADAM22 surface expression is mediated by phosphorylation-dependent interaction with 14-3-3 protein family members. *J Cell Sci* **119,** 3296-3305.

Graff JM, Thies RS, Song JJ, Celeste AJ, Melton DA (1994) Studies with a Xenopus BMP receptor suggest that ventral mesoderm-inducing signals override dorsal signals in vivo. *Cell* **79,** 169-179.

Habas R, Dawid IB, He X (2003) Coactivation of Rac and Rho by Wnt/Frizzled signaling is required for vertebrate gastrulation. *Genes Dev.* **17,** 295-309.

Habas R, Kato Y, He X (2001) Wnt/Frizzled activation of Rho regulates vertebrate gastrulation and requires a novel Formin homology protein Daam1. *Cell* **107,** 843-854.

Haglund K, Schmidt MH, Wong ES, Guy GR, Dikic I (2005) Sprouty2 acts at the Cbl/CIN85 interface to inhibit epidermal growth factor receptor downregulation. *EMBO Rep.* **6,** 635-641.

Halbleib JM, Nelson WJ (2006) Cadherins in development: cell adhesion, sorting, and tissue morphogenesis. *Genes Dev.* **20,** 3199-3214.

Hanafusa H, Torii S, Yasunaga T, Nishida E (2002) Sprouty1 and Sprouty2 provide a control mechanism

for the Ras/MAPK signalling pathway. *Nat.Cell Biol.* **4,** 850-858.

Heggem MA, Bradley RS (2003b) The cytoplasmic domain of Xenopus NF-protocadherin interacts with TAF1/set. *Dev.Cell* **4,** 419-429.

Heggem MA, Bradley RS (2003a) The cytoplasmic domain of Xenopus NF-protocadherin interacts with TAF1/set. *Dev.Cell* **4,** 419-429.

Heisenberg CP, Tada M, Rauch GJ, Saude L, Concha ML, Geisler R, Stemple DL, Smith JC, Wilson SW (2000) Silberblick/Wnt11 mediates convergent extension movements during zebrafish gastrulation. *Nature* **405,** 76-81.

Hinrichs MV, Gatica M, Allende CC, Allende JE (1995) Site-directed mutants of the beta subunit of protein kinase CK2 demonstrate the important role of Pro-58. *FEBS Lett.* **368,** 211-214.

Hirano S, Suzuki ST, Redies C (2003) The cadherin superfamily in neural development: diversity, function and interaction with other molecules. *Front Biosci.* **8,** d306-d355.

Huelsken J, Behrens J (2002) The Wnt signalling pathway. *Journal of Cell Science* **115,** 3977-3978.

Hukriede NA, Tsang TE, Habas R, Khoo PL, Steiner K, Weeks DL, Tam PP, Dawid IB (2003) Conserved requirement of Lim1 function for cell movements during gastrulation. *Dev.Cell* **4,** 83-94.

Hyodo-Miura J, Urushiyama S, Nagai S, Nishita M, Ueno N, Shibuya H (2002) Involvement of NLK and Sox11 in neural induction in Xenopus development. *Genes Cells* **7,** 487-496.

Ibrahim H, Winklbauer R (2001) Mechanisms of mesendoderm internalization in the Xenopus gastrula: lessons from the ventral side. *Dev.Biol.* **240,** 108-122.

Iouzalen N, Camonis J, Moreau J (1998) Identification and Characterization in Xenopus of XsmgGDS, a RalB Binding Protein. *Biochemical and Biophysical Research Communications* **250,** 359-363.

Ishitani T, Kishida S, Hyodo-Miura J, Ueno N, Yasuda J, Waterman M, Shibuya H, Moon RT, Ninomiya-Tsuji J, Matsumoto K (2003) The TAK1-NLK mitogen-activated protein kinase cascade functions in the Wnt-5a/Ca(2+) pathway to antagonize Wnt/beta-catenin signaling. *Mol.Cell Biol.* **23,** 131-139.

Ishitani T, Ninomiya-Tsuji J, Nagai S, Nishita M, Meneghini M, Barker N, Waterman M, Bowerman B, Clevers H, Shibuya H, Matsumoto K (1999) The TAK1-NLK-MAPK-related pathway antagonizes signalling between beta-catenin and transcription factor TCF. *Nature* **399,** 798-802.

Jarrett O, Stow JL, Yap AS, Key B (2002) Dynamin-dependent endocytosis is necessary for convergent-extension movements in Xenopus animal cap explants. *Int.J Dev.Biol.* **46,** 467-473.

Katanaev VL, Ponzielli R, Semeriva M, Tomlinson A (2005) Trimeric G protein-dependent frizzled signaling in Drosophila. *Cell* **120,** 111-122.

Keller R (2002) Shaping the vertebrate body plan by polarized embryonic cell movements. *Science* **298,** 1950-1954.

Keller R, Davidson LA, Shook DR (2003) How we are shaped: the biomechanics of gastrulation. *Differentiation* **71,** 171-205.

Kim SH, Yamamoto A, Bouwmeester T, Agius E, Robertis EM (1998) The role of paraxial protocadherin in selective adhesion and cell movements of the mesoderm during Xenopus gastrulation. *Development* **125,** 4681-4690.

Kim SW, Park JI, Spring CM, Sater AK, Ji H, Otchere AA, Daniel JM, McCrea PD (2004) Non-canonical Wnt signals are modulated by the Kaiso transcriptional repressor and p120-catenin. *Nat.Cell Biol.* **6,** 1212-1220.

Kinoshita N, Iioka H, Miyakoshi A, Ueno N (2003) PKC delta is essential for Dishevelled function in a noncanonical Wnt pathway that regulates Xenopus convergent extension movements. *Genes Dev.* **17,** 1663-1676.

Kishida S, Yamamoto H, Kikuchi A (2004) Wnt-3a and Dvl induce neurite retraction by activating Rho-associated kinase. *Mol.Cell Biol.* **24,** 4487-4501.

Kuhl M, Geis K, Sheldahl LC, Pukrop T, Moon RT, Wedlich D (2001) Antagonistic regulation of convergent extension movements in Xenopus by Wnt/beta-catenin and Wnt/Ca2+ signaling. *Mech.Dev.* **106,** 61-76.

Kuhl M, Sheldahl LC, Park M, Miller JR, Moon RT (2000) The Wnt/Ca2+ pathway: a new vertebrate Wnt signaling pathway takes shape. *Trends Genet.* **16,** 279-283.

Kumagai A, Dunphy WG (1999) Binding of 14-3-3 proteins and nuclear export control the intracellular localization of the mitotic inducer Cdc25. *Genes Dev.* **13,** 1067-1072.

Kuroda H, Inui M, Sugimoto K, Hayata T, Asashima M (2002) Axial protocadherin is a mediator of prenotochord cell sorting in Xenopus. *Dev.Biol.* **244,** 267-277.

Kusakabe M, Nishida E (2004) The polarity-inducing kinase Par-1 controls Xenopus gastrulation in cooperation with 14-3-3 and aPKC. *EMBO J* **23,** 4190-4201.

Kwan KM, Kirschner MW (2003) Xbra functions as a switch between cell migration and convergent extension in the Xenopus gastrula. *Development* **130,** 1961-1972.

Latinkic BV, Mercurio S, Bennett B, Hirst EM, Xu Q, Lau LF, Mohun TJ, Smith JC (2003) Xenopus Cyr61 regulates gastrulation movements and modulates Wnt signalling. *Development* **130,** 2429-2441.

Lau JM, Wu C, Muslin AJ (2006) Differential role of 14-3-3 family members in Xenopus development. *Dev.Dyn.* **235,** 1761-1776.

Lawrence PA, Casal J, Struhl G (2002) Towards a model of the organisation of planar polarity and pattern in the Drosophila abdomen. *Development* **129,** 2749-2760.

Levine E, Lee CH, Kintner C, Gumbiner BM (1994) Selective disruption of E-cadherin function in early Xenopus embryos by a dominant negative mutant. *Development* **120,** 901-909.

Litchfield DW (2003) Protein kinase CK2: structure, regulation and role in cellular decisions of life and death. *Biochem.J* **369,** 1-15.

Logan CY, Nusse R (2004) The Wnt signaling pathway in development and disease. *Annu.Rev.Cell Dev.Biol.* **20,** 781-810.

Marsden M, DeSimone DW (2003) Integrin-ECM interactions regulate cadherin-dependent cell adhesion and are required for convergent extension in Xenopus. *Curr.Biol.* **13,** 1182-1191.

Medina A, Swain RK, Kuerner KM, Steinbeisser H (2004) Xenopus paraxial protocadherin has signaling functions and is involved in tissue separation. *EMBO J* **23,** 3249-3258.

Meggio F, Boldyreff B, Marin O, Pinna LA, Issinger OG (1992) Role of the beta subunit of casein kinase-2

on the stability and specificity of the recombinant reconstituted holoenzyme. *Eur.J Biochem.* **204,** 293-297.

Miller JR, McClay DR (1997) Characterization of the role of cadherin in regulating cell adhesion during sea urchin development. *Dev.Biol.* **192,** 323-339.

Miyakoshi A, Ueno N, Kinoshita N (2004) Rho guanine nucleotide exchange factor xNET1 implicated in gastrulation movements during Xenopus development. *Differentiation* **72,** 48-55.

Moeller H, Jenny A, Schaeffer HJ, Schwarz-Romond T, Mlodzik M, Hammerschmidt M, Birchmeier W (2006) Diversin regulates heart formation and gastrulation movements in development. *Proc.Natl.Acad.Sci U.S.A* **103,** 15900-15905.

Moon RT, Campbell RM, Christian JL, McGrew LL, Shih J, Fraser S (1993) Xwnt-5A: a maternal Wnt that affects morphogenetic movements after overexpression in embryos of Xenopus laevis. *Development* **119,** 97-111.

Munoz R, Larrain J (2006) xSyndecan-4 regulates gastrulation and neural tube closure in Xenopus embryos. *ScientificWorldJournal.* **6,** 1298-1301.

Munoz R, Moreno M, Oliva C, Orbenes C, Larrain J (2006) Syndecan-4 regulates non-canonical Wnt signalling and is essential for convergent and extension movements in Xenopus embryos. *Nat.Cell Biol.* **8,** 492-500.

Myers DC, Sepich DS, Solnica-Krezel L (2002a) Bmp activity gradient regulates convergent extension during zebrafish gastrulation. *Dev.Biol.* **243,** 81-98.

Myers DC, Sepich DS, Solnica-Krezel L (2002b) Convergence and extension in vertebrate gastrulae: cell movements according to or in search of identity? *Trends Genet.* **18,** 447-455.

Nelson KK, Nelson RW (2004) Cdc42 Effector Protein 2 (XCEP2) is required for normal gastrulation and contributes to cellular adhesion in Xenopus laevis. *BMC.Dev.Biol.* **4,** 13.

Niefind K, Guerra B, Ermakowa I, Issinger OG (2001) Crystal structure of human protein kinase CK2: insights into basic properties of the CK2 holoenzyme. *EMBO J* **20,** 5320-5331.

Nobes CD, Hall A (1999) Rho GTPases control polarity, protrusion, and adhesion during cell movement. *J Cell Biol.* **144,** 1235-1244.

Nubler-Jung (1987) Insect epidermis: disturbance of supracellular tissue polarity does not prevent the expression of cell polarity. *Roux's Arch.Dev.Biol.* **196,** 286-289.

Obenauer JC, Yaffe MB (2004) Computational prediction of protein-protein interactions. *Methods Mol.Biol.* **261,** 445-468.

Ohkawara B, Yamamoto TS, Tada M, Ueno N (2003) Role of glypican 4 in the regulation of convergent extension movements during gastrulation in Xenopus laevis. *Development* **130,** 2129-2138.

Oishi I, Suzuki H, Onishi N, Takada R, Kani S, Ohkawara B, Koshida I, Suzuki K, Yamada G, Schwabe GC, Mundlos S, Shibuya H, Takada S, Minami Y (2003) The receptor tyrosine kinase Ror2 is involved in non-canonical Wnt5a/JNK signalling pathway. *Genes Cells* **8,** 645-654.

Park M, Moon RT (2002) The planar cell-polarity gene stbm regulates cell behaviour and cell fate in vertebrate embryos. *Nat.Cell Biol.* **4,** 20-25.

Paulson AF, Mooney E, Fang X, Ji H, McCrea PD (2000) Xarvcf, Xenopus member of the p120 catenin

subfamily associating with cadherin juxtamembrane region. *J Biol.Chem.* **275,** 30124-30131.

Penzo-Mendez A, Umbhauer M, Djiane A, Boucaut JC, Riou JF (2003) Activation of Gbetagamma signaling downstream of Wnt-11/Xfz7 regulates Cdc42 activity during Xenopus gastrulation. *Dev.Biol.* **257,** 302-314.

Piddini E, Vincent JP (2003) Modulation of developmental signals by endocytosis: different means and many ends. *Curr.Opin.Cell Biol.* **15,** 474-481.

Pulina MV, Rizzuto R, Brini M, Carafoli E (2006) Inhibitory interaction of the plasma membrane Na+/Ca2+ exchangers with the 14-3-3 proteins. *J Biol.Chem.* **281,** 19645-19654.

Rangarajan J, Luo T, Sargent TD (2006) PCNS: a novel protocadherin required for cranial neural crest migration and somite morphogenesis in Xenopus. *Dev.Biol.* **295,** 206-218.

Rhee SG (2001) Regulation of phosphoinositide-specific phospholipase C. *Annu.Rev.Biochem.* **70,** 281-312.

Rijsewijk F, Schuermann M, Wagenaar E, Parren P, Weigel D, Nusse R (1987) The Drosophila homolog of the mouse mammary oncogene int-1 is identical to the segment polarity gene wingless. *Cell* **50,** 649-657.

Roffers-Agarwal J, Xanthos JB, Miller JR (2005) Regulation of actin cytoskeleton architecture by Eps8 and Abi1. *BMC.Cell Biol.* **6,** 36.

Rong J, Li S, Sheng G, Wu M, Coblitz B, Li M, Fu H, Li XJ (2007) 14-3-3 protein interacts with Huntingtin-associated protein 1 and regulates its trafficking. *J Biol.Chem.* **282,** 4748-4756.

Ryan PJ, Gillespie LL (1994) Phosphorylation of phospholipase C gamma 1 and its association with the FGF receptor is developmentally regulated and occurs during mesoderm induction in Xenopus laevis. *Dev.Biol.* **166,** 101-111.

Sano K, Tanihara H, Heimark RL, Obata S, Davidson M, St John T, Taketani S, Suzuki S (1993) Protocadherins: a large family of cadherin-related molecules in central nervous system. *EMBO J* **12,** 2249-2256.

Sasai N, Nakazawa Y, Haraguchi T, Sasai Y (2004) The neurotrophin-receptor-related protein NRH1 is essential for convergent extension movements. *Nat.Cell Biol.* **6,** 741-748.

Sato A, Khadka DK, Liu W, Bharti R, Runnels LW, Dawid IB, Habas R (2006) Profilin is an effector for Daam1 in non-canonical Wnt signaling and is required for vertebrate gastrulation. *Development* **133,** 4219-4231.

Schwarz-Romond T, Asbrand C, Bakkers J, Kuhl M, Schaeffer HJ, Huelsken J, Behrens J, Hammerschmidt M, Birchmeier W (2002) The ankyrin repeat protein Diversin recruits Casein kinase Iepsilon to the beta-catenin degradation complex and acts in both canonical Wnt and Wnt/JNK signaling. *Genes Dev.* **16,** 2073-2084.

Scita G, Nordstrom J, Carbone R, Tenca P, Giardina G, Gutkind S, Bjarnegard M, Betsholtz C, Di Fiore PP (1999) EPS8 and E3B1 transduce signals from Ras to Rac. *Nature* **401,** 290-293.

Sivak JM, Petersen LF, Amaya E (2005) FGF signal interpretation is directed by Sprouty and Spred proteins during mesoderm formation. *Dev.Cell* **8,** 689-701.

Sokol SY (1996) Analysis of Dishevelled signalling pathways during Xenopus development. *Curr.Biol.* **6,** 1456-1467.

Solnica-Krezel L (2005) Conserved patterns of cell movements during vertebrate gastrulation. *Curr.Biol.* **15,** R213-R228.

Strutt H, Strutt D (2005) Long-range coordination of planar polarity in Drosophila. *Bioessays* **27,** 1218-1227.

Sumanas S, Strege P, Heasman J, Ekker SC (2000) The putative wnt receptor Xenopus frizzled-7 functions upstream of beta-catenin in vertebrate dorsoventral mesoderm patterning. *Development* **127,** 1981-1990.

Tada M, Smith JC (2000) Xwnt11 is a target of Xenopus Brachyury: regulation of gastrulation movements via Dishevelled, but not through the canonical Wnt pathway. *Development* **127,** 2227-2238.

Tahinci E, Symes K (2003) Distinct functions of Rho and Rac are required for convergent extension during Xenopus gastrulation. *Dev.Biol.* **259,** 318-335.

Takeuchi M, Nakabayashi J, Sakaguchi T, Yamamoto TS, Takahashi H, Takeda H, Ueno N (2003) The prickle-related gene in vertebrates is essential for gastrulation cell movements. *Curr.Biol.* **13,** 674-679.

Tanegashima K, Zhao H, Dawid IB (2006) WGEF activates Rho in the Wnt-PCP pathway and controls convergent extension during Xenopus gastrulation. *11th international Xenopus conference, Kazusa, Japan*.

Tao Q, Yokota C, Puck H, Kofron M, Birsoy B, Yan D, Asashima M, Wylie CC, Lin X, Heasman J (2005) Maternal wnt11 activates the canonical wnt signaling pathway required for axis formation in Xenopus embryos. *Cell* **120,** 857-871.

Thorpe CJ, Moon RT (2004) nemo-like kinase is an essential co-activator of Wnt signaling during early zebrafish development. *Development* **131,** 2899-2909.

Topczewski J, Sepich DS, Myers DC, Walker C, Amores A, Lele Z, Hammerschmidt M, Postlethwait J, Solnica-Krezel L (2001) The zebrafish glypican knypek controls cell polarity during gastrulation movements of convergent extension. *Dev.Cell* **1,** 251-264.

Ulrich F, Krieg M, Schotz EM, Link V, Castanon I, Schnabel V, Taubenberger A, Mueller D, Puech PH, Heisenberg CP (2005) Wnt11 functions in gastrulation by controlling cell cohesion through Rab5c and E-cadherin. *Dev.Cell* **9,** 555-564.

Unterseher F, Hefele JA, Giehl K, De Robertis EM, Wedlich D, Schambony A (2004) Paraxial protocadherin coordinates cell polarity during convergent extension via Rho A and JNK. *EMBO J* **23,** 3259-3269.

Veeman MT, Axelrod JD, Moon RT (2003) A second canon. Functions and mechanisms of beta-catenin-independent Wnt signaling. *Dev.Cell* **5,** 367-377.

Vidalain PO, Boxem M, Ge H, Li S, Vidal M (2004) Increasing specificity in high-throughput yeast two-hybrid experiments. *Methods* **32,** 363-370.

Wacker S, Brodbeck A, Lemaire P, Niehrs C, Winklbauer R (1998) Patterns and control of cell motility in the Xenopus gastrula. *Development* **125,** 1931-1942.

Wacker S, Grimm K, Joos T, Winklbauer R (2000) Development and control of tissue separation at gastrulation in Xenopus. *Dev.Biol.* **224,** 428-439.

Wallingford JB, Rowning BA, Vogeli KM, Rothbacher U, Fraser SE, Harland RM (2000) Dishevelled controls cell polarity during Xenopus gastrulation. *Nature* **405,** 81-85.

Wang HY, Malbon CC (2003) Wnt signaling, Ca2+, and cyclic GMP: visualizing Frizzled functions. *Science* **300,** 1529-1530.

Wessely O, Kim JI, Geissert D, Tran U, De Robertis EM (2004) Analysis of Spemann organizer formation in Xenopus embryos by cDNA macroarrays. *Dev.Biol.* **269,** 552-566.

Wilhelm V, Rojas P, Gatica M, Allende CC, Allende JE (1995) Expression of the subunits of protein kinase CK2 during oogenesis in Xenopus laevis. *Eur.J Biochem.* **232,** 671-676.

Winklbauer R, Medina A, Swain RK, Steinbeisser H (2001) Frizzled-7 signalling controls tissue separation during Xenopus gastrulation. *Nature* **413,** 856-860.

Witzel S, Zimyanin V, Carreira-Barbosa F, Tada M, Heisenberg CP (2006) Wnt11 controls cell contact persistence by local accumulation of Frizzled 7 at the plasma membrane. *J Cell Biol.* **175,** 791-802.

Wu C, Muslin AJ (2002) Role of 14-3-3 proteins in early Xenopus development. *Mech.Dev.* **119,** 45-54.

Wu J, Klein TJ, Mlodzik M (2004) Subcellular localization of frizzled receptors, mediated by their cytoplasmic tails, regulates signaling pathway specificity. *PLoS.Biol.* **2,** E158.

Yagi T, Takeichi M (2000) Cadherin superfamily genes: functions, genomic organization, and neurologic diversity. *Genes Dev.* **14,** 1169-1180.

Yamamoto A, Amacher SL, Kim SH, Geissert D, Kimmel CB, De Robertis EM (1998) Zebrafish paraxial protocadherin is a downstream target of spadetail involved in morphogenesis of gastrula mesoderm. *Development* **125,** 3389-3397.

Yamamoto A, Kemp C, Bachiller D, Geissert D, De Robertis EM (2000) Mouse paraxial protocadherin is expressed in trunk mesoderm and is not essential for mouse development. *Genesis.* **27,** 49-57.

Yamashita S, Miyagi C, Carmany-Rampey A, Shimizu T, Fujii R, Schier AF, Hirano T (2002) Stat3 Controls Cell Movements during Zebrafish Gastrulation. *Dev.Cell* **2,** 363-375.

Yokota C, Kofron M, Zuck M, Houston DW, Isaacs H, Asashima M, Wylie CC, Heasman J (2003) A novel role for a nodal-related protein; Xnr3 regulates convergent extension movements via the FGF receptor. *Development* **130,** 2199-2212.

Yoshida K, Yoshitomo-Nakagawa K, Seki N, Sasaki M, Sugano S (1998) Cloning, expression analysis, and chromosomal localization of BH-protocadherin (PCDH7), a novel member of the cadherin superfamily. *Genomics* **49,** 458-461.

Yu A, Rual JF, Tamai K, Harada Y, Vidal M, He X, Kirchhausen T (2007) Association of Dishevelled with the clathrin AP-2 adaptor is required for Frizzled endocytosis and planar cell polarity signaling. *Dev.Cell* **12,** 129-141.

Zeng X, Tamai K, Doble B, Li S, Huang H, Habas R, Okamura H, Woodgett J, He X (2005) A dual-kinase mechanism for Wnt co-receptor phosphorylation and activation. *Nature* **438,** 873-877.

Abbreviations

Ab	antibody
AC	animal cap
ARVCF	armadillo repeat gene deleted in velo-cardio-facial syndrome
3-AT	3-amino-1,2,4-triazole
AXPC	axial protocadherin
AXPCc	cytoplasmic domain of axial protocadherin
BCR	blastcoel roof
bFGF	basic FGF
BMP	bone morphogenesis protein
bp	base pair
BSA	bovine serum albumin
CE	convergent extension
CK	casein kinase
Co-IP	co-immunoprecipitation
C-terminal	carboxy-terminal
DAG	diacylglycerol
DEPC	diethylpyrocarbonate
DMF	N,N-dimethylformamide
DMSO	dimethylsulfoxide
DN	dominant negative
DNA	desoxyribonucleic acid
dNTP	desoxynucleotidetriphosphate
Dsh	dishevelled
DTT	dithiothreitol
ECL	enhanced chemoluminescence
ECM	extracellular matrix
EDTA	ethylenediaminetetraacetate
FGF	fibroblast growth factor
FGFR	fibroblast growth factor receptor
Fz	frizzled
GEF	guanine nucleotide exchange factor
GFP	green fluorescent protein
GPCR	G-protein-coupled receptor
GSK3	glycogen synthase kinase 3
GST	glutathione S-transferase
HA	hemagglutinin

HSPG	heparan sulfate proteoglycan
Ig	immmunoglobulin
JNK	Jun N-terminal kinase
kb	Kilobase pair
kDa	Kilo Dalton
LiOAC	lithium acetate
LRP	low density lipoprotein receptor related protein
β-ME	β-mercaptoethanol
MO	morpholino oligonucleotide
NLK	Nemo-like kinase
N-ternimal	amino-terminal
ORF	open reading frame
PAGE	polyacrylamide gel electrophoresis
PAPC	paraxial protocadherin
PAPCc	cytoplasmic domain of paraxial protocadherin
PBS	phosphate buffered saline
PEG	polyethylene glycol
PCP	planar cell polarity
PCR	polymerase chain reaction
PI3K	phosphatidylinositol-3 kinase
PKC	protein kinase C
PLC	phospholipase C
PMA	phorbol-12-myristat-13-acetate
PMSF	phenylmethylsulfonylfluorid
RNA	ribonucleic acid
rpm	rounds per minute
RT	reverse transcription
RTK	receptor tyrosine kinase
SDS	sodium dodecyl sulfate
SH2	Src homology 2
SH3	Src homology 3
Spred	sprouty-related protein
Spry	sprouty
TCA	trichloracetic acid
Tris	tris(-hydroxymethyl)-aminomethane
UTR	untranslated region
X-Gal	5-bromo-4-chloro-3-indolyl-β-D-galactopyranoside

Index of Tables and Figures

Acknowledgements

This study has been performed in the Institute of Human Genetics, University of Heidelberg. I would like to thank Prof. Herbert Steinbeisser for offering me the opportunity to enter the fascinating Developmental Biology field and for his patient supervision and inspiring discussions. I am so fortunate to meet such a person on my scientific way. I am thankful to Prof. Thomas Holstein for taking over my supervision in the Faculty of Biology.

Thanks to all the colleagues in Steinbeisser lab for the pleasent working atmosphere, stimulating discussions and sharing their experiences, especially, Corinna Berger, Isabelle Köster, Klaus-Michael Kürner, Rajeeb K. Swain, Katja Hess and Patricia Janicki. Thank Kirsten Linsmeier for expert technical assistance. I also thank colleagues in Prof. Christof Niehrs´lab for generous help, especially, Jinlong Shen. Prof. Hans Jansen´s help and advice with yeast two-hybrid screen and Dr. Engel´s help with confocal microscopy at Nikon Imaging Center are highly appreciated. Thank all members of Institute of Human Genetics for their help, especially sequencing service.

I want to thank Kürner KM for providing activin and Amaya E, Dominguez I, Kumagai A, McCrea PD, Moreau J, Nishida E and Staub O for kindly providing plasmids and yeast two-hybrid library. The work presented in this thesis was supported by the Deutsche Forschungsgemeinschaft (STE-613/4-1).

Finally, great thanks go to my wife, Dr. Ling Zhang, for her constant support in terms of both family and academic affairs. I appreciate greatly that my daughter, Xintong Wang, understands me so fully as to endure the separation from me during my graduate work. Also I am in great debt to my father and parents-in-law for their support and taking care of my daughter.